

Supporting Information

Design of functional isocyanate-free poly(oxazolidone)s under mild conditions

Maliheh Razavi-Esfali^{a,b}, Thomas Habets^a, Fabiana Siragusa^a, Bruno Grignard^{a,c}, Haritz Sardon^{b*} and Christophe Detrembleur^{a*}

^a Center for Education and Research on Macromolecules (CERM), CESAM Research Unit, University of Liege, Sart-Tilman B6a, 4000 Liege, Belgium

^b POLYMAT, University of the Basque Country UPV/EHU, Joxe Mari Korta Center, Avda. Tolosa 7, 20018 Donostia-San Sebastian, Spain

^c FRITCO2T Platform, University of Liege, Sart-Tilman B6a, 4000 Liege, Belgium

Table of Contents

1-	Materials and instrumentation	3
A-	Materials	3
B-	Instrumentation	3
2-	Poly(<i>oxo</i> -carbonate)s characterizations	5
3-	Poly(<i>oxo</i> -carbonate)s degradation	8
4-	Characterizations of bis(oxazolidone) with allyl functionality	9
5-	Polymerization experimental setup and optimization reactions	14
6-	Kinetic of the polymerization reaction for P2b	16
7-	NMR of polymers (Table 2, entry 1-5).....	18
8-	SEC analyses of hydrated polymers	20
9-	NMR characterizations of hydrated polymers (Table 2, entry 1-5)	24
10-	Solubility of all synthesized polymers.....	42
11-	TGA characterization of pure polymers	43
12-	Slow TGA characterization and derivative curves of pure polymers.....	45
13-	NMR spectra of dehydrated polymers.....	48
14-	SEC chromatogram of dehydrated polymers.....	63
15-	TGA of dehydrated samples	66
16-	DSC characterization of hydrated polymers.....	69
17-	DSC characterization of dehydrated polymers	72
18-	Mechanical test	75
19-	Chemical stability	76
20-	Structure characterizations of P2b-Sulfoxide (oxidation to sulfoxide)	79
21-	Structure characterizations of P2b-Sulfone (oxidation to sulfone)	85
22-	TGA characterization of post-modified polymers.....	92
23-	Structure characterizations of P2b-Sulfonium (S-alkylated).....	93
24-	DSC characterization of alkylated polymer.....	98
25-	References	99

1- Materials and instrumentation

A- Materials

1,4-Butanediol (97%), 1,8-Diazabicyclo[5.4.0]undec-7-ene (DBU, 99%), Allylamine (98%), 2,2'-(Ethylenedioxy)diethanethiol (95%), 1,4-Butanedithiol (97%), 2,2-Dimethoxy-2-phenyl acetophenone (DMPA, 99%), Hydrogen peroxide solution 30%, Iodomethane (99%), Diphenyldiselenid (98%), 1,4-Benzenedimethanethiol (98%) were purchased from Sigma Aldrich. Ethylene Glycol Bis(3-mercaptopropionate) (98%) was purchased from TCI. 1,6-Hexanedithiol (97%) was purchased from Thermo Scientific. The following were selected as mixtures of photoinitiators: a blend of 2-hydroxy-2-methylpropiophenone phenyl bis(2,4,6-trimethylbenzoyl)-phosphine oxide and ethylphenyl(2,4,6-trimethylbenzoyl) phosphinate (Omnirad 2022), a blend of ethyl phenyl(2,4,6-trimethylbenzoyl) phosphinate and phenyl bis(2,4,6-trimethylbenzoyl)-phosphineoxide (Omnirad 2100). All photoinitiators mixtures used were from IGM Resins (Netherlands). The structures of free radical photoinitiators–mixtures are presented in Scheme S1. All other chemicals and reagents were purchased from commercial sources and used as received.

4,4'-(ethane-1,2-diyl)bis(4-methyl-5-methylene-1,3-dioxolan-2-one) (Bis α CC) was synthesized as reported by our group [1].

Dialysis membrane Spectra/Por 7 (MWCO 1 kD) was purchased from Repligen.

B- Instrumentation

Nuclear Magnetic Resonance (NMR) Spectroscopy

All NMR analyses were performed using a Bruker 400 MHz spectrometer at 25 °C in the Fourier transform mode. 16 scans for ¹H spectra and 512 scans for ¹³C spectra were recorded.

Size exclusion chromatography (SEC)

Number-average molecular weight (M_n), weight-average molecular weight (M_w), and dispersity ($D = M_w/M_n$) of the polymers were assessed by using a size exclusion chromatography (SEC) with a polystyrene calibration in dimethylformamide (DMF) containing LiBr (0.025 M) at 55 °C (flow rate: 1 mL/min) with a Waters chromatograph equipped with three columns (PSS gram 1000Å (x2), 30 Å) and a precolumn, a dual absorbance detector (Waters 2487) and a refractive index detector (Waters 2414).

Thermogravimetric analysis (TGA)

TGA of the polymers were measured on TGA2 instrument from Mettler Toledo. To determine the mass loss of polymers, 4-7 mg of each sample were heated at 10 °C/min from 30 to 50 °C and flushed for 10 min at 50 °C and then heated at 20 °C/min until 600 °C under an N₂ atmosphere (20 mL/min). To assign the dehydration temperature, 4-7 mg of each sample were heated at 2 °C/min from 30 to 250 °C under N₂ atmosphere (20 ml/min).

Differential scanning calorimetry (DSC)

DSC of all samples was acquired using a DSC 250 (TA Instruments) with a liquid nitrogen cooling system and a N₂ sample flow rate of 50 mL/min. 3–5 mgs of each sample were loaded into aluminum pans, hermetically sealed, and run using a heat/cool/heat method. To determine the T_g of polymers with hydroxyoxazolidone linkages, samples were heated from 25 to 90 °C at a heating rate of 10 °C/min, cooled to –40 °C at a rate of 10 °C/min. The temperature modulated segment was set with an amplitude of 2 °C with a period of 60 seconds. Finally, the sample was heated again to 200 °C at a rate of 2 °C/min.

The final heating curve was used for thermal property evaluation. To assign the T_g for dehydrated polymers, samples were heated to 140 °C at a heating rate of 10 °C/min, cooled to -80 °C at a rate of 10 °C/min, and finally heated again to 160 °C at a rate of 10 °C/min.

Fourier Transform Infrared Spectra (F-TIR)

FTIR was performed using a Nicolet IS5 spectrometer (Thermo Fisher Scientific) equipped with a diamond attenuated transmission.

Tensile tests

Tensile tests were conducted at room temperature using an Instron 34TM-10 equipped with a load cell of 500 N at a speed of 5 mm.min⁻¹. Measurements were repeated 5 times on dogbone-shaped samples (ASTM-D638-V) with a thickness of around 0.15 mm. The samples were prepared by compression molding and were cut at room temperature using a Qualitest die cutter.

Compression molding

Polymer samples were cut into little pieces and pressed between Teflon sheets over steel plates in a Carver press. **P2a** was pressed at a temperature of 70 °C for 3x15 min under a pressure of 6 ton metric. The process was achieved in three steps to correctly eliminate air bubbles trapped in the polymer film. **P2a-dehydrated** was pressed at 50 °C for 15 min under a pressure of 6 ton metric. The steel plates were then removed from the hot press and cooled rapidly in a press at room-temperature.

2- Poly(*oxo*-carbonate)s characterizations

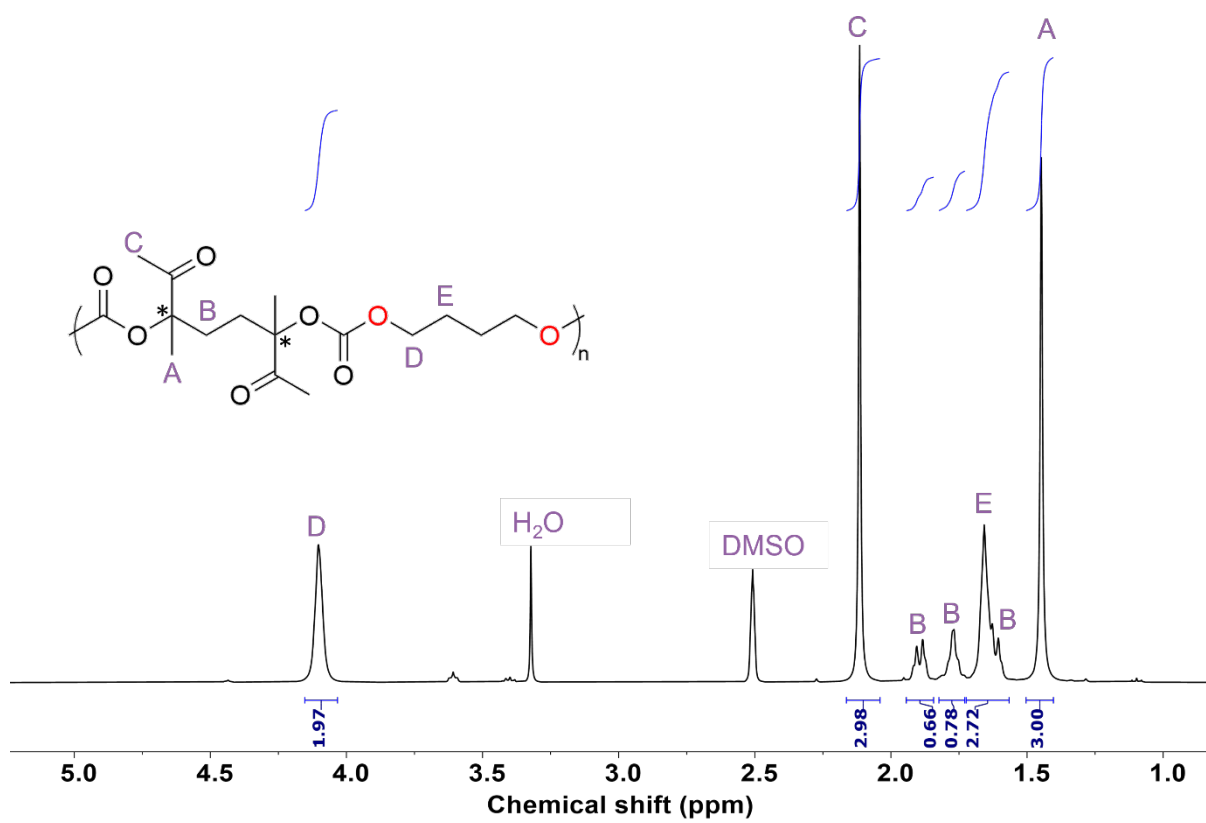


Figure S1. ¹H-NMR spectrum of pure PC (400 MHz, DMSO-*d*₆).

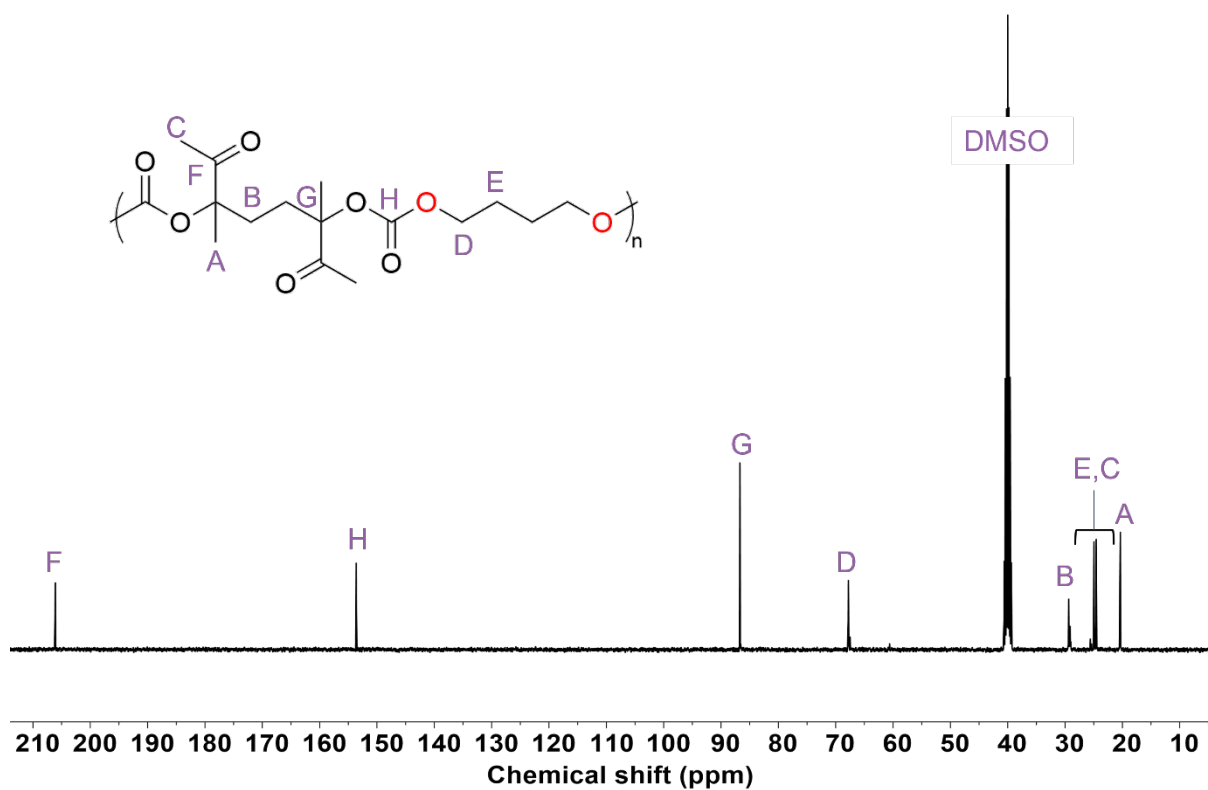


Figure S2. ^{13}C -NMR spectrum of pure PC (100 MHz, $\text{DMSO-}d_6$).

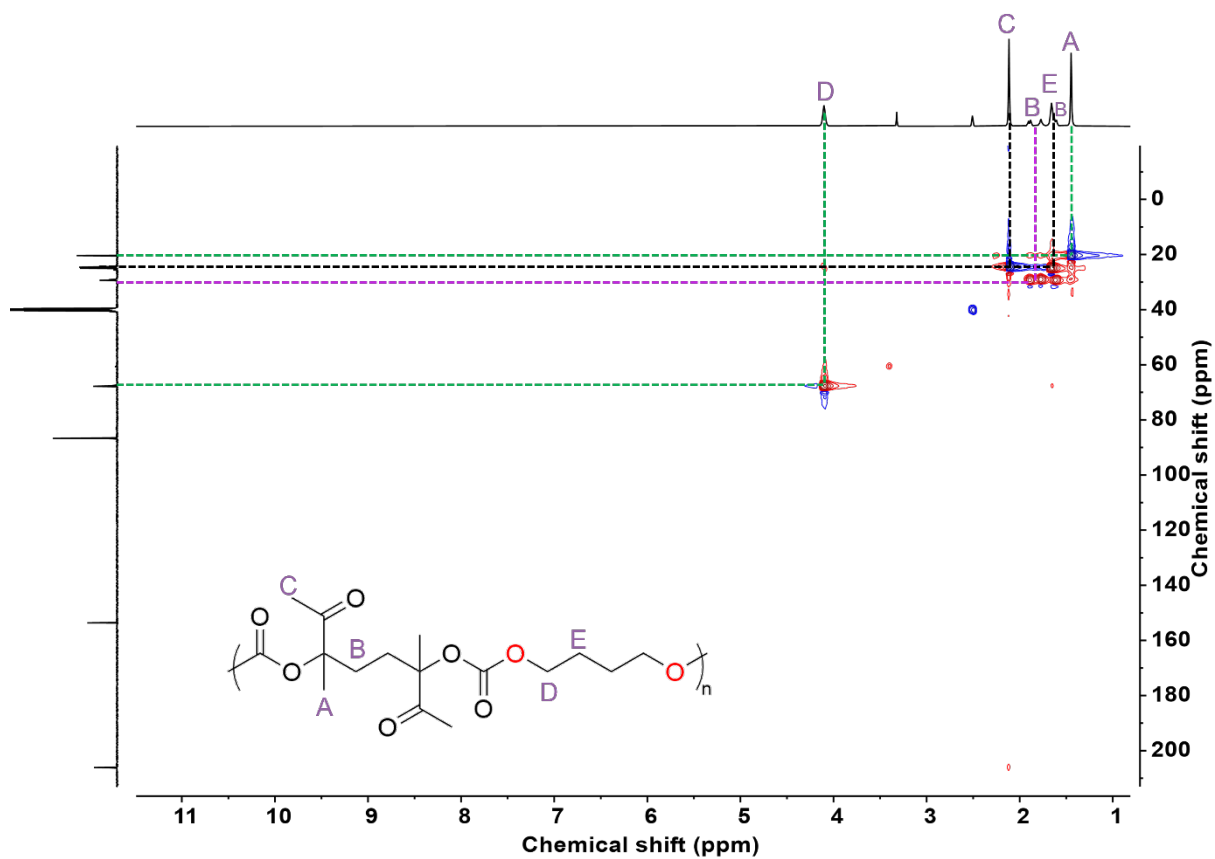


Figure S3. ^1H - ^{13}C HSQC NMR spectrum of pure PC (400 MHz, $\text{DMSO-}d_6$).

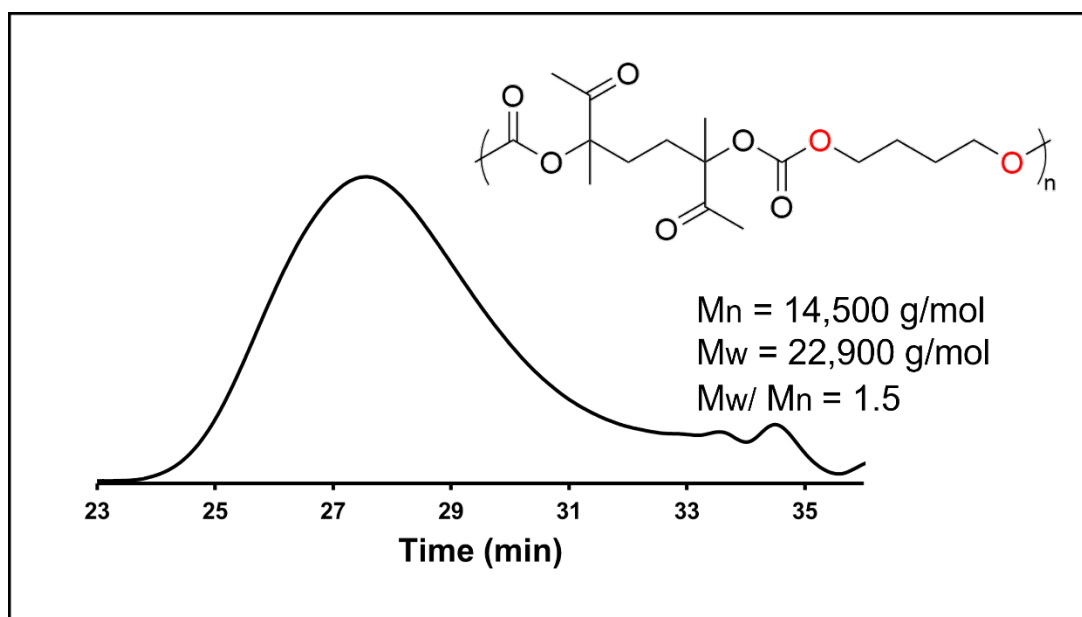


Figure S4. SEC chromatogram of poly(*oxo*-carbonate) PC (in DMF/LiBr).

4- Characterizations of bis(oxazolidone) with allyl functionality

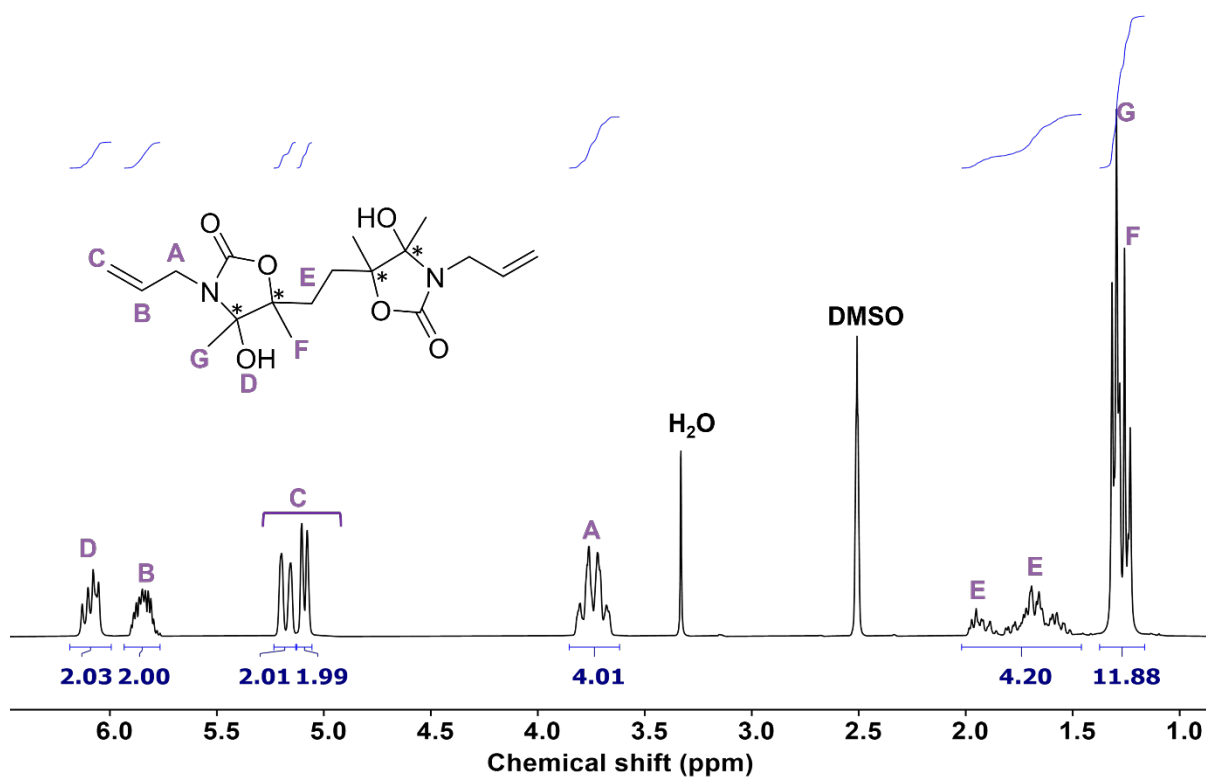


Figure S7. ¹H-NMR spectrum of monomer 1 (400 MHz, DMSO-*d*₆).

¹H NMR (400 MHz, DMSO-*d*₆): $\delta = 6.09$ ppm (m, 2H), $\delta = 5.84$ ppm (m, 2H), $\delta = 5.18$ (m, 2H), $\delta = 5.09$ (m, 2H), $\delta = 3.73$ (m, 4H), $\delta = 1.49$ - 2.01 (m, 4H), $\delta = 1.16$ - 1.37 (m, 12H).

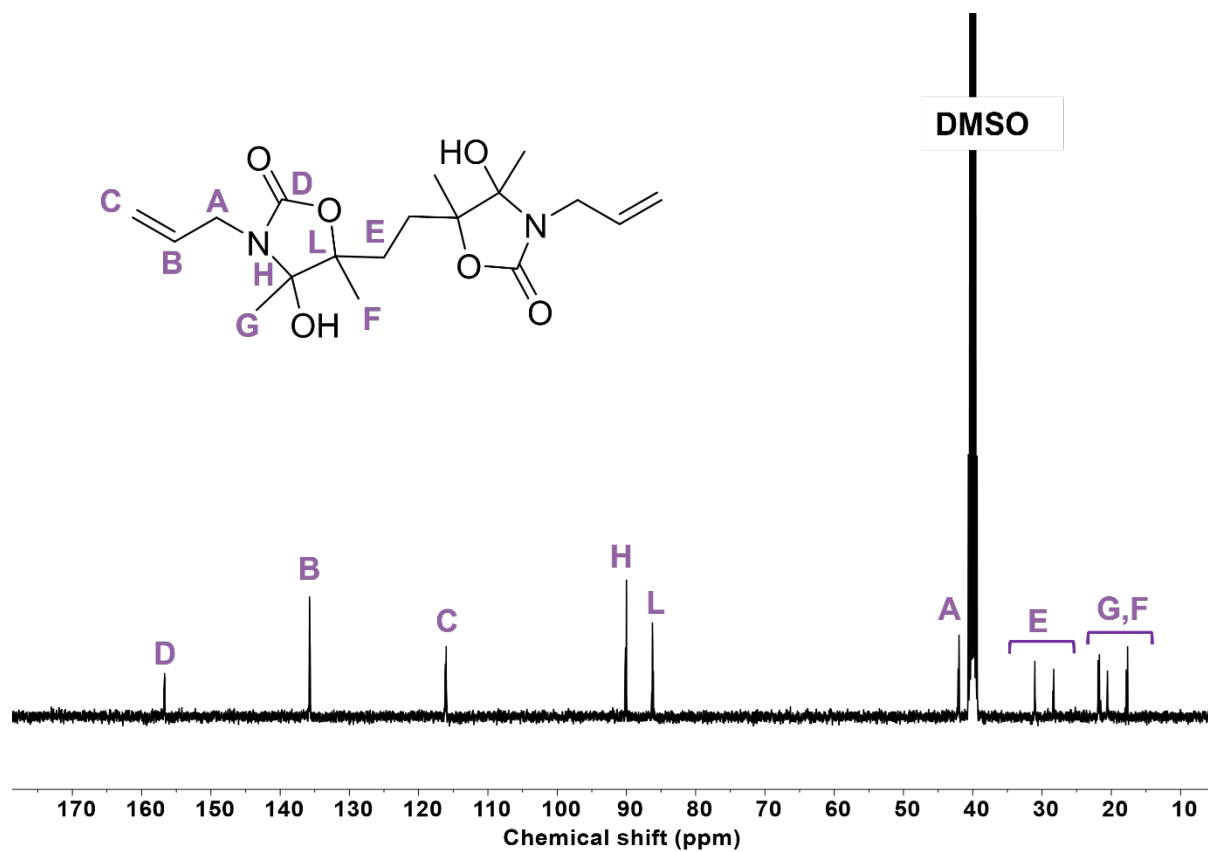


Figure S8. ^{13}C -NMR spectrum of monomer **1** (100 MHz, $\text{DMSO-}d_6$).

^{13}C NMR (100 MHz, $\text{DMSO-}d_6$): $\delta = 156.7$ ppm, $\delta = 135.7$ ppm, $\delta = 116.1$ ppm, $\delta = 90.1$ ppm, $\delta = 86.2$ ppm, $\delta = 42.1$ ppm, $\delta = 31.03$ ppm, $\delta = 28.3$ ppm, $\delta = 21.8$ ppm, $\delta = 20.6$ ppm, $\delta = 17.7$ ppm.

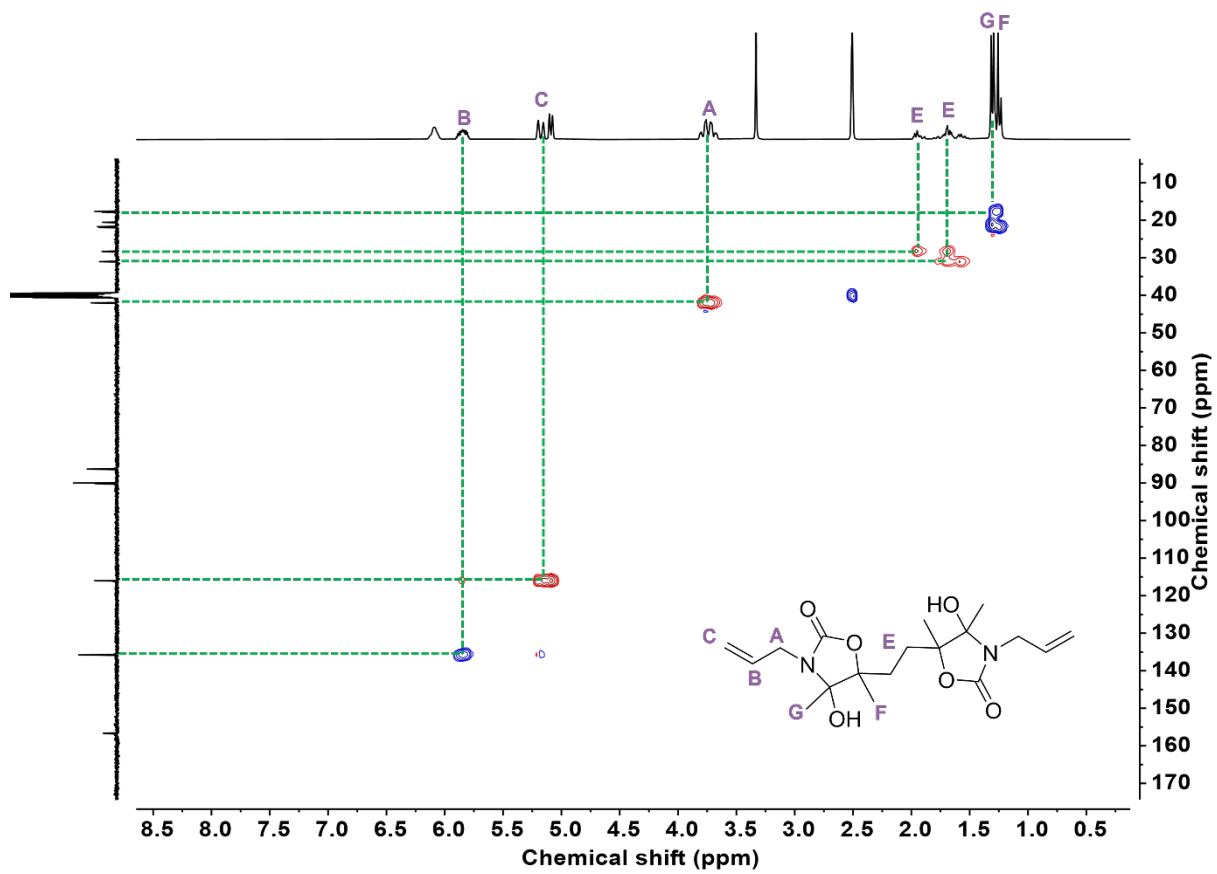


Figure S9. ^1H - ^{13}C HSQC NMR spectrum of monomer 1 (400 MHz, $\text{DMSO-}d_6$).

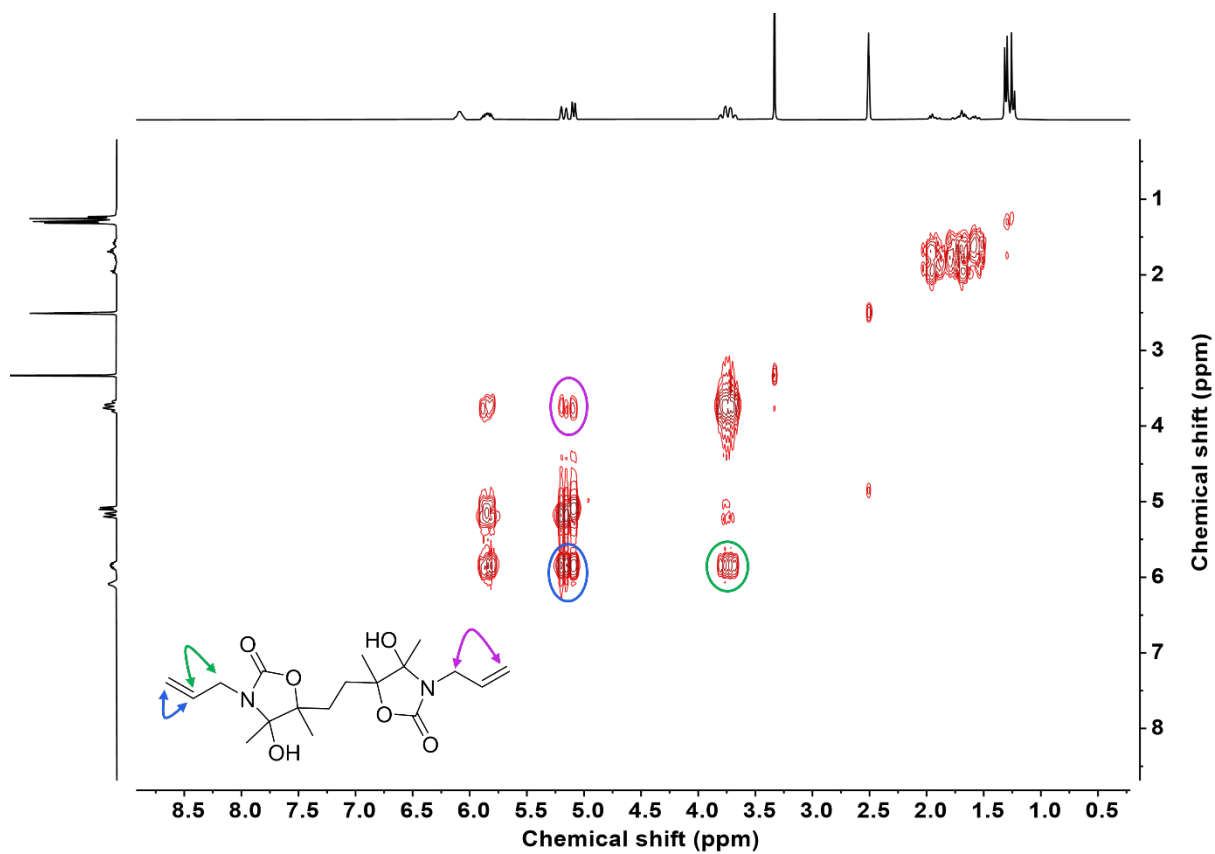


Figure S10. COSY NMR spectrum of monomer **1** (400 MHz, DMSO-*d*₆).

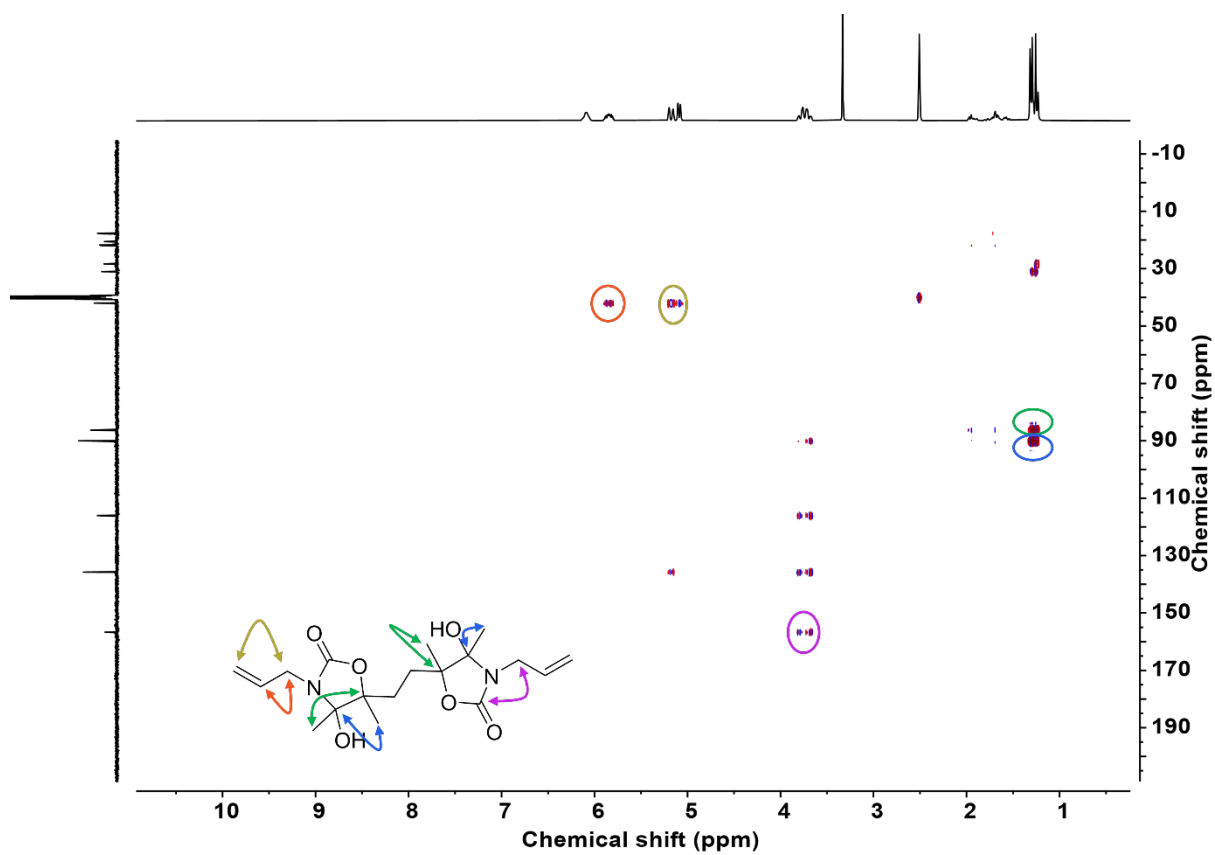


Figure S11. HMBC NMR spectrum of monomer **1** (400 MHz, DMSO-*d*₆).

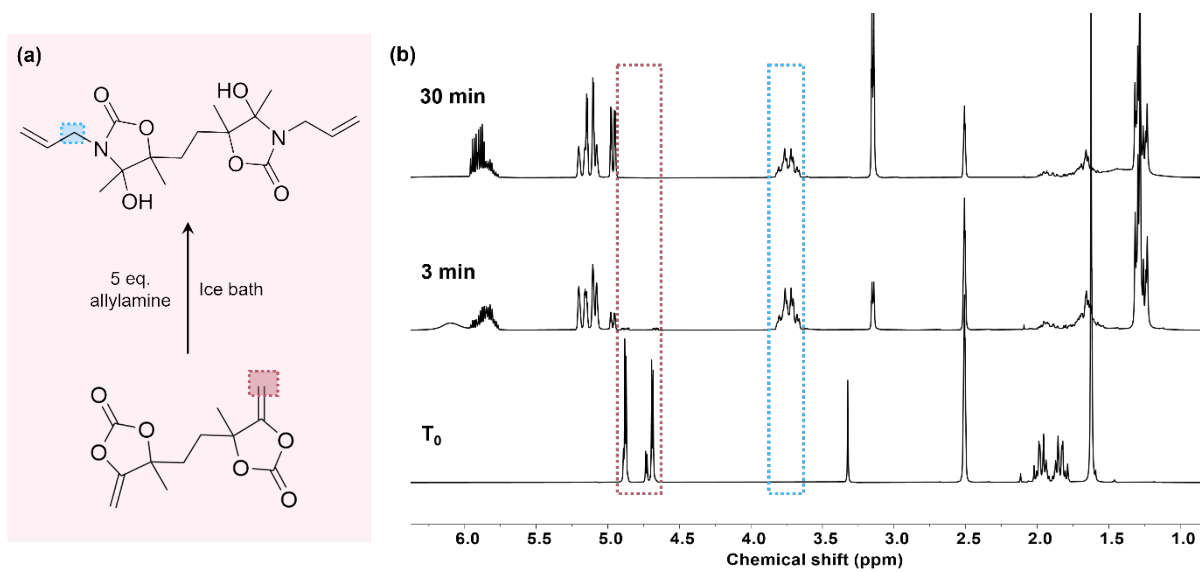


Figure S12. (a) The reaction between Bis α CC and allylamine; (b) Kinetics of the reaction monitored by ^1H -NMR (400 MHz, $\text{DMSO-}d_6$), T_0 represents the time before addition of allylamine.

5- Polymerization experimental setup and optimization reactions

The reaction setup is displayed in Figure S13. However, as our setup does not include a temperature regulation system, we verified that the UV lamp did not generate too much heat during a reaction. We therefore monitored the reaction over 24h using a temperature probe. As shown in Figure S14, the temperature was measured to be of 23 °C over all the course of the experiment.



Figure S13. Photopolymerization setup using Omnicure series 2000, 200 W.



Figure S14. Photopolymerization apparatus, featuring an Omnicure series 2000, 200 W system integrated with a thermostat unit, (a) at the beginning ; (b) after 24 h of reaction

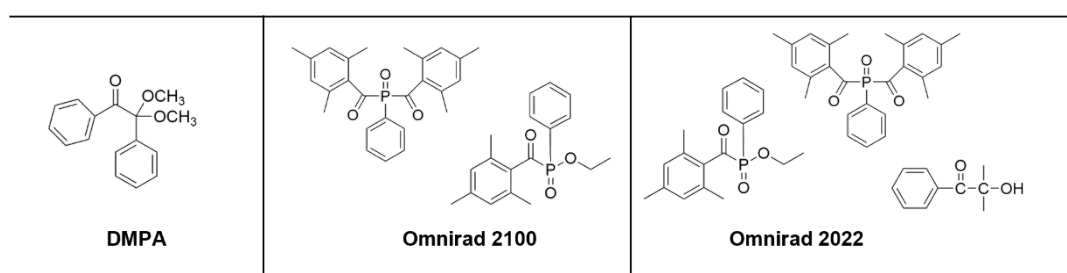
Optimization of the reaction conditions

To a glass vial, monomer **1** (400 mg, 1.08 mmol, 1 equiv) and 2,2'-(Ethylenedioxy)diethanethiol (**2a**, 1.08 mmol, 1 equiv) were added followed by the addition of the initiator (5 mol% vs monomer **1**, 0.054 mmol, (13.9 mg for DMPA, 17.08 mg for Omnirad 2100, 22.5 mg for Omnirad 2022, see Scheme S1

for the structure of initiators). Then a specific amount of solvent was added to control the concentration of the mixture. The reaction mixture was then stirred under irradiation for 24 h. After that, a small amount of the crude product was withdrawn for $^1\text{H-NMR}$ characterization to determine the monomer conversion and SEC analysis to investigate the relative molar mass of the polymers.

The conversion of monomer **1** was determined by comparison of the relative intensities of the peaks corresponding to allyl protons at 5.13 ppm of the monomer **1** and the methylene group of oxazolidones (N-CH_2) at $\delta = 3.16$ ppm of the produced polymer according to the equation:

$$\text{Conv.} = 1 - \frac{I(5.13)/2}{\frac{I(5.13)}{2} + \frac{I(3.16)}{2}} \quad (\text{Eq.S1})$$



Scheme S1. Structure of the free-radical photoinitiators.

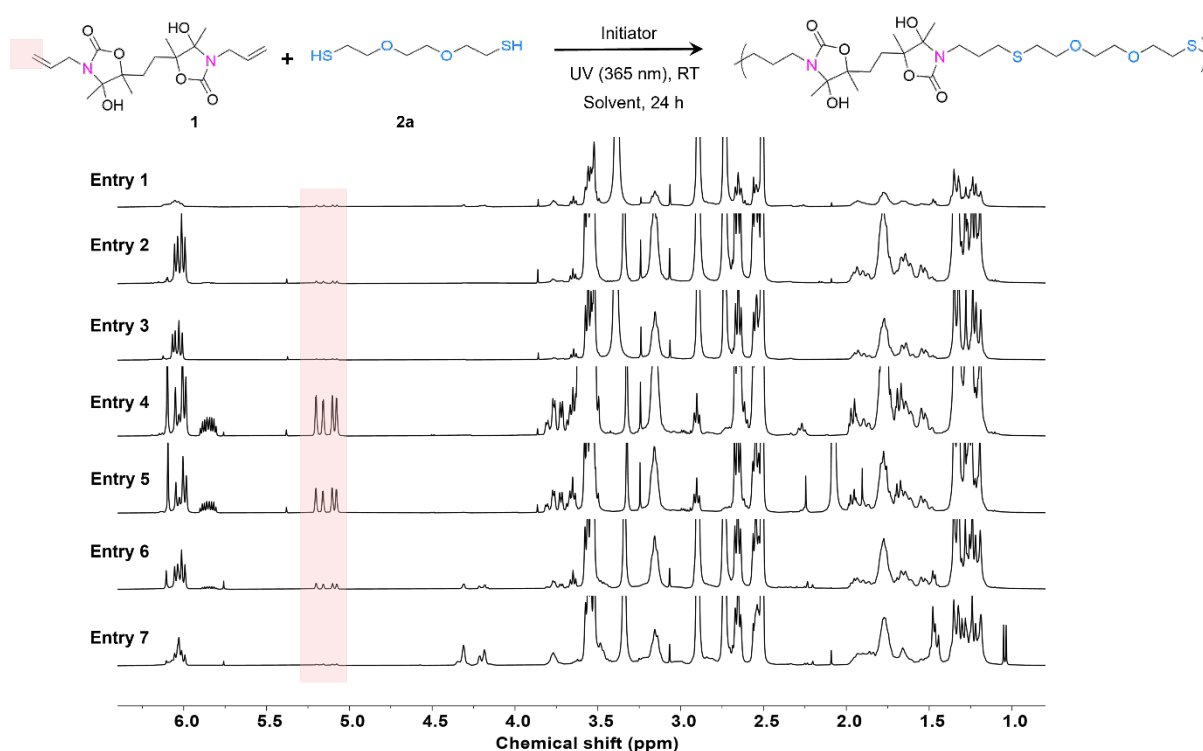


Figure S15. Thiol-ene photopolymerization of monomer **1** and dithiol **2a**; $^1\text{H-NMR}$ spectrum of crude products of each optimization reaction (400 MHz, $\text{DMSO-}d_6$). Results are summarized in Table 1.

6- Kinetic of the polymerization reaction for P2b

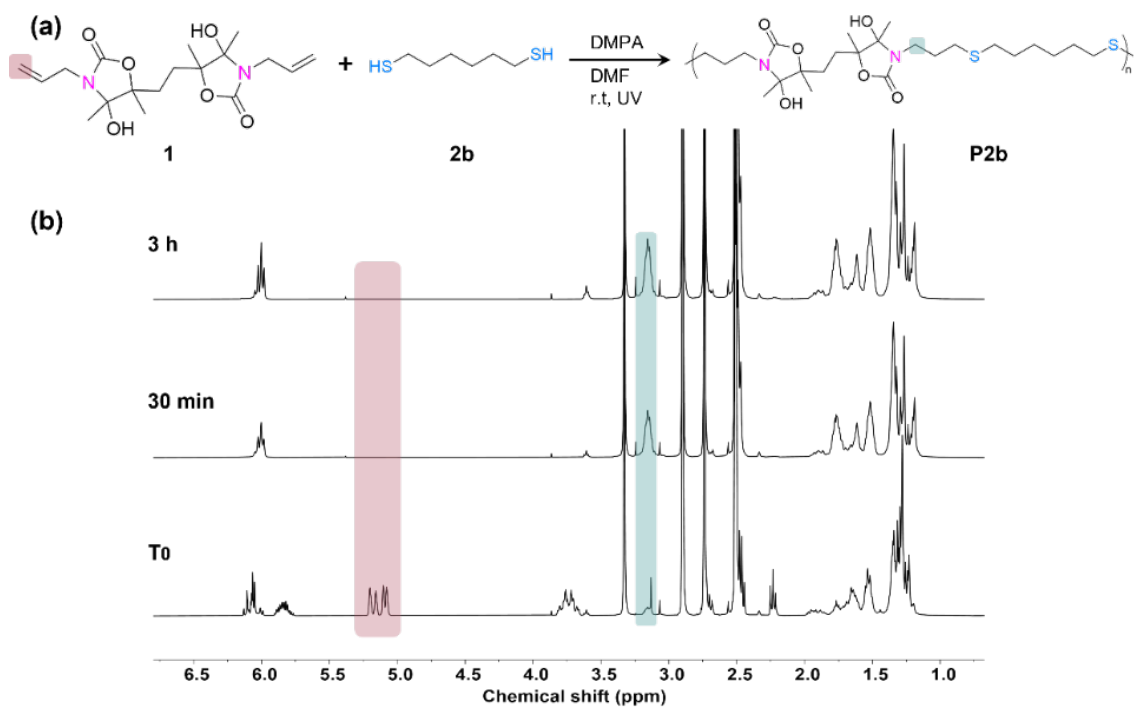


Figure S16. (a) Scheme of photopolymerization reaction between monomer **1** and dithiol **2b**; (b) ¹H-NMR spectroscopy of photopolymerization of **1** and **2b** along time (400 MHz, DMSO-*d*₆).

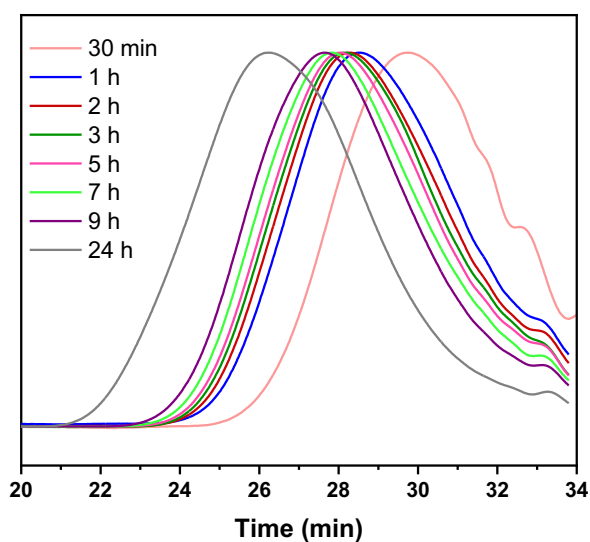


Figure S17. SEC chromatograms along time for thiol-ene polymerization of **1** and **2b** (in DMF/LiBr).

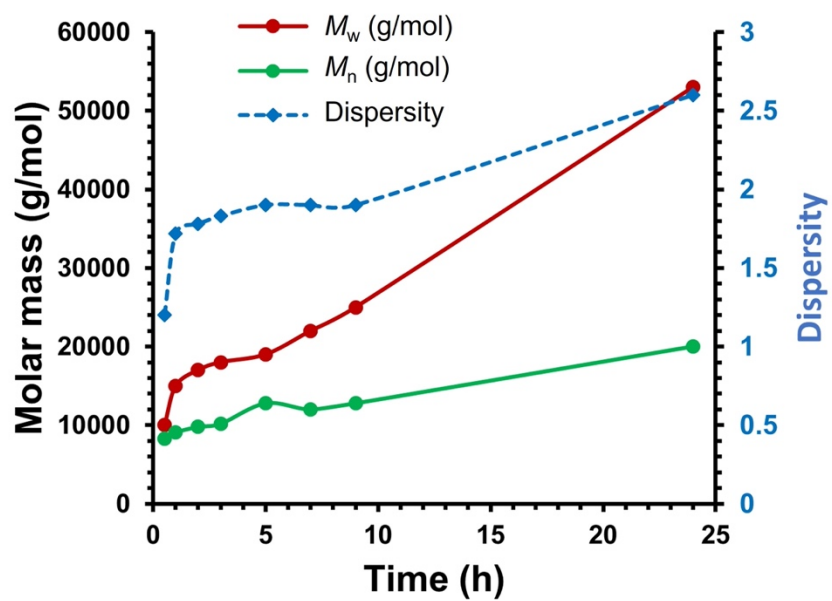


Figure S18. M_w and dispersity evolution for thiol-ene polymerization of **1** and **2b** along time using SEC (in DMF/LiBr).

7- NMR of polymers (Table 2, entry 1-5)

For **P2a**, the conversion of monomer **1** was determined by comparison of the integrals of the peaks corresponding to allyl protons at 5.13 ppm of **1** and the oxazolidone linkages (N-CH₂, δ = 3.15 ppm) of the produced polymer according to the equation:

$$Conv. = 1 - \left(\frac{I(5.13)/2}{I(5.13) + I(3.15)/2} \right) \quad (\text{Eq.S2})$$

For **P2b**, the conversion of monomer **1** was determined by comparison of the integrals of the peaks corresponding to allyl protons at 5.13 ppm of **1** and the oxazolidone linkages (N-CH₂, δ = 3.16 ppm) of the produced polymer according to the equation:

$$Conv. = 1 - \left(\frac{I(5.13)/2}{I(5.13) + I(3.16)/2} \right) \quad (\text{Eq.S3})$$

For **P2c**, the conversion of monomer **1** was determined by comparison of the integrals of the peaks corresponding to allyl protons at 5.13 ppm of **1** and the ester moiety (O-CH₂, δ = 4.25 ppm) of the produced polymer according to the equation:

$$Conv. = 1 - \left(\frac{I(5.13)/2}{I(5.13) + I(4.25)/2} \right) \quad (\text{Eq.S4})$$

For **P2d**, the conversion of monomer **1** was determined by comparison of the integrals of the peaks corresponding to allyl protons at 5.13 ppm of **1** and the the oxazolidone linkages (N-CH₂, δ = 3.15 ppm) of the produced polymer according to the equation:

$$Conv. = 1 - \left(\frac{I(5.13)/2}{I(5.13) + I(3.15)/2} \right) \quad (\text{Eq.S5})$$

For **P2e**, the conversion of monomer **1** was determined by comparison of the integrals of the peaks corresponding to allyl protons at 5.13 ppm of **1** and thioether bond (CH₂-S, δ = 2.41 ppm) of the produced polymer according to the equation:

$$Conv. = 1 - \left(\frac{I(5.13)/2}{I(5.13) + I(2.41)/2} \right) \quad (\text{Eq.S6})$$

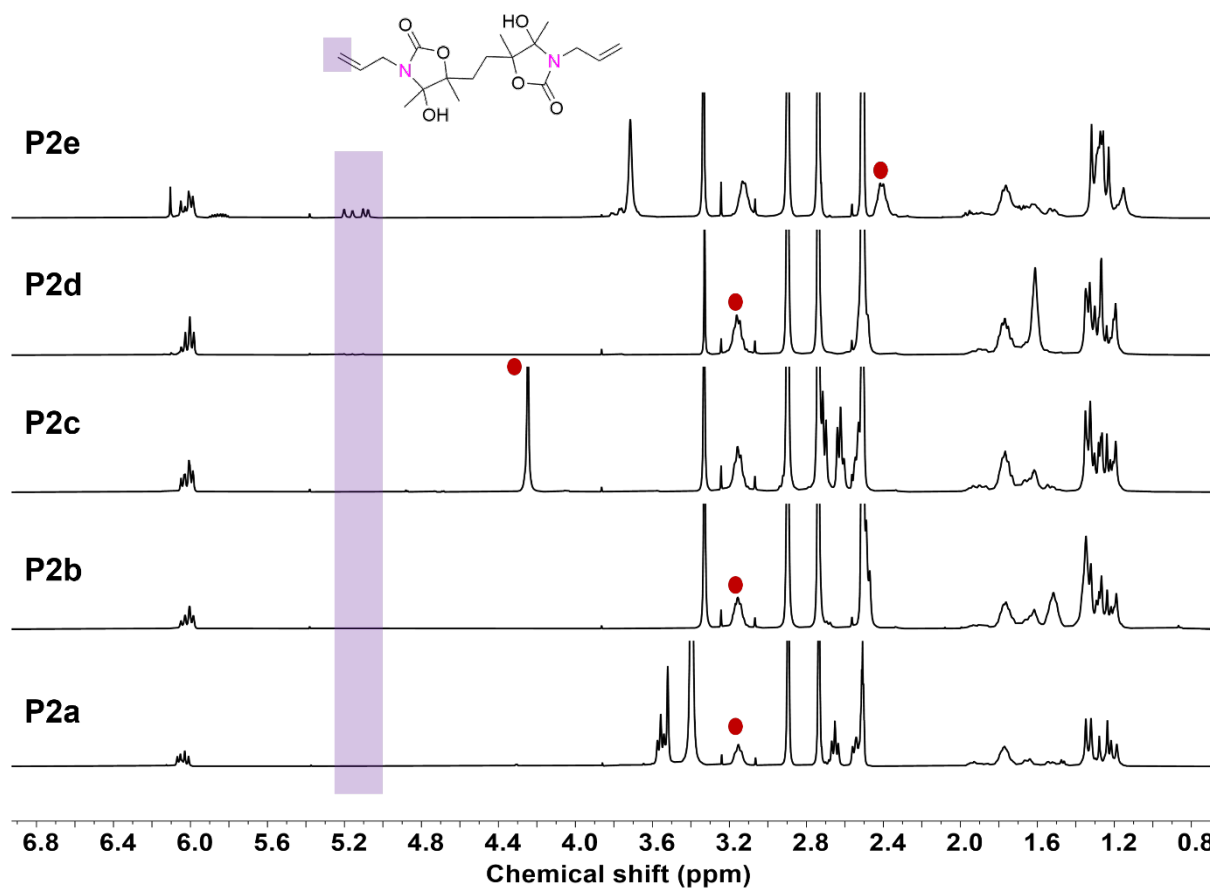


Figure S19. ¹H-NMR spectrum of crude hydrated polymers (400 MHz, DMSO-*d*₆).

8- SEC analyses of hydrated polymers

Table S1. Molecular characteristics of crude and pure copolymers

Entry	Polymer	Crude polymers			Pure polymers		
		M_n^a (g/mol)	M_w^a (g/mol)	Dispersity ^a	M_n^b (g/mol)	M_w^b (g/mol)	Dispersity ^b
1	P2a	27,000	116,000	4.2	31,000	101,000	3.2
2	P2b	19,000	71,000	3.7	20,000	57,000	2.7
3	P2c	18,000	54,000	2.9	21,000	64,000	3
4	P2d	22,000	55,000	2.5	23,000	69,000	3
5	P2e	7,000	19,000	2.7	8,000	20,000	2.5

^aDetermined on crude polymers, ^bDetermined on pure polymers by SEC in DMF/LiBr calibrated with PS standards

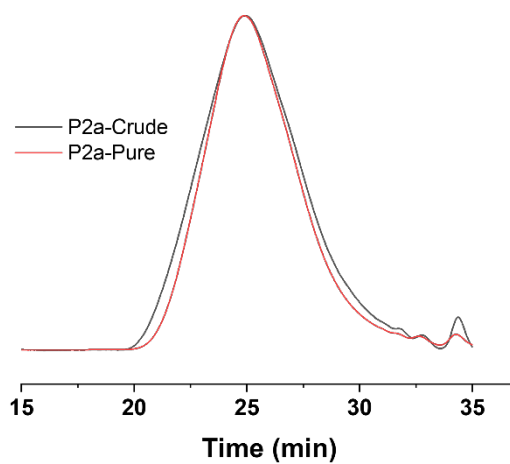


Figure S20. SEC chromatogram, overlay of crude and pure **P2a** (in DMF/LiBr).

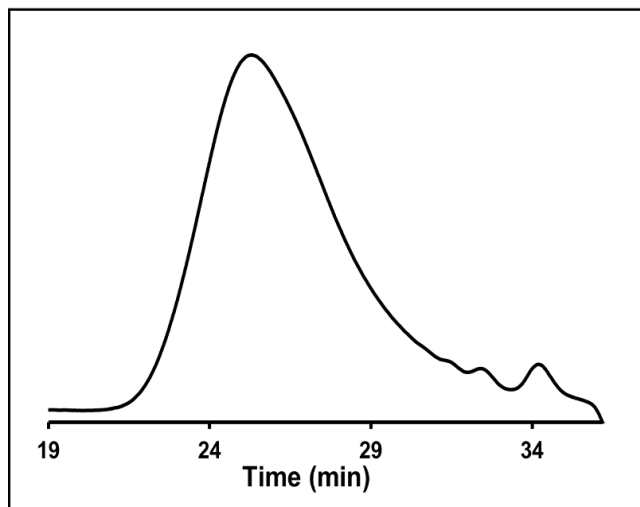
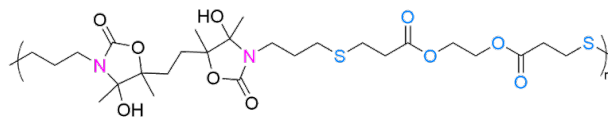


Figure S23. SEC chromatogram of purified **P2c** (in DMF/LiBr).

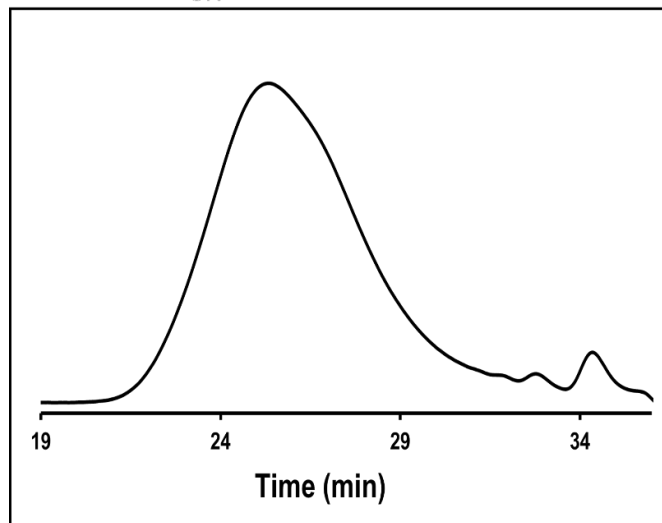
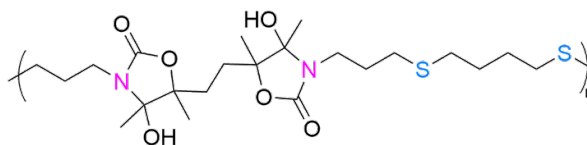


Figure S24. SEC chromatogram of purified **P2d** (in DMF/LiBr).

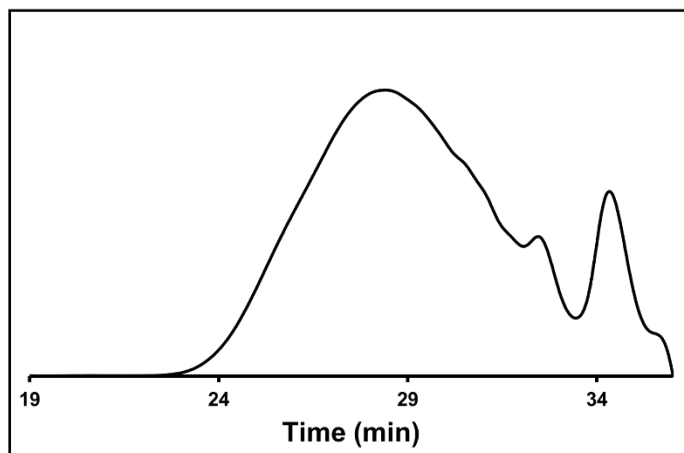
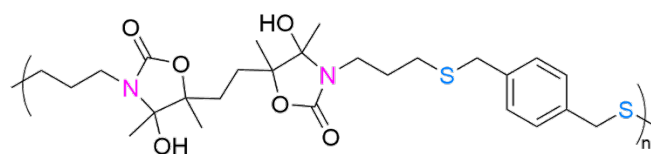


Figure S25. SEC chromatogram of purified **P2e** (in DMF/LiBr).

9- NMR characterizations of hydrated polymers (Table 2, entry 1-5)

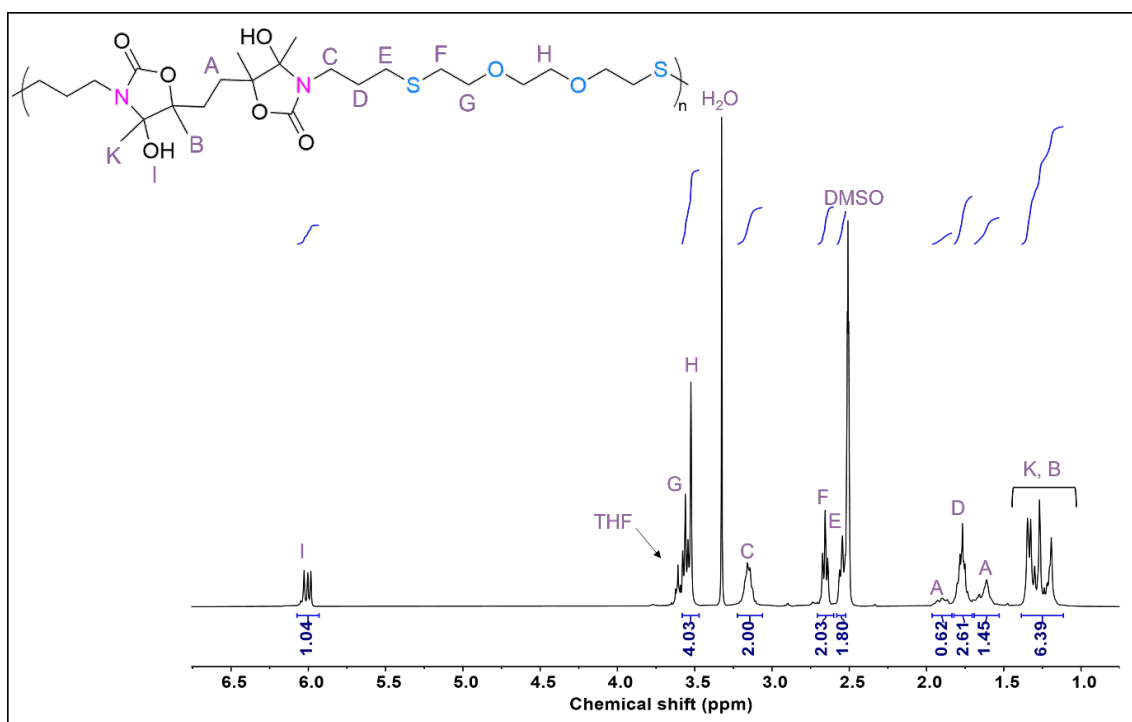


Figure S26. ¹H-NMR spectrum of purified P2a (400 MHz, DMSO-*d*₆).

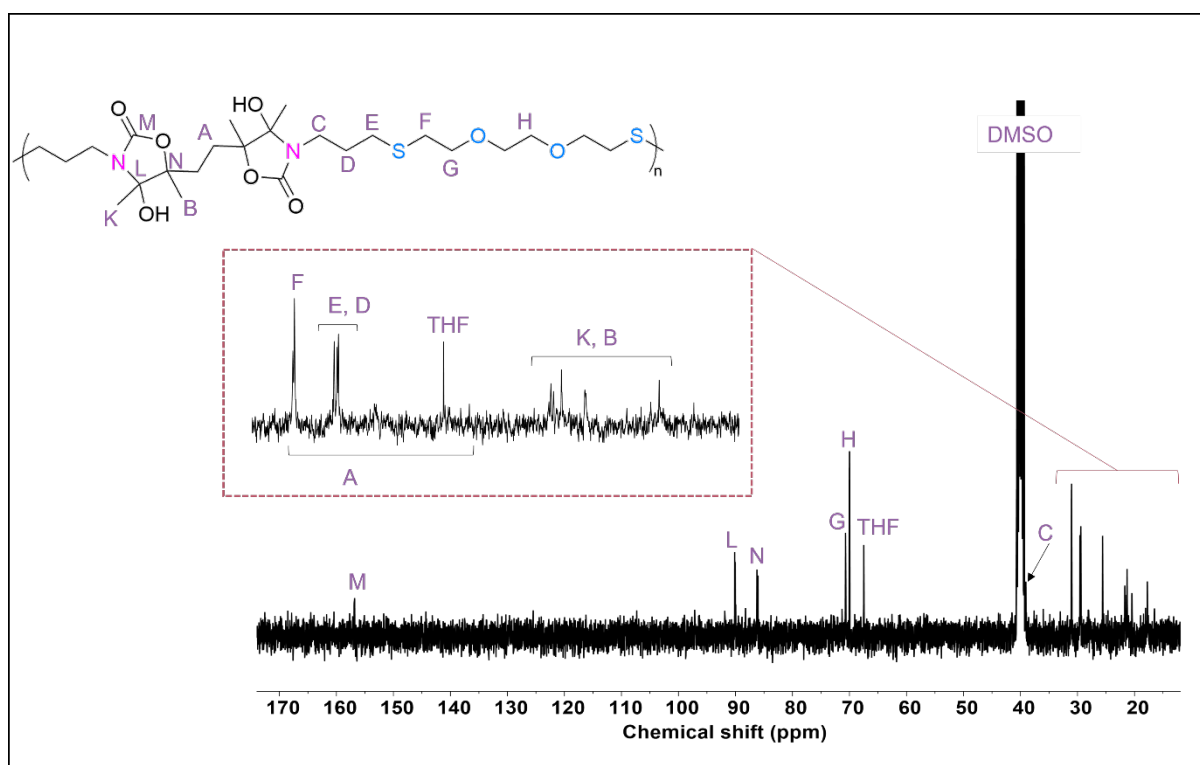


Figure S27. ¹³C-NMR spectrum of purified P2a (100 MHz, DMSO-*d*₆).

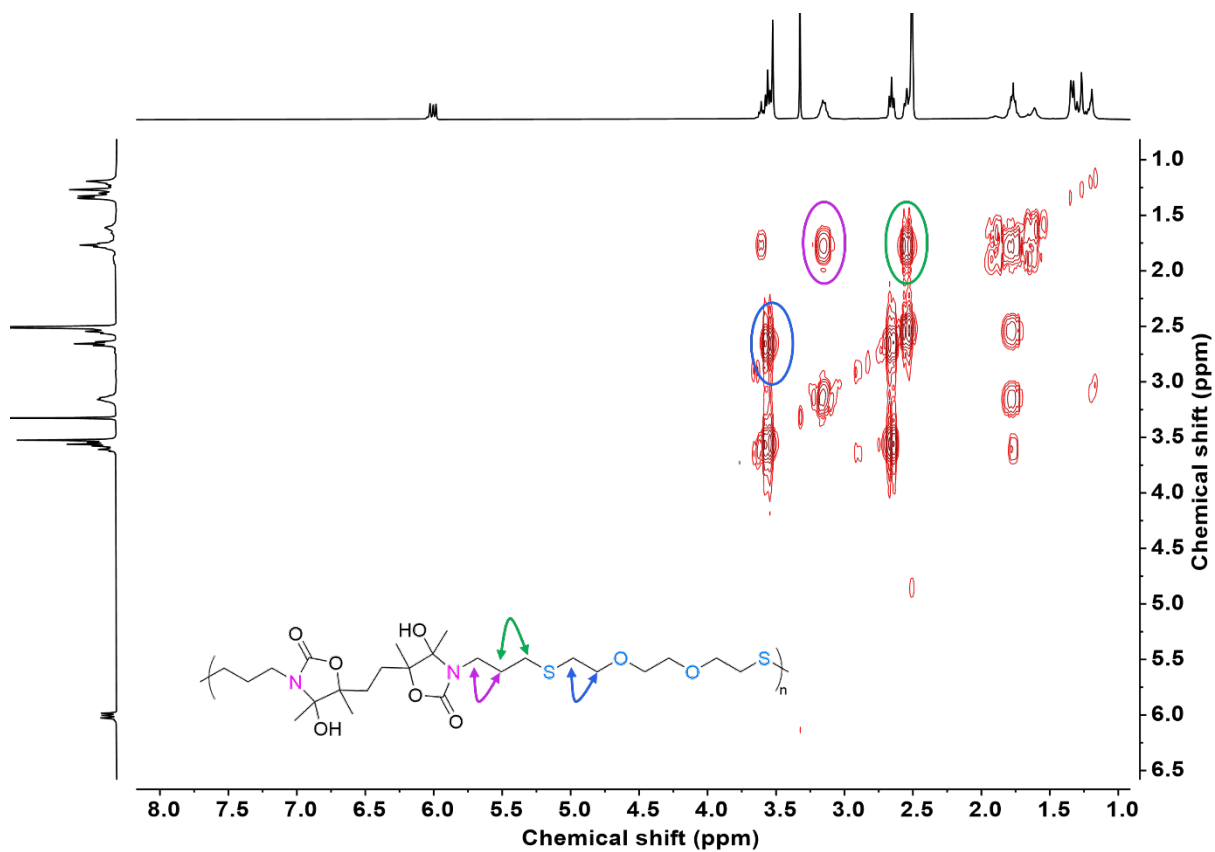


Figure S28. COSY NMR spectrum of purified **P2a** (400 MHz, DMSO- d_6).

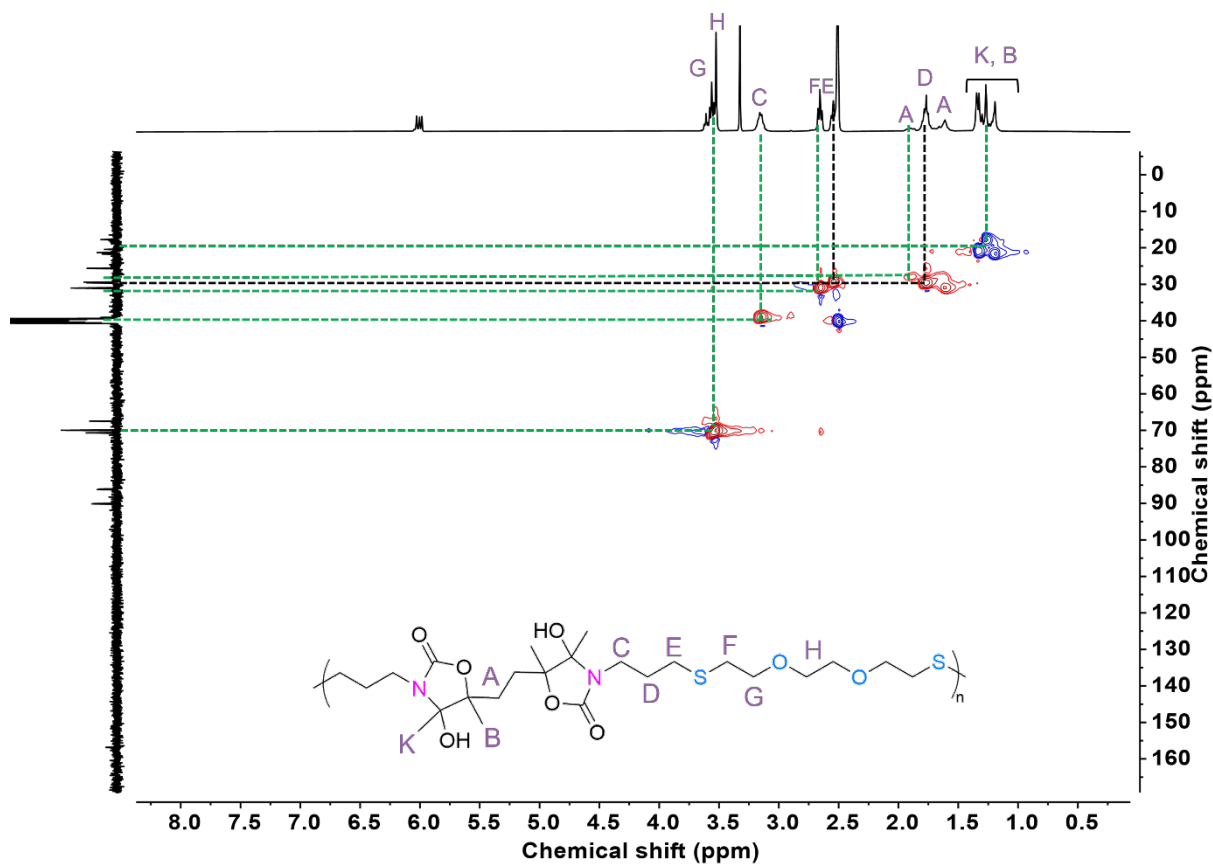


Figure S29. ^1H - ^{13}C HSQC NMR spectrum of purified **P2a** (400 MHz, DMSO- d_6).

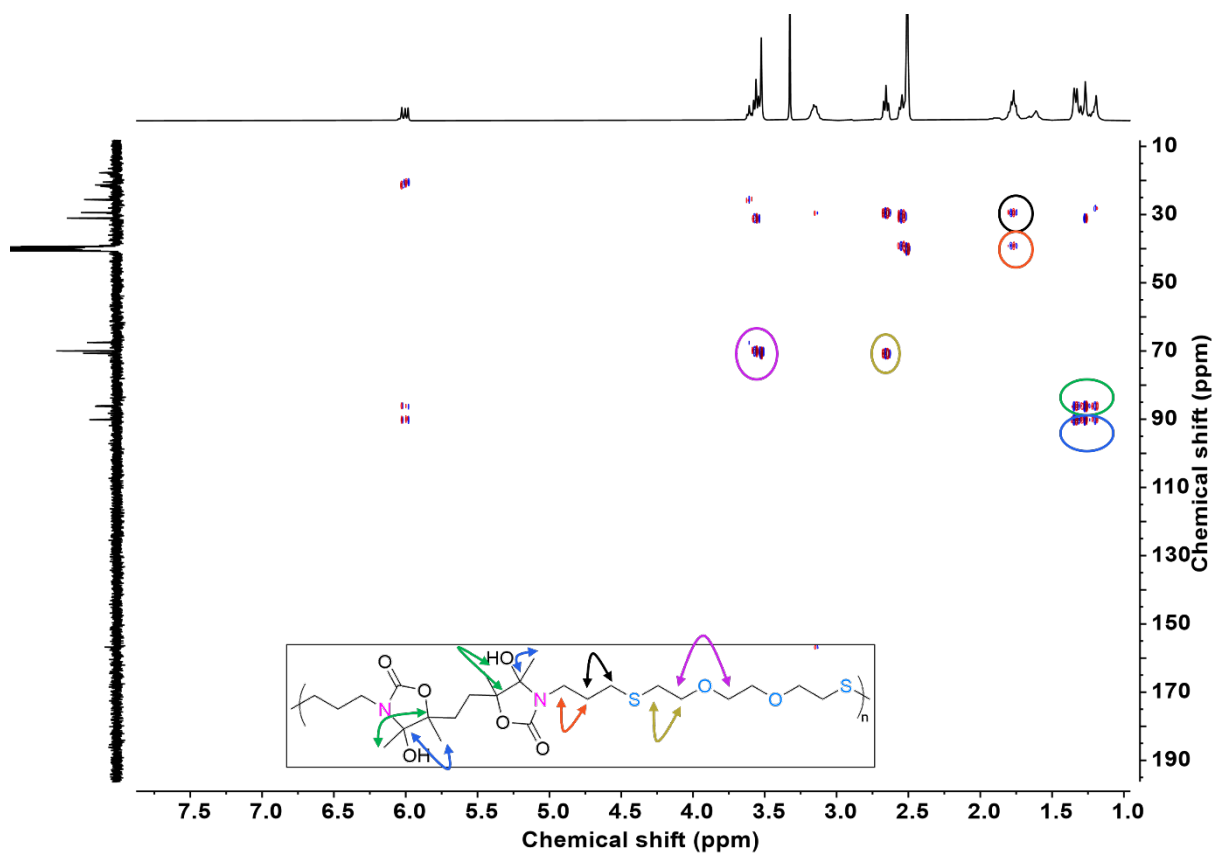


Figure S30. HMBC NMR spectrum of purified P2a (400 MHz, DMSO- d_6).

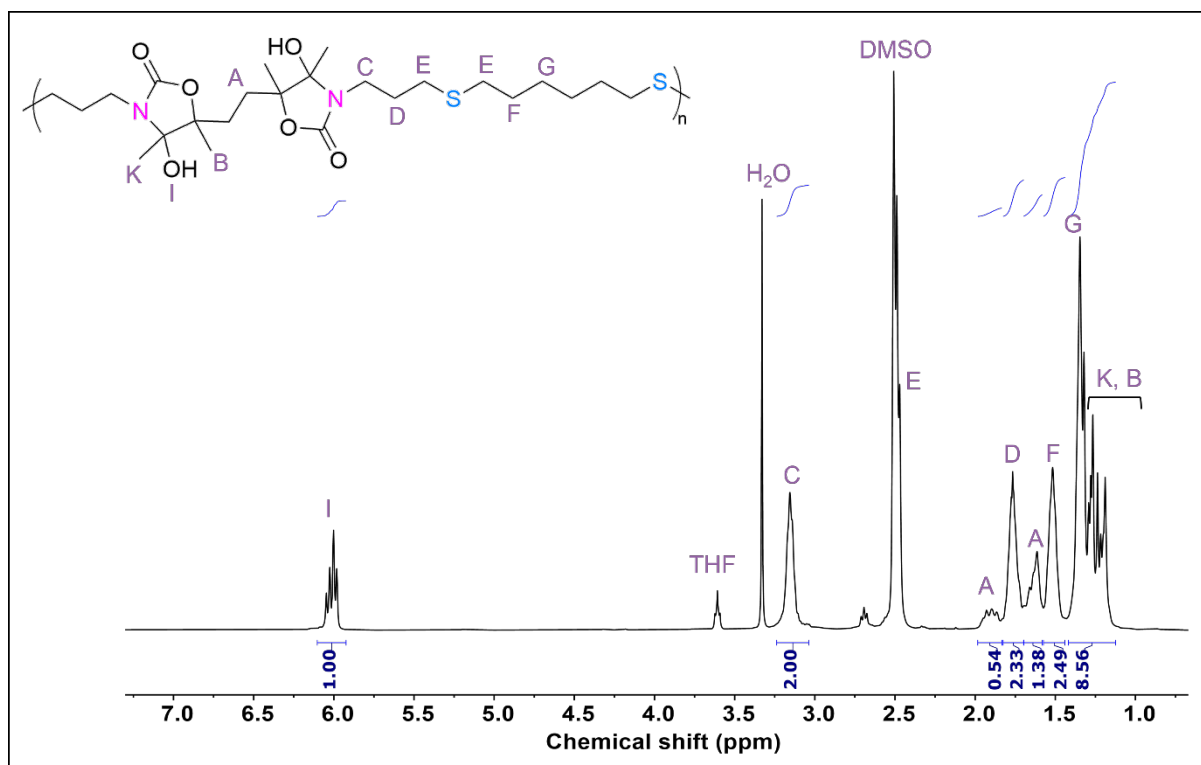


Figure S31. $^1\text{H-NMR}$ spectrum of purified **P2b** (400 MHz, $\text{DMSO-}d_6$).

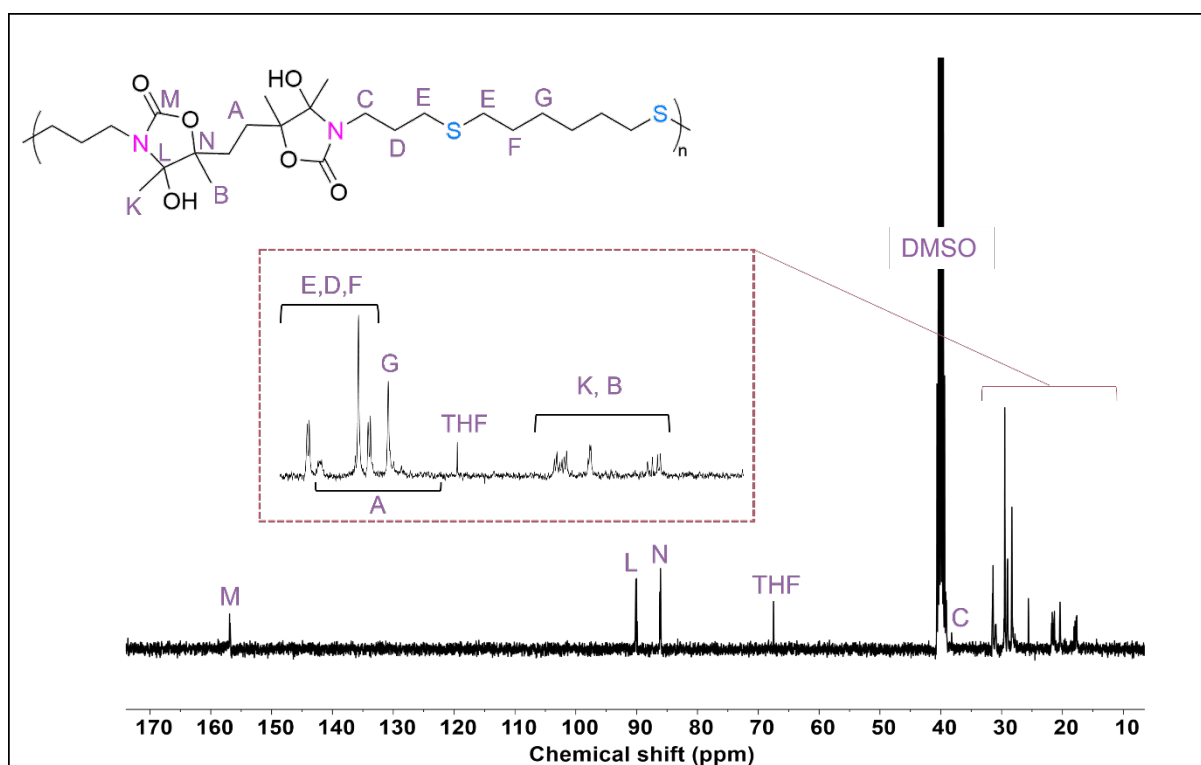


Figure S32. $^{13}\text{C-NMR}$ spectrum of purified **P2b** (100 MHz, $\text{DMSO-}d_6$).

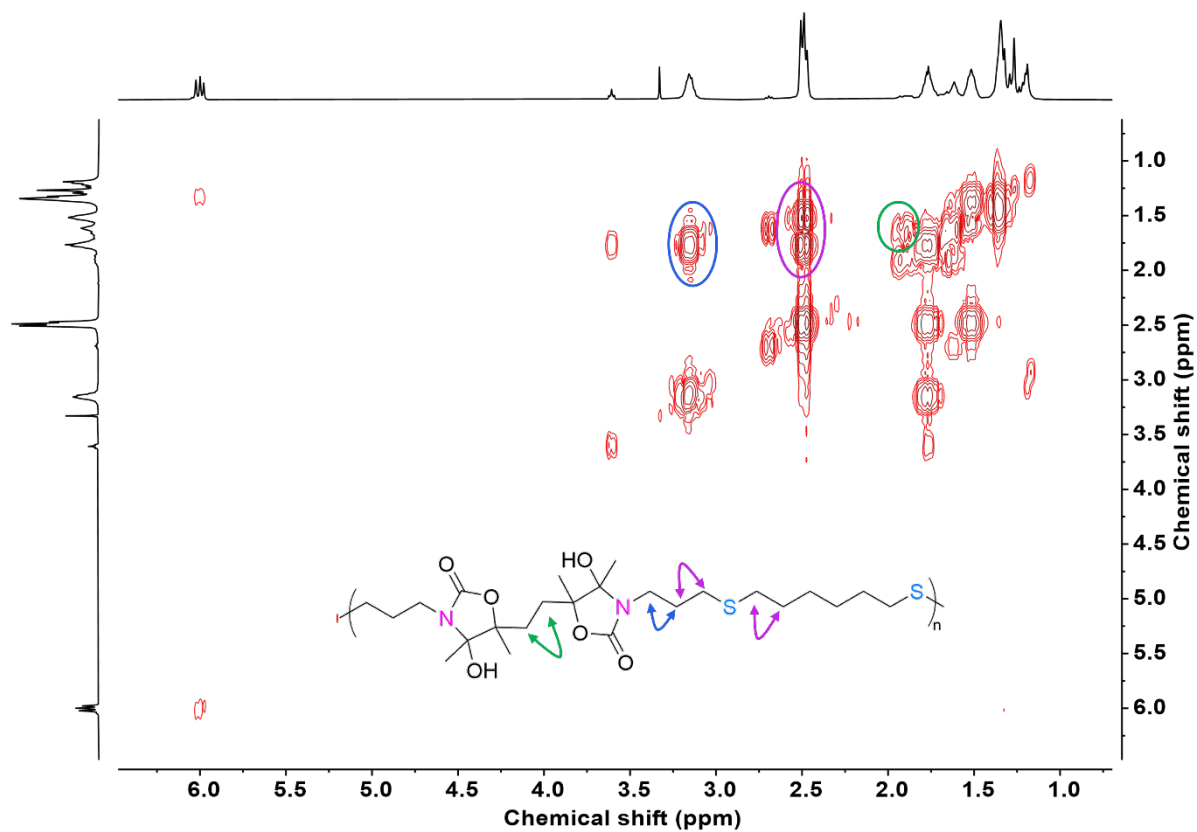


Figure S33. COSY NMR spectrum of purified **P2b** (400 MHz, DMSO- d_6).

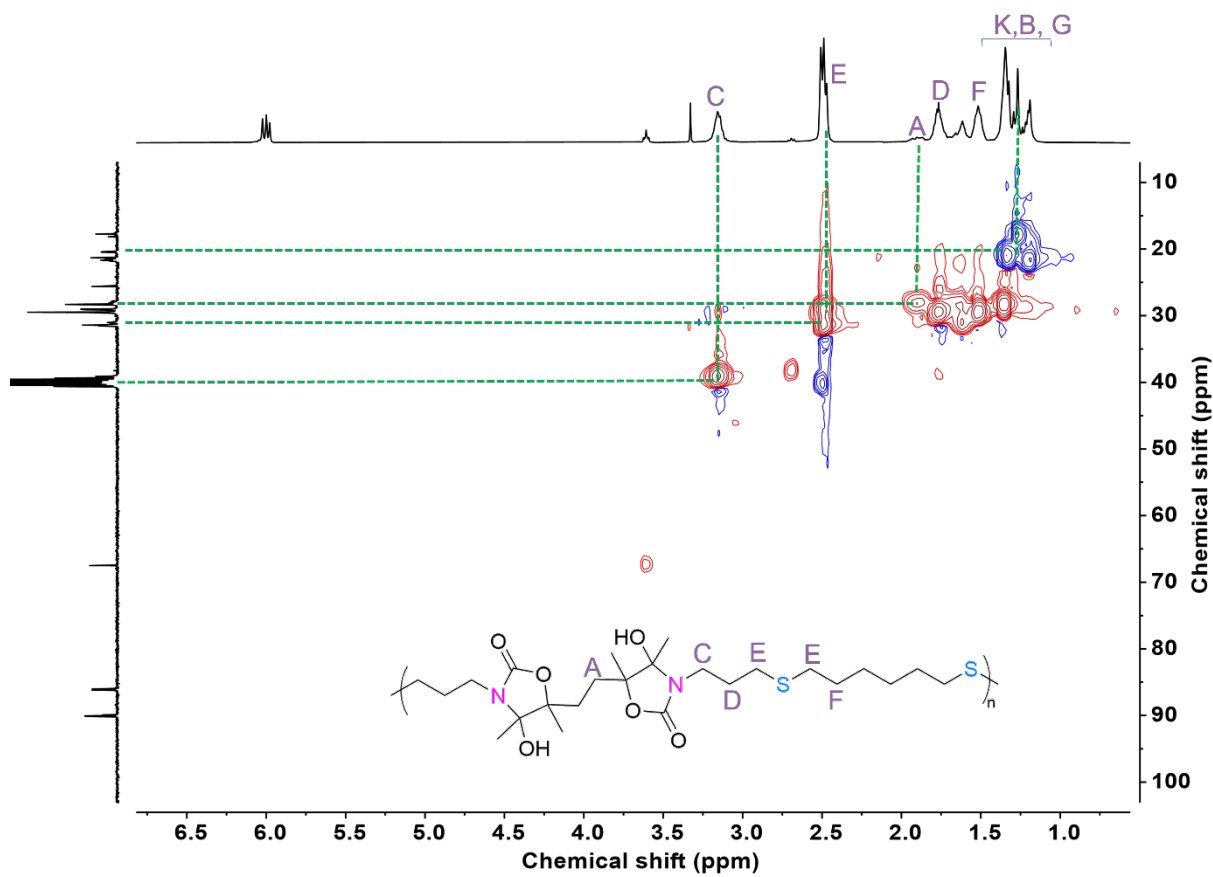


Figure S34. ^1H - ^{13}C HSQC NMR spectrum of purified **P2b** (400 MHz, $\text{DMSO-}d_6$).

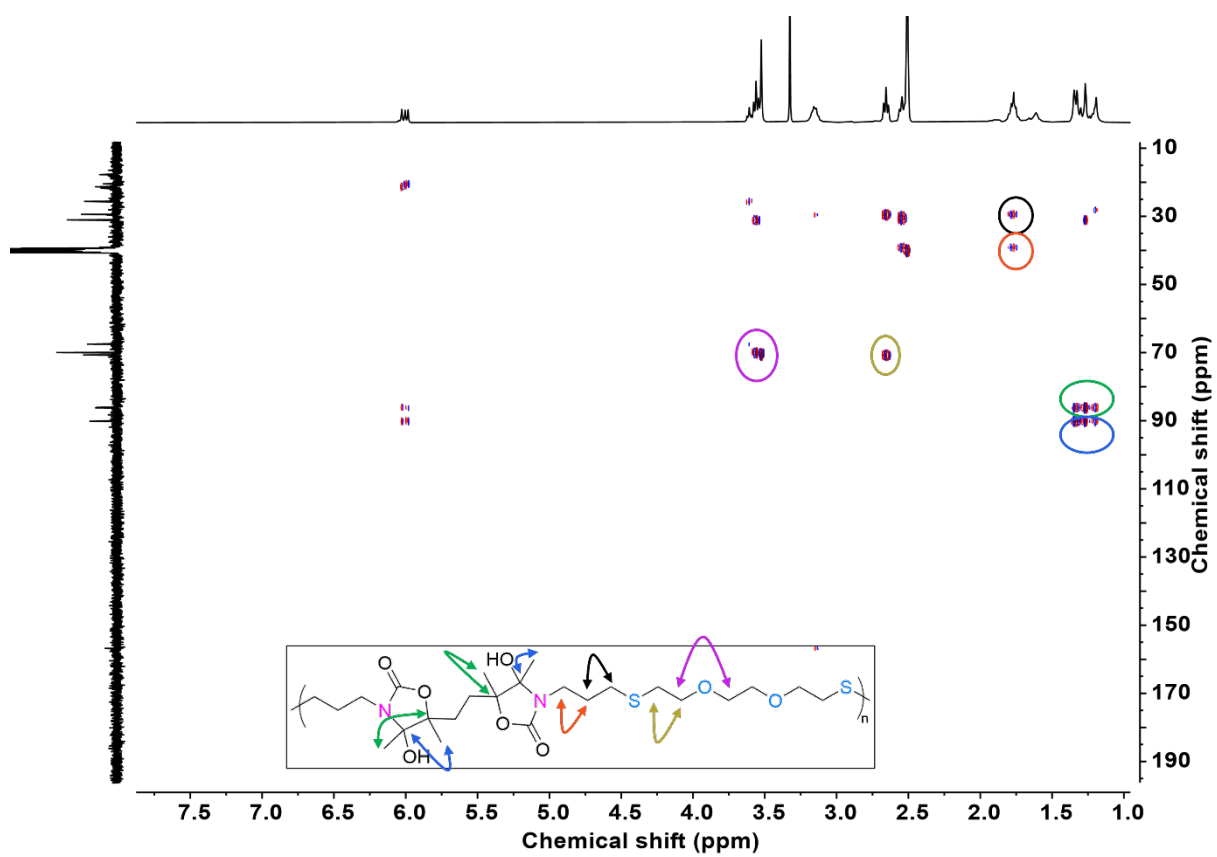


Figure S35. HMBC NMR spectrum of purified **P2b** (400 MHz, $\text{DMSO-}d_6$).

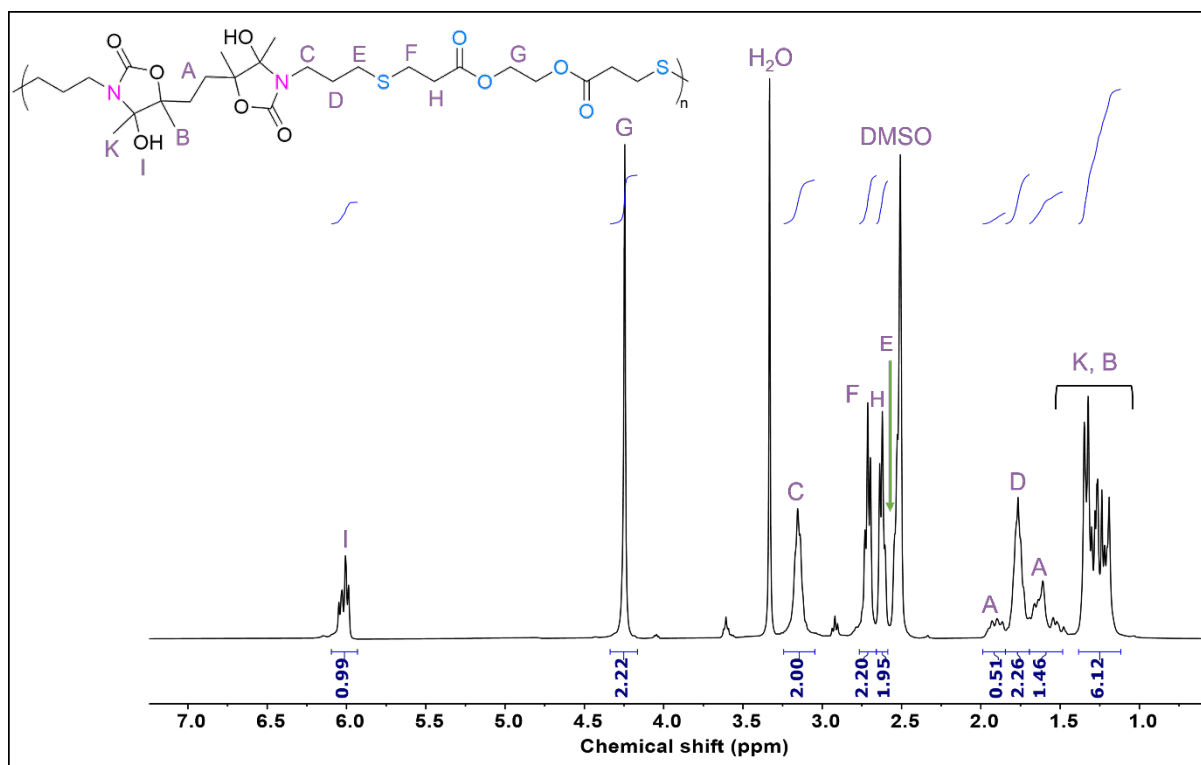


Figure S36. ¹H-NMR spectrum of purified P2c (400 MHz, DMSO-*d*₆).

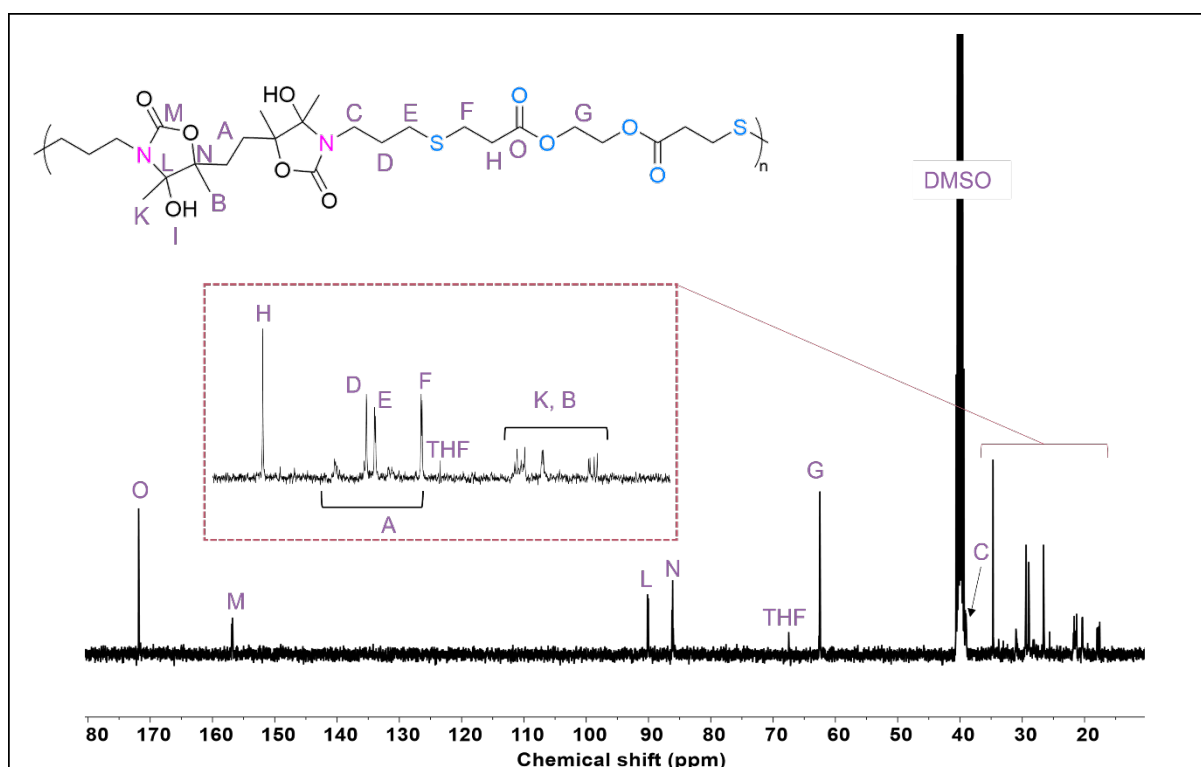


Figure S37. ¹³C-NMR spectrum of purified P2c (100 MHz, DMSO-*d*₆).

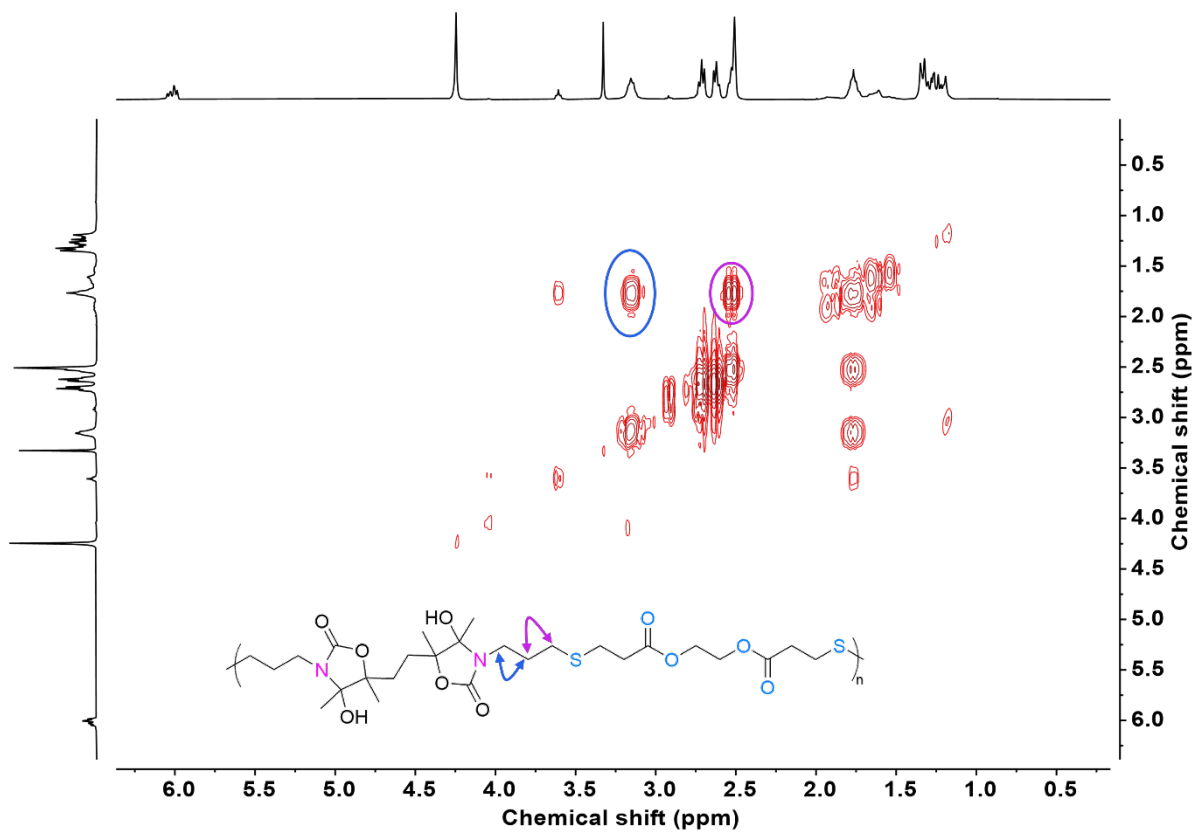


Figure S38. COSY NMR spectrum of purified P2c (400 MHz, $\text{DMSO-}d_6$).

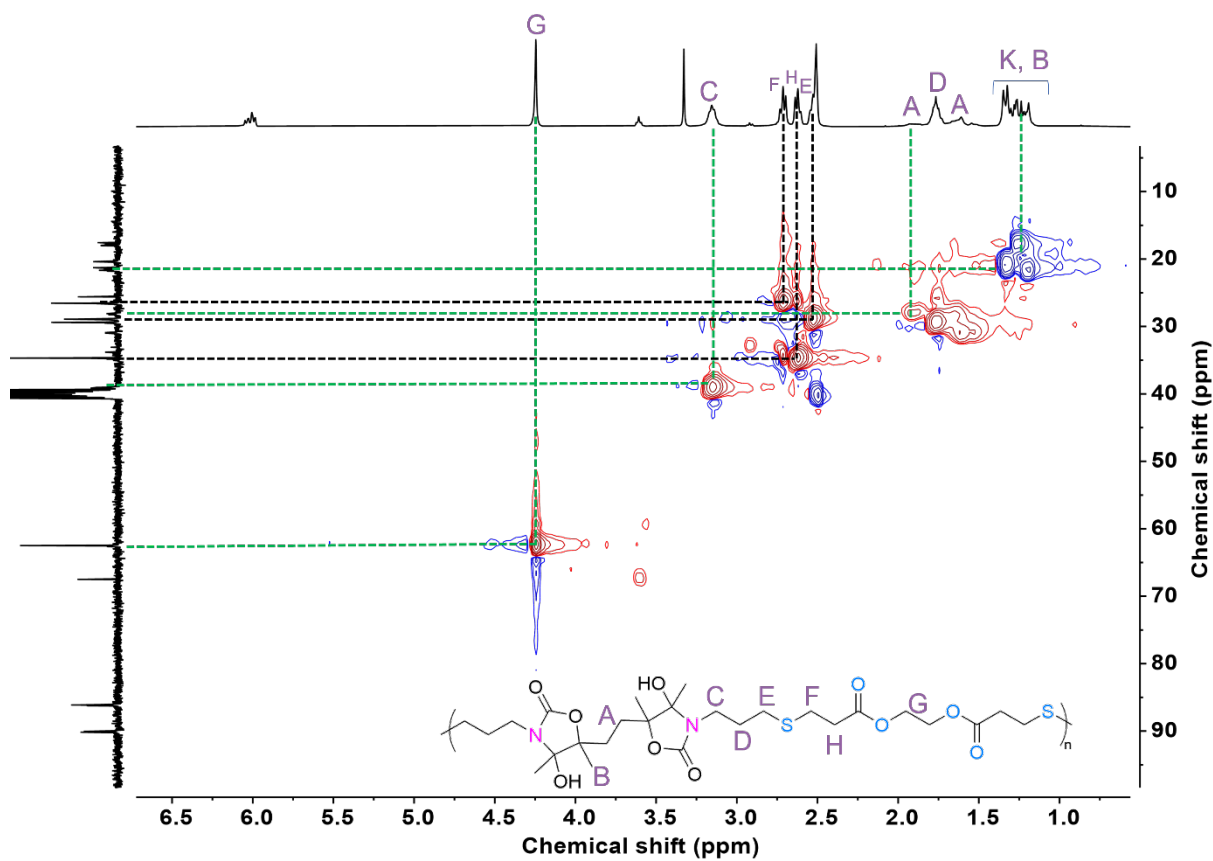


Figure S39. ^1H - ^{13}C HSQC NMR spectrum of purified P2c (400 MHz, $\text{DMSO-}d_6$).

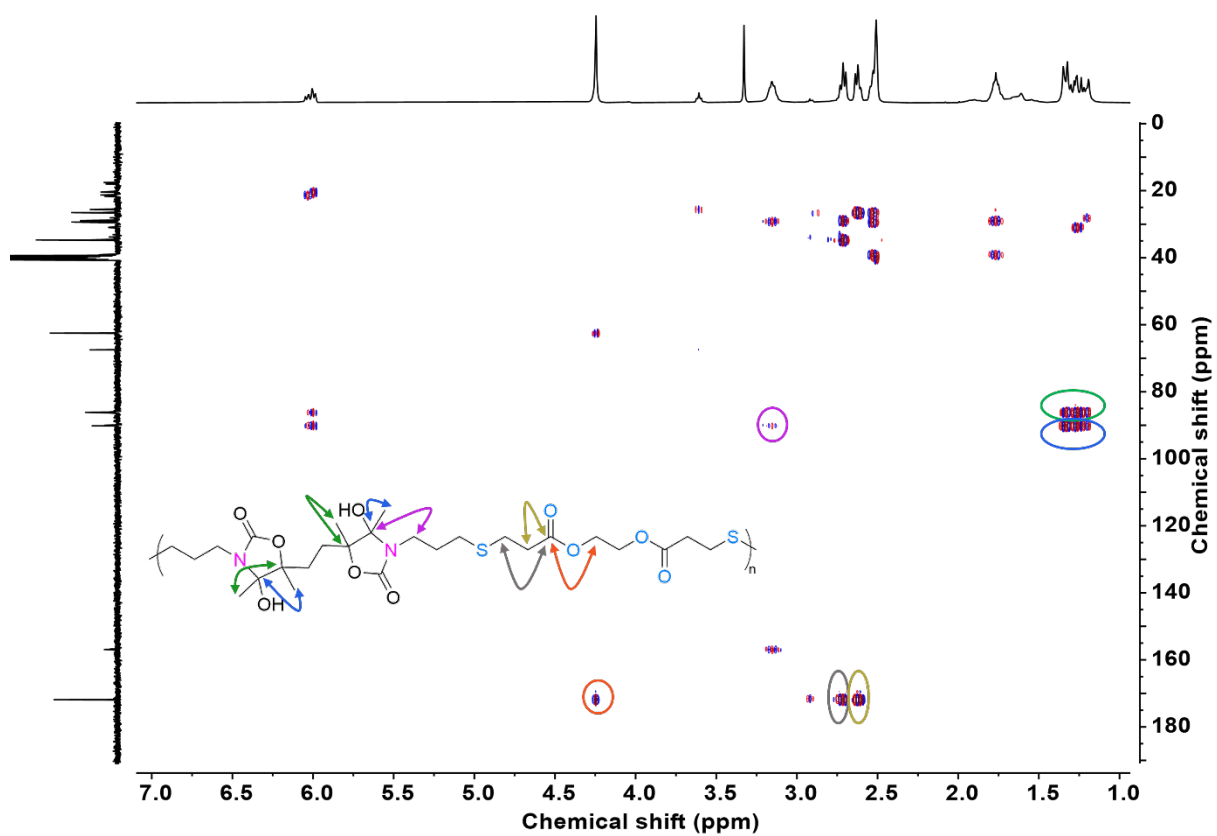


Figure S40. HMBC NMR spectrum of purified P2c (400 MHz, DMSO-*d*₆).

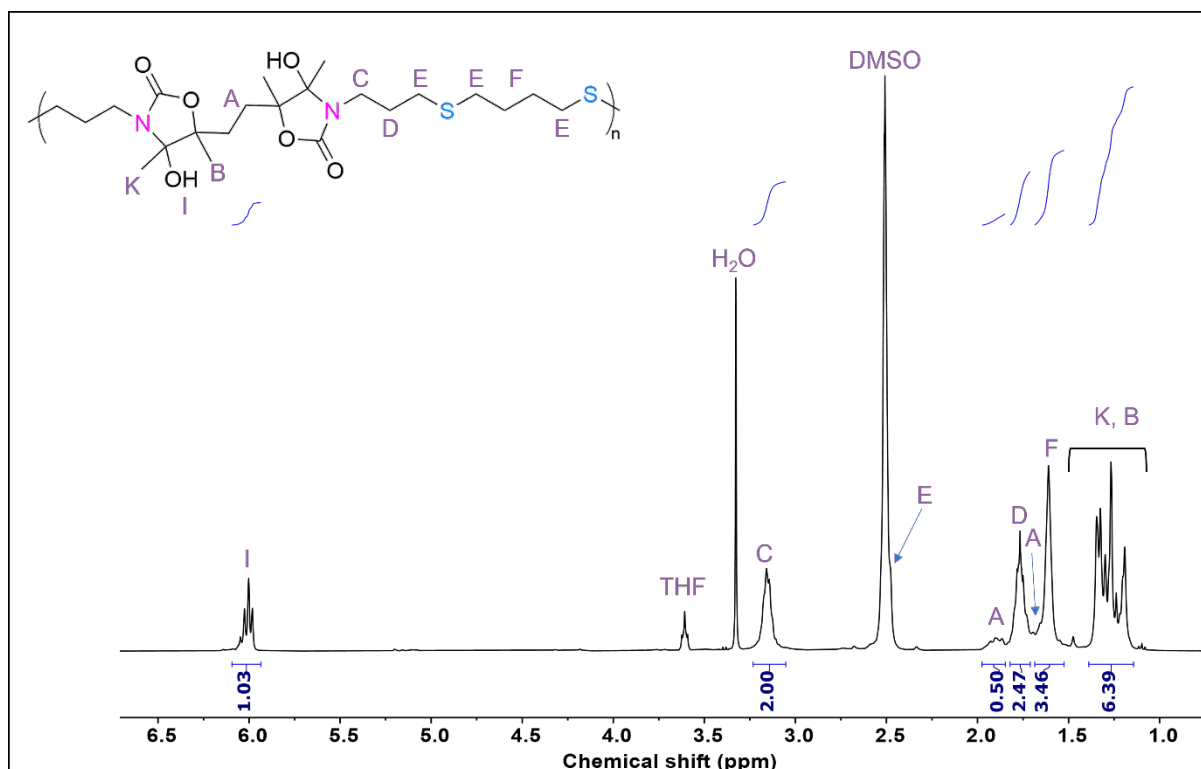


Figure S41. $^1\text{H-NMR}$ spectrum of purified **P2d** (400 MHz, $\text{DMSO-}d_6$).

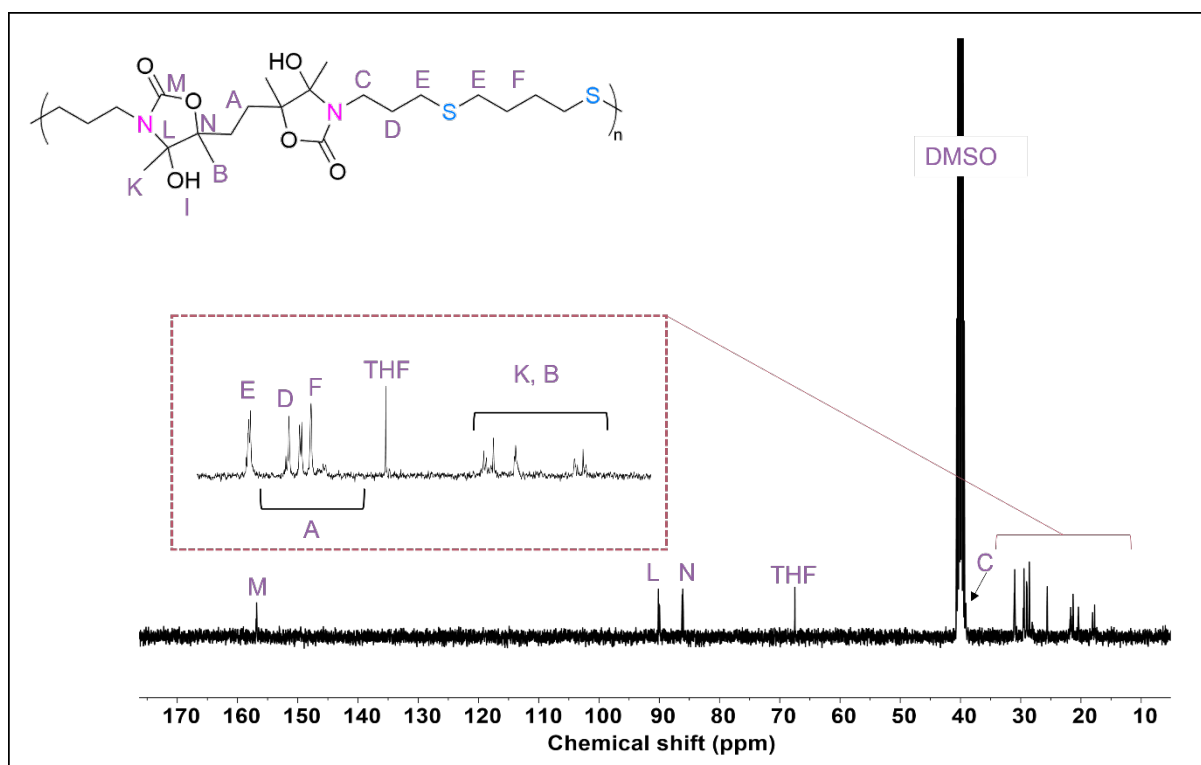


Figure S42. $^{13}\text{C-NMR}$ spectrum of purified **P2d** (100 MHz, $\text{DMSO-}d_6$).

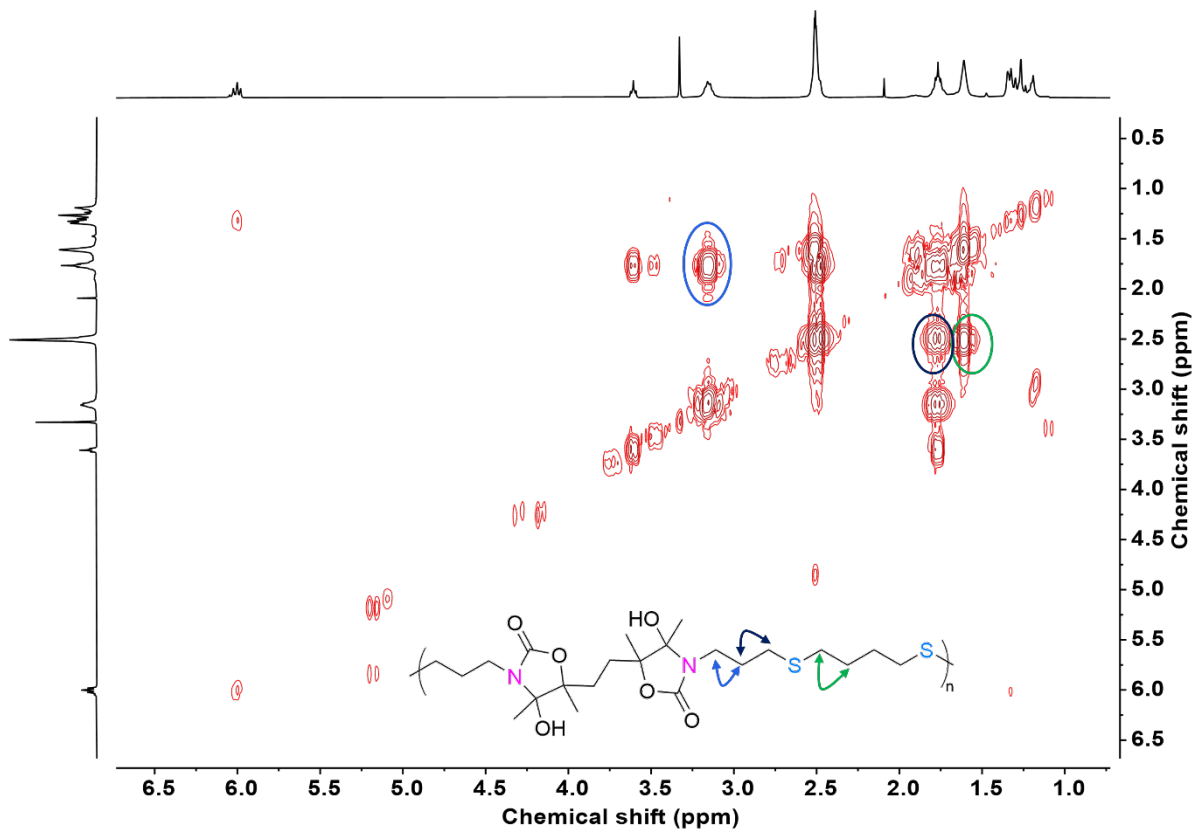


Figure S43. COSY NMR spectrum of purified **P2d** (400 MHz, DMSO-*d*₆).

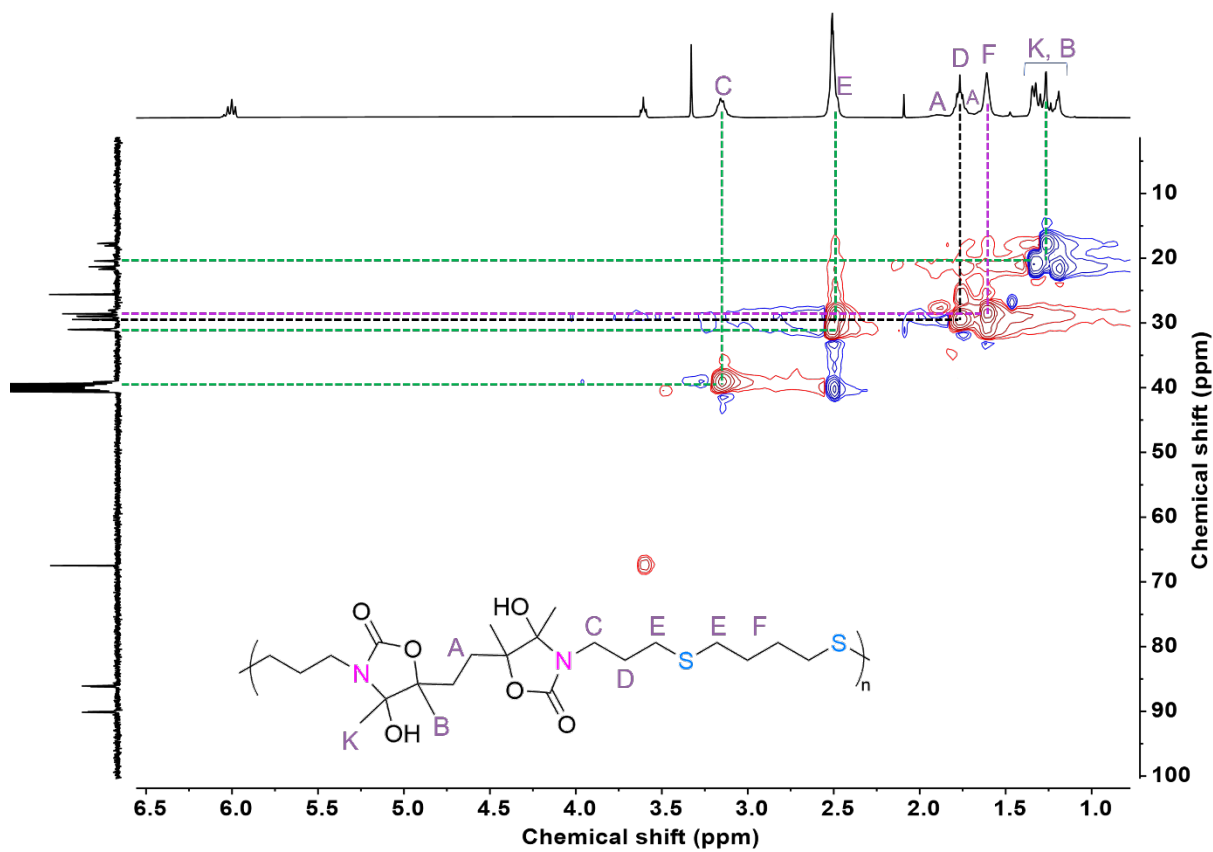


Figure S44. ^1H - ^{13}C HSQC NMR spectrum of purified **P2d** (400 MHz, $\text{DMSO-}d_6$).

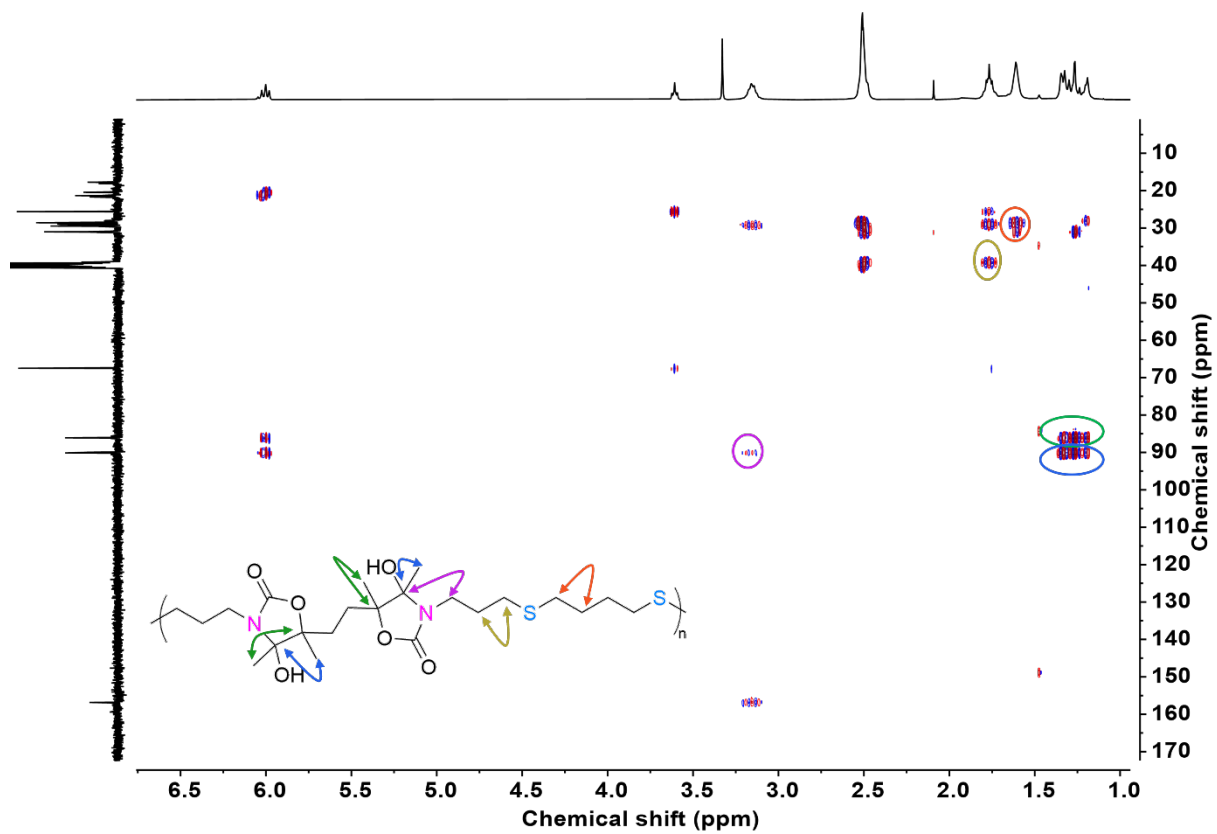


Figure S45. HMBC NMR spectrum of purified P2d (400 MHz, DMSO- d_6).

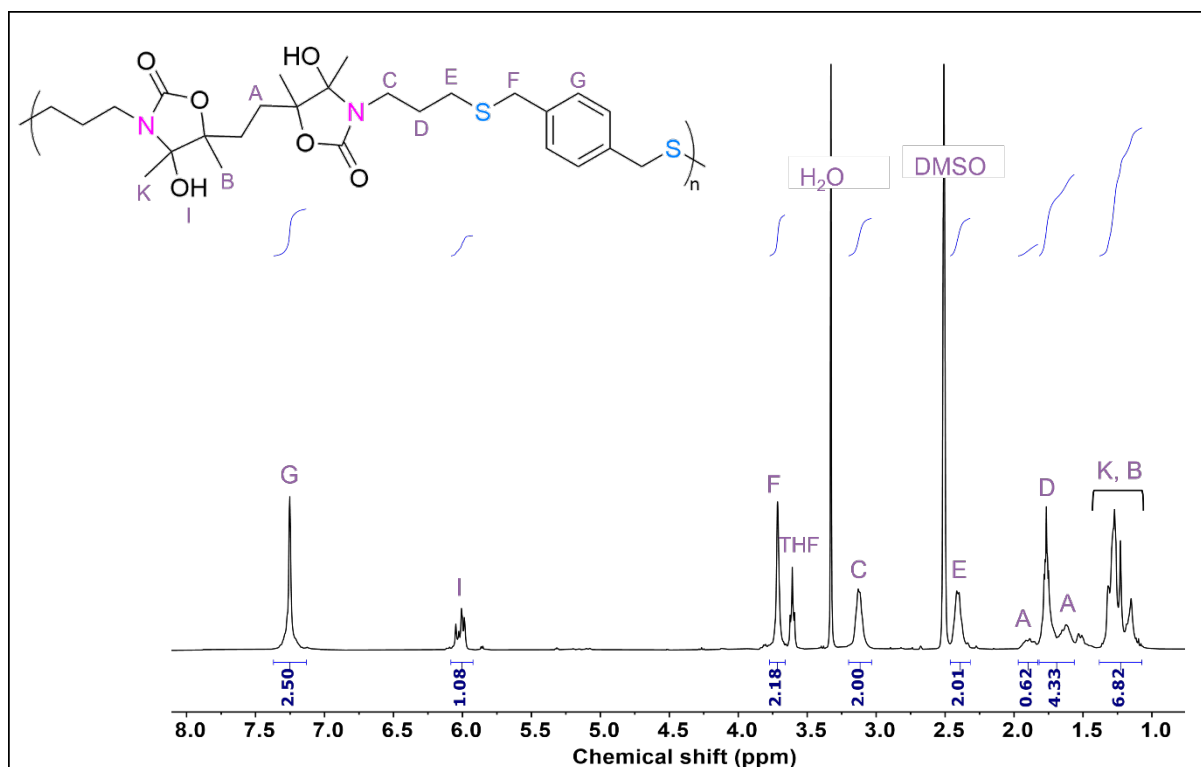


Figure S46. $^1\text{H-NMR}$ spectrum of purified P2e (400 MHz, $\text{DMSO-}d_6$).

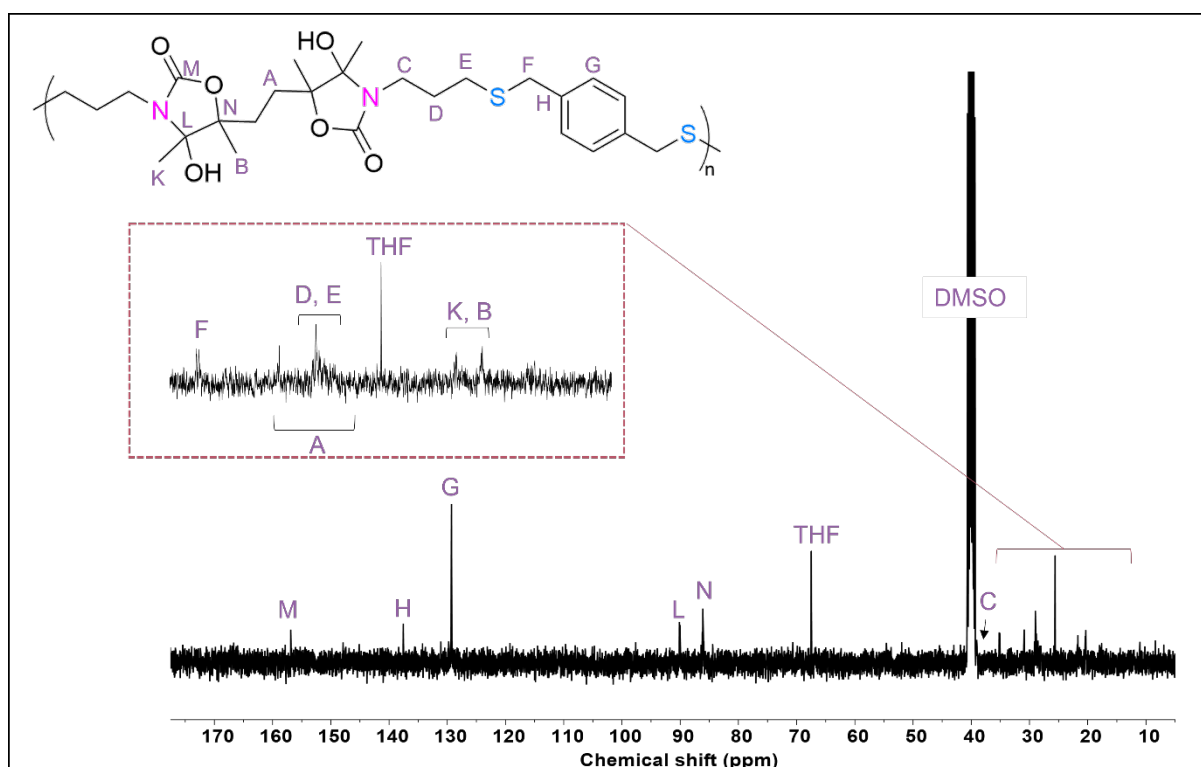


Figure S47. $^{13}\text{C-NMR}$ spectrum of purified P2e (100 MHz, $\text{DMSO-}d_6$).

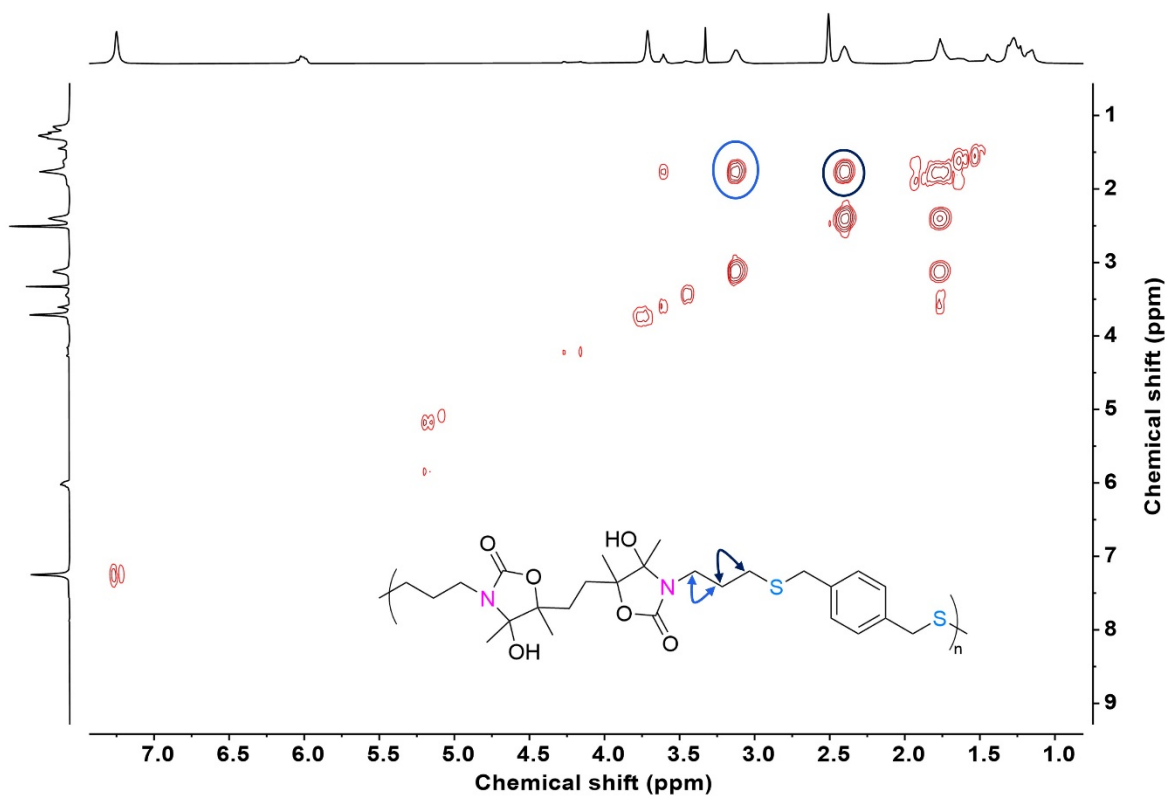


Figure S48. COSY NMR spectrum of purified **P2e** (400 MHz, DMSO- d_6).

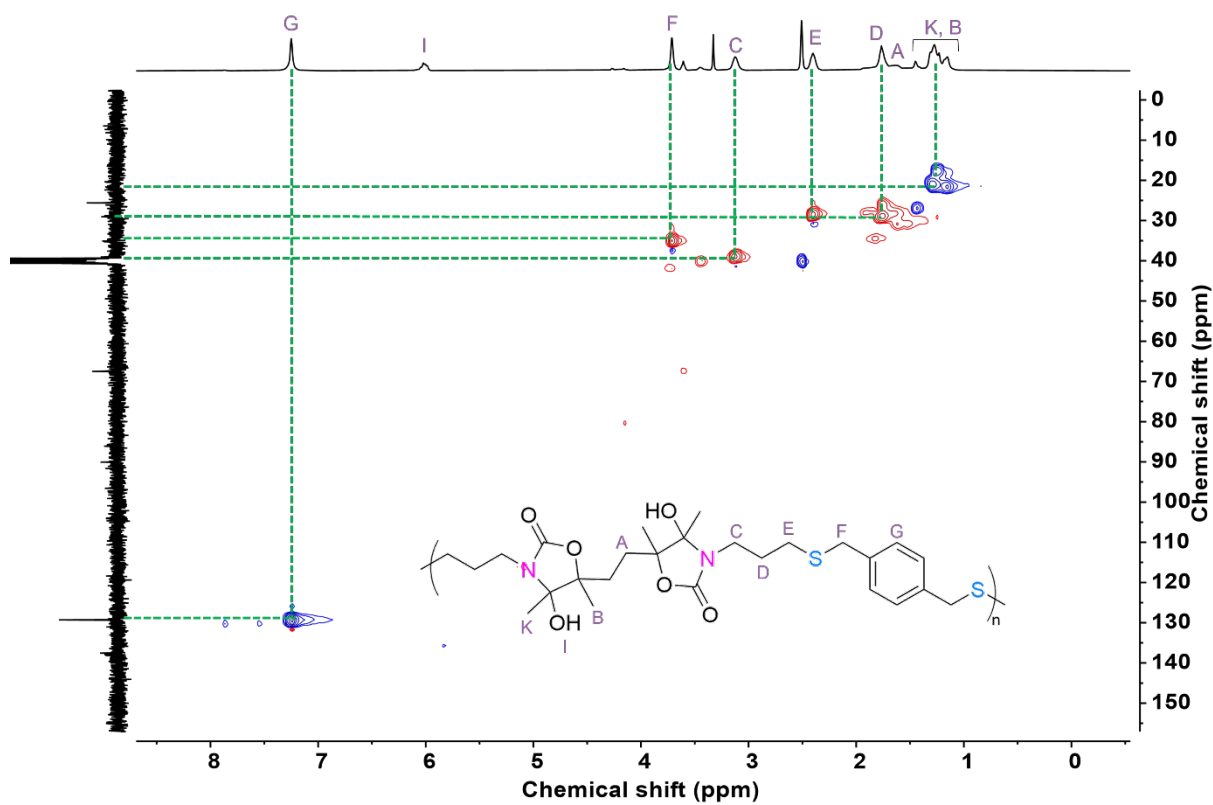


Figure S49. ^1H - ^{13}C HSQC NMR spectrum of purified P2e (400 MHz, $\text{DMSO-}d_6$).

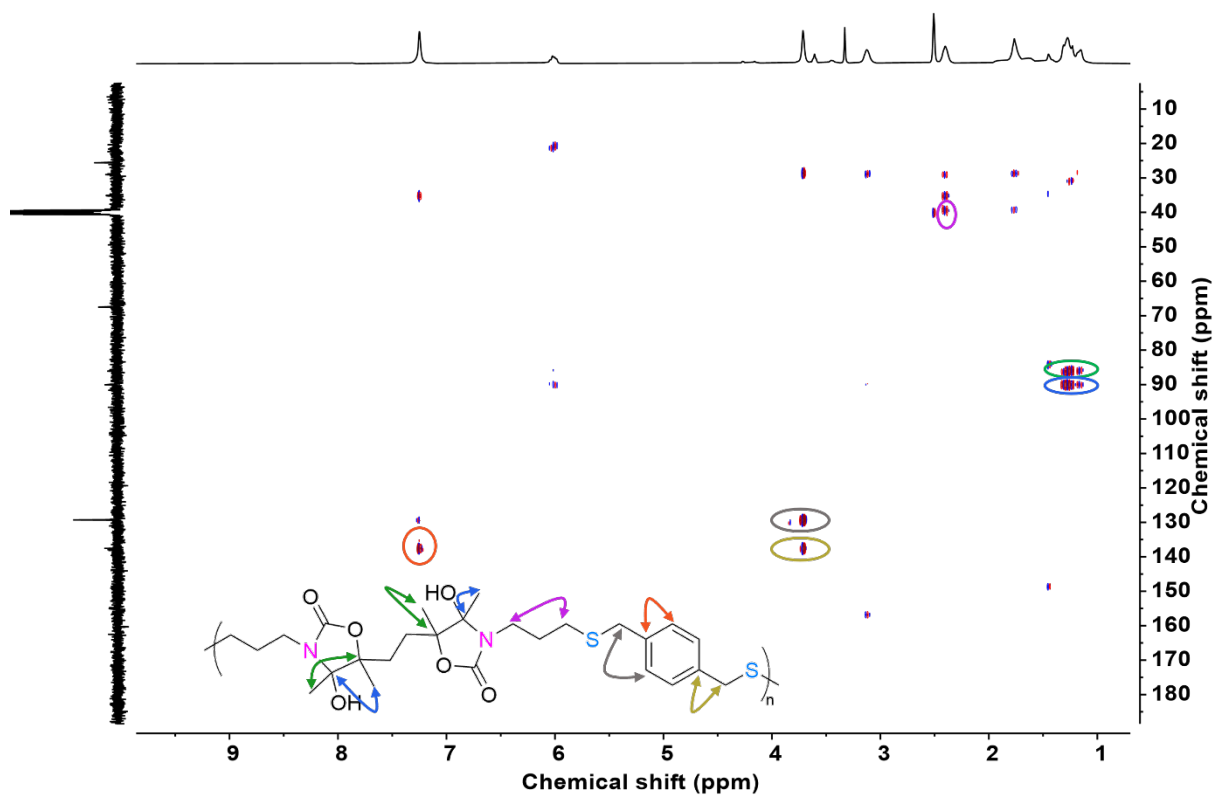


Figure S50. HMBC NMR spectrum of purified **P2e** (400 MHz, $\text{DMSO-}d_6$).

10- Solubility of all synthesized polymers

The polymer was cut into small pieces and 50 mg were immersed in 6 mL of DMF, DMSO, THF, or water for 48 h to determine solubility. Results are given in Table S2, categorizing them qualitatively as either soluble or not soluble.

Table S2. Solubility table of all synthesized polymers

		DMF	DMSO	THF	Water
Hydrated polymers	P2a	✓	✓	✓	✗
	P2b	✓	✓	✓	✗
	P2c	✓	✓	✓	✗
	P2d	✓	✓	✓	✗
	P2e	✓	✓	✓	✗
Dehydrated polymers	P2a-dehydrated	✓	✓	✓	✗
	P2b-dehydrated	✓	✓	✓	✗
	P2c-dehydrated	✓	✓	✓	✗
	P2d-dehydrated	✓	✓	✓	✗
	P2e-dehydrated	✓	✓	✓	✗
Post-modified polymers	P2b-Sulfoxide	✓	✓	✗	✗
	P2b-Sulfone	✓	✓	✗	✗
	P2b-Sulfonium	✗	✓	✗	✓

11- TGA characterization of pure polymers

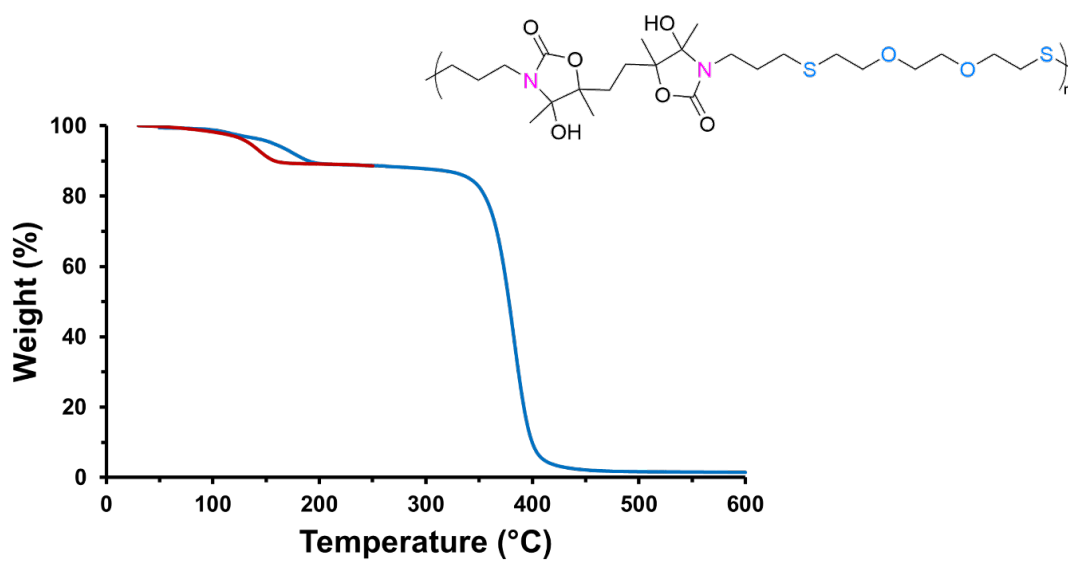


Figure S51. TGA thermogram of **P2a** at a heating rate of 20 K/min (blue) and 2 K/min (red)

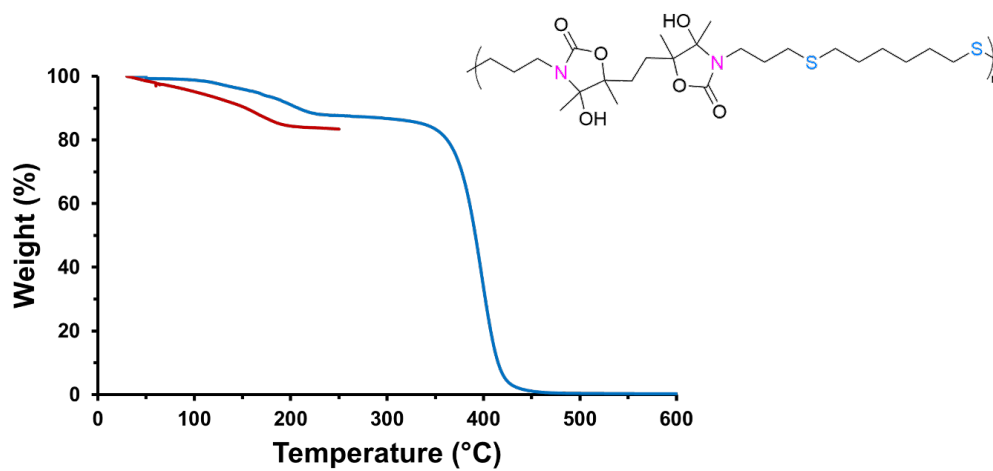


Figure S52. TGA thermogram of **P2b** at a heating rate of 20 K/min (blue) and 2 K/min (red)

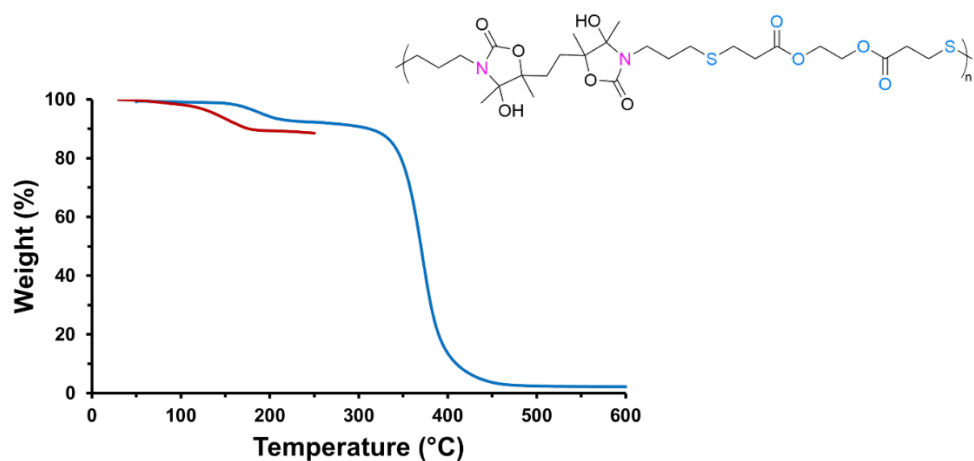


Figure S53. TGA thermogram of P2c at a heating rate of 20 K/min (blue) and 2 K/min (red)

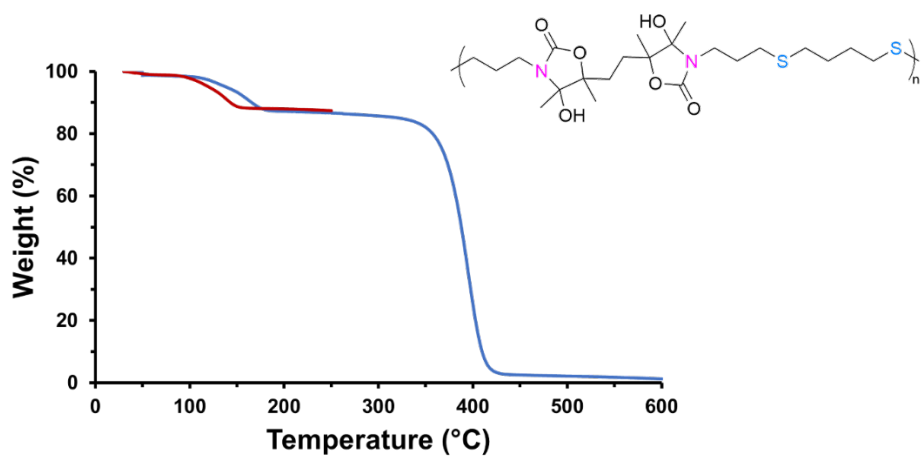


Figure S54. TGA thermogram of P2d at a heating rate of 20 K/min (blue) and 2 K/min (red)

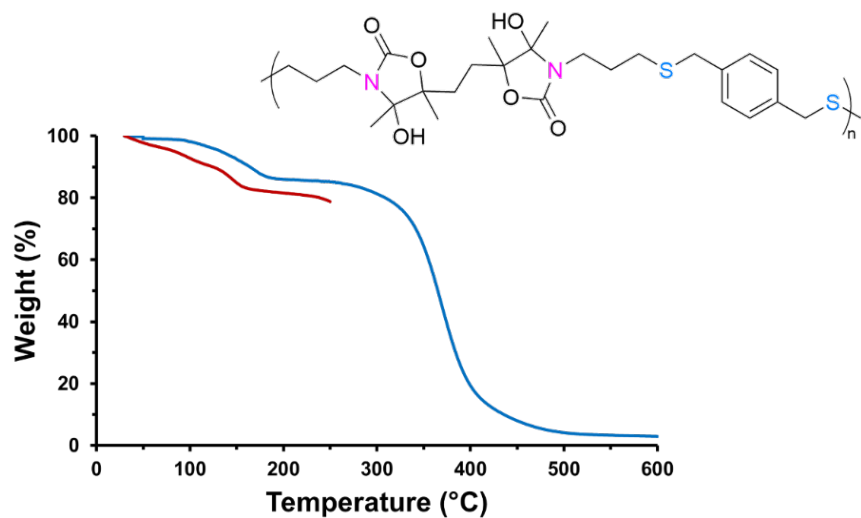


Figure S55. TGA thermogram of P2e at a heating rate of 20 K/min (blue) and 2 K/min (red)

12- Slow TGA characterization and derivative curves of pure polymers

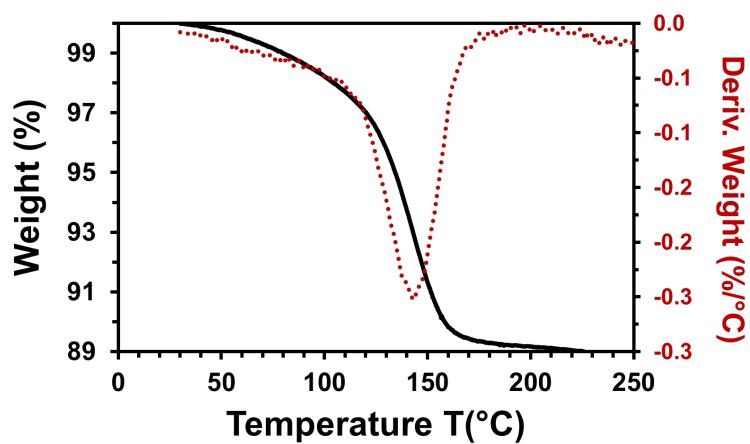


Figure S56. The slow TGA curve of **P2a** at the heating rate of 2 K/min and its derivative curve to determine the $T_{\text{dehy.}}$

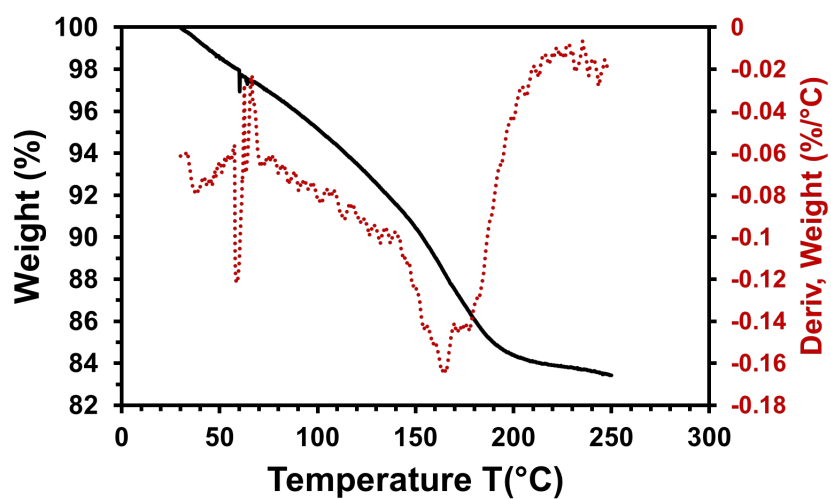


Figure S57. The slow TGA curve of **P2b** at the heating rate of 2 K/min and its derivative curve to determine the $T_{\text{dehy.}}$

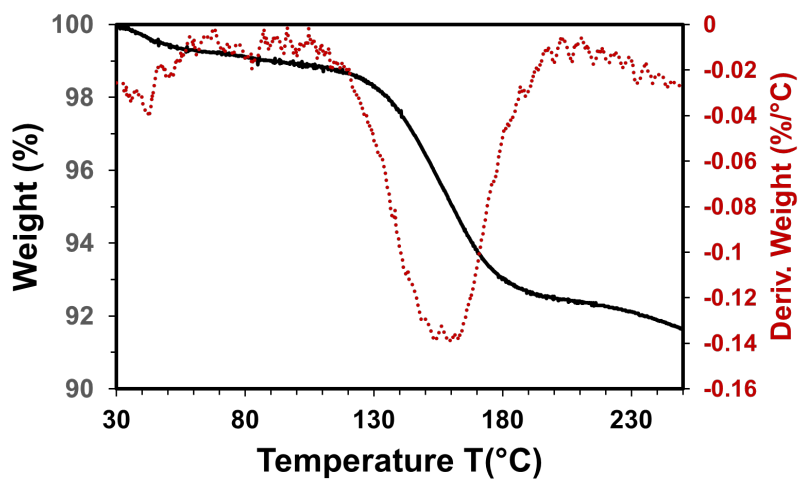


Figure S58. The slow TGA curve of P2c at the heating rate of 2 K/min and its derivative curve to determine the T_{dehy} .

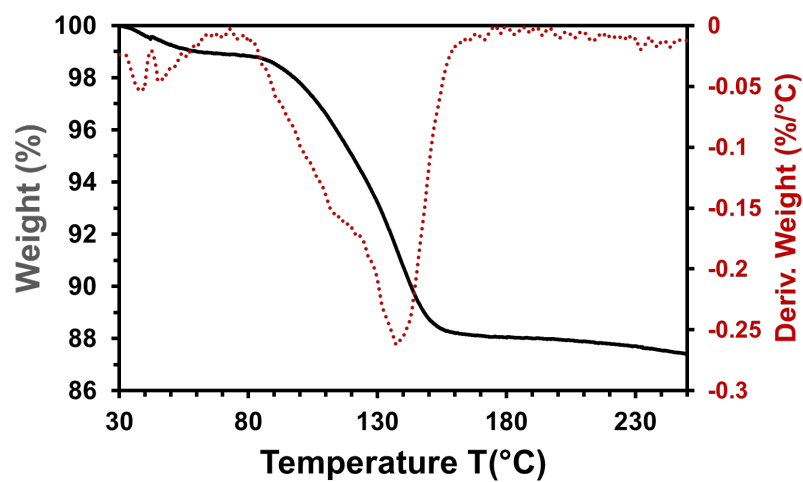


Figure S59. The slow TGA curve of P2d at the heating rate of 2 K/min and its derivative curve to determine the T_{dehy} .

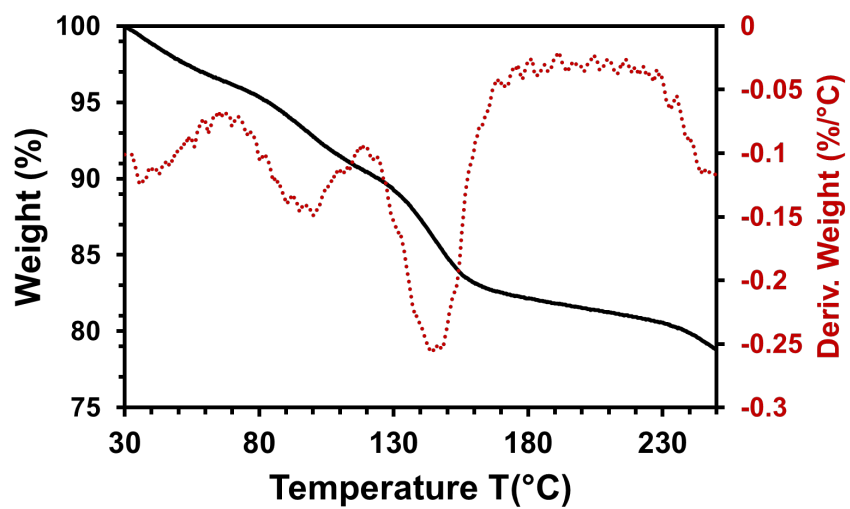


Figure S60. The slow TGA curve of **P2e** at the heating rate of 2 K/min and its derivative curve to determine the T_{dehy}

13-NMR spectra of dehydrated polymers

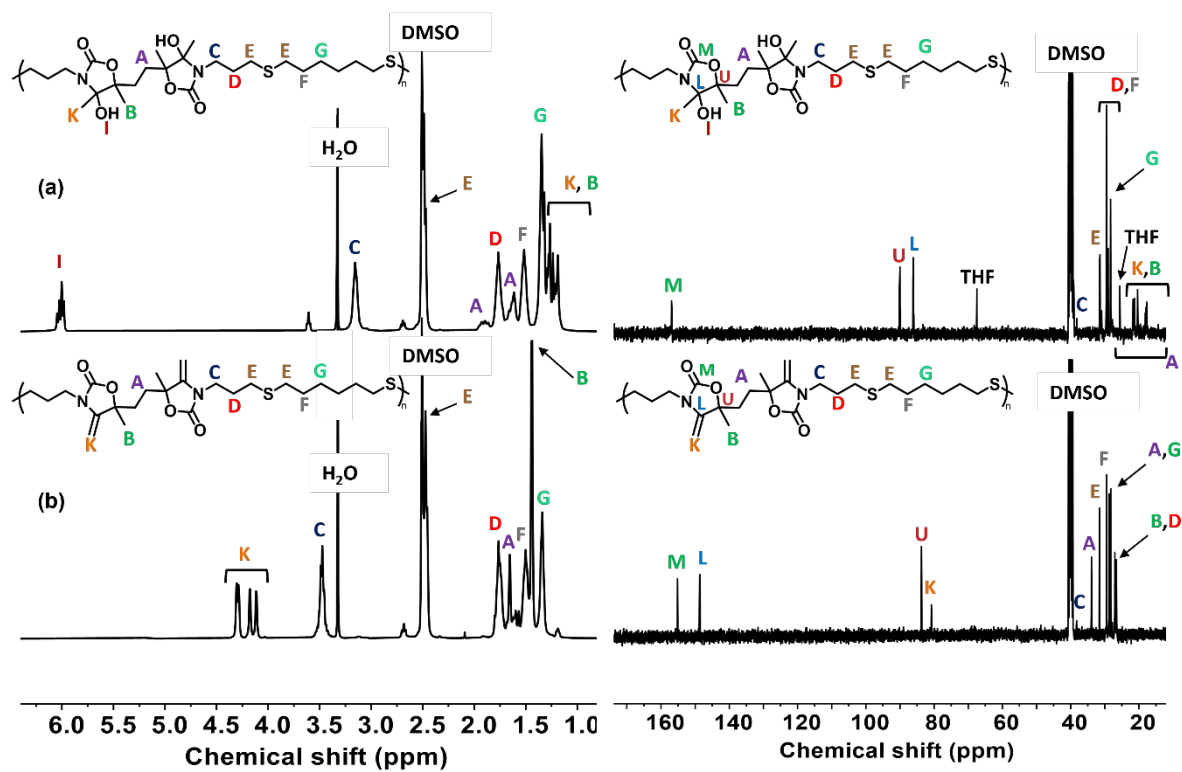


Figure S61. ^1H -NMR spectra (left, 400 MHz, $\text{DMSO-}d_6$) and ^{13}C -NMR spectra (right, 100 MHz, $\text{DMSO-}d_6$) of (a) **P2b** and (b) **P2b-dehydrated**.

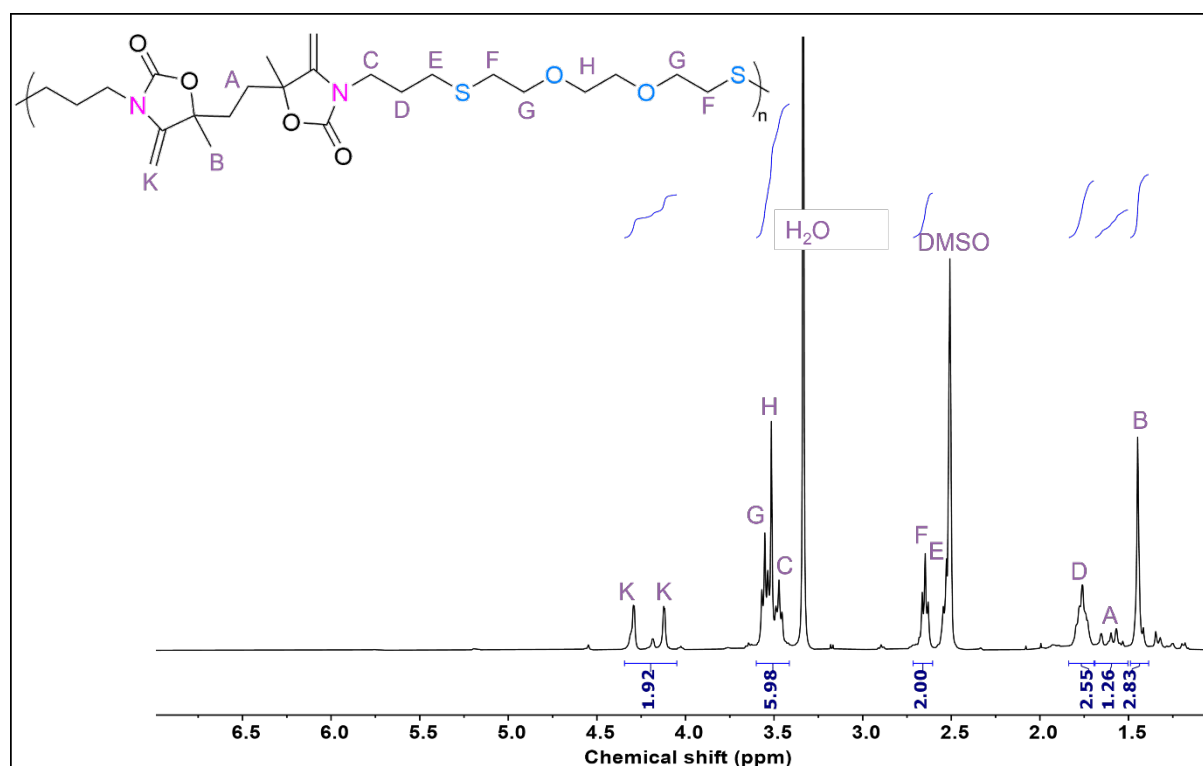


Figure S62. ^1H -NMR spectrum of P2a-dehydrated (400 MHz, $\text{DMSO-}d_6$).

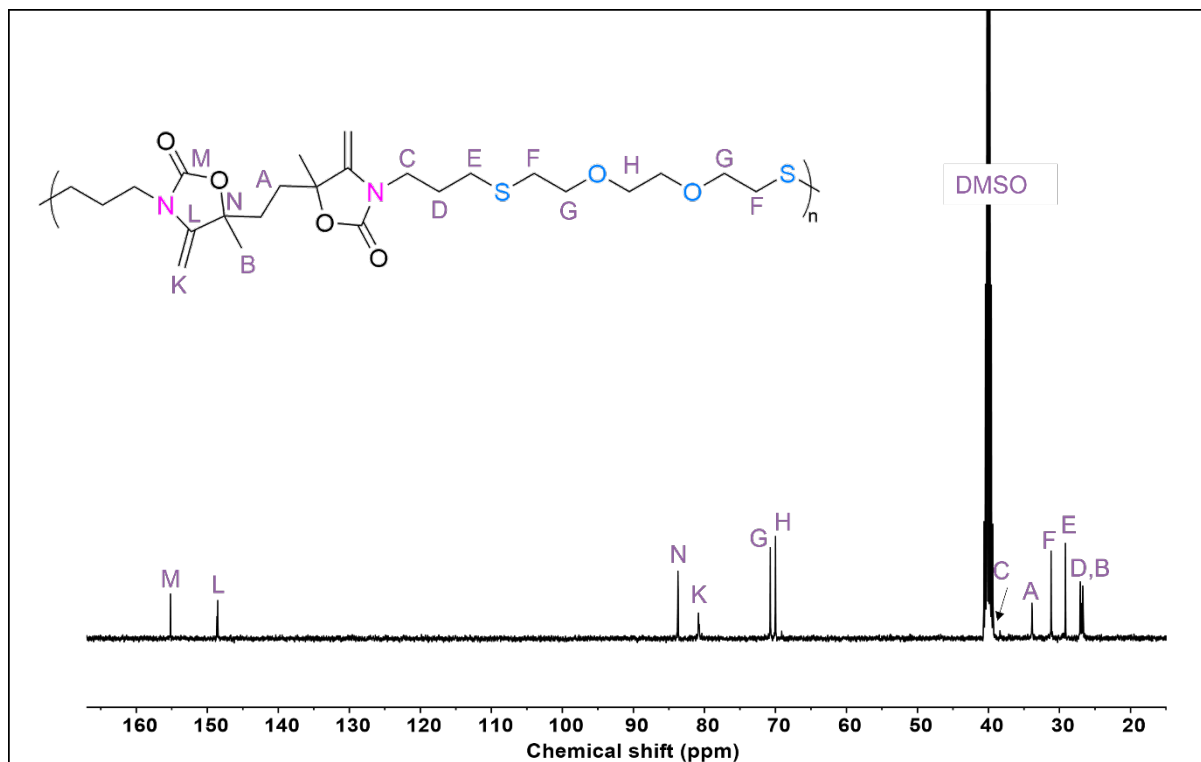


Figure S63. ^{13}C -NMR spectrum of P2a-dehydrated (100 MHz, $\text{DMSO-}d_6$).

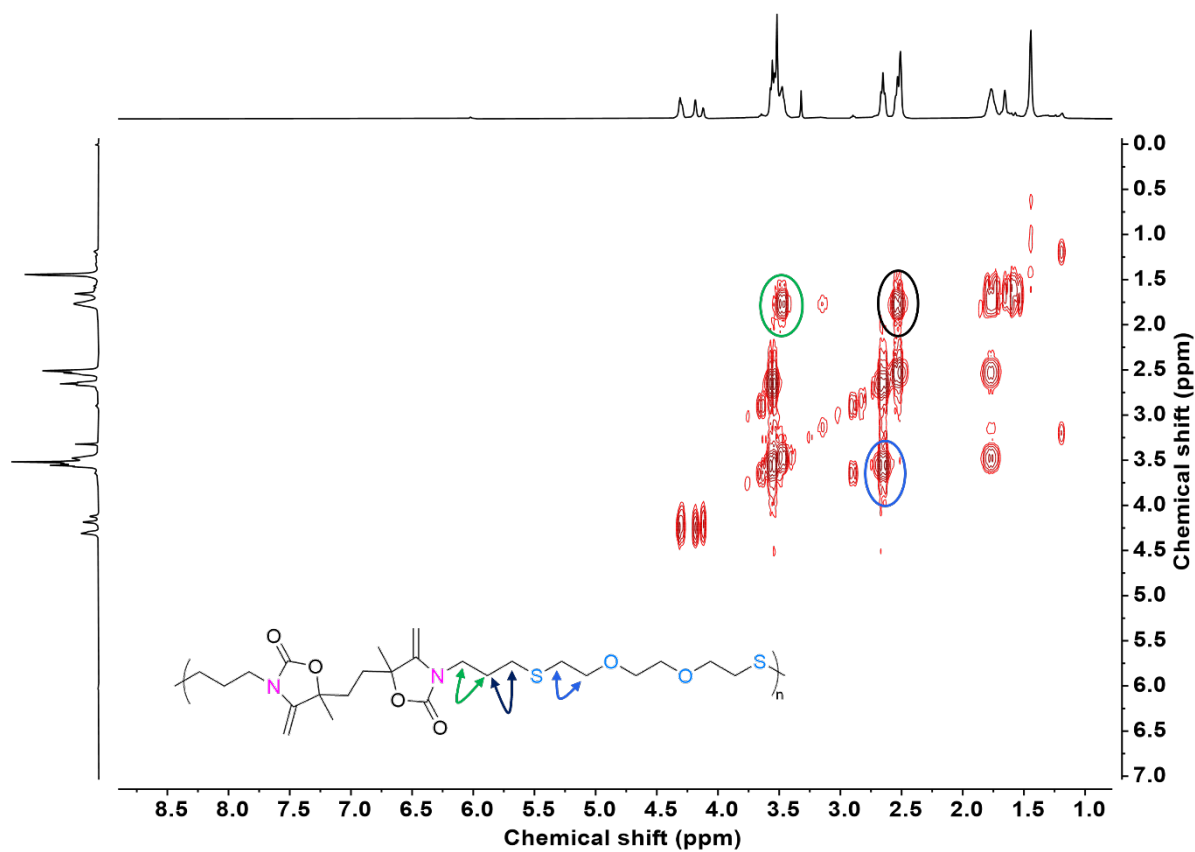


Figure S64. COSY NMR spectrum of P2a-dehydrated (400 MHz, DMSO-*d*₆).

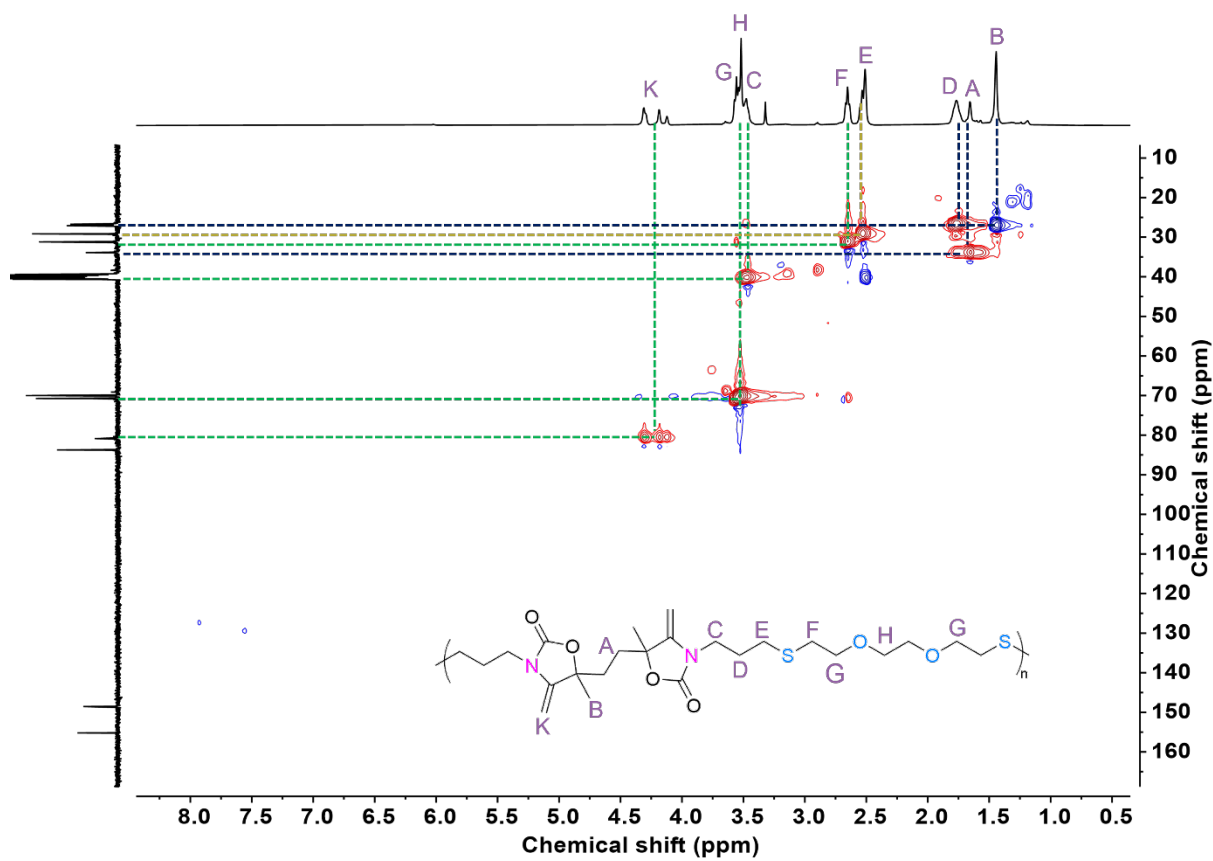


Figure S65. ¹H-¹³C HSQC NMR spectrum of P2a-dehydrated (400 MHz, DMSO-*d*₆).

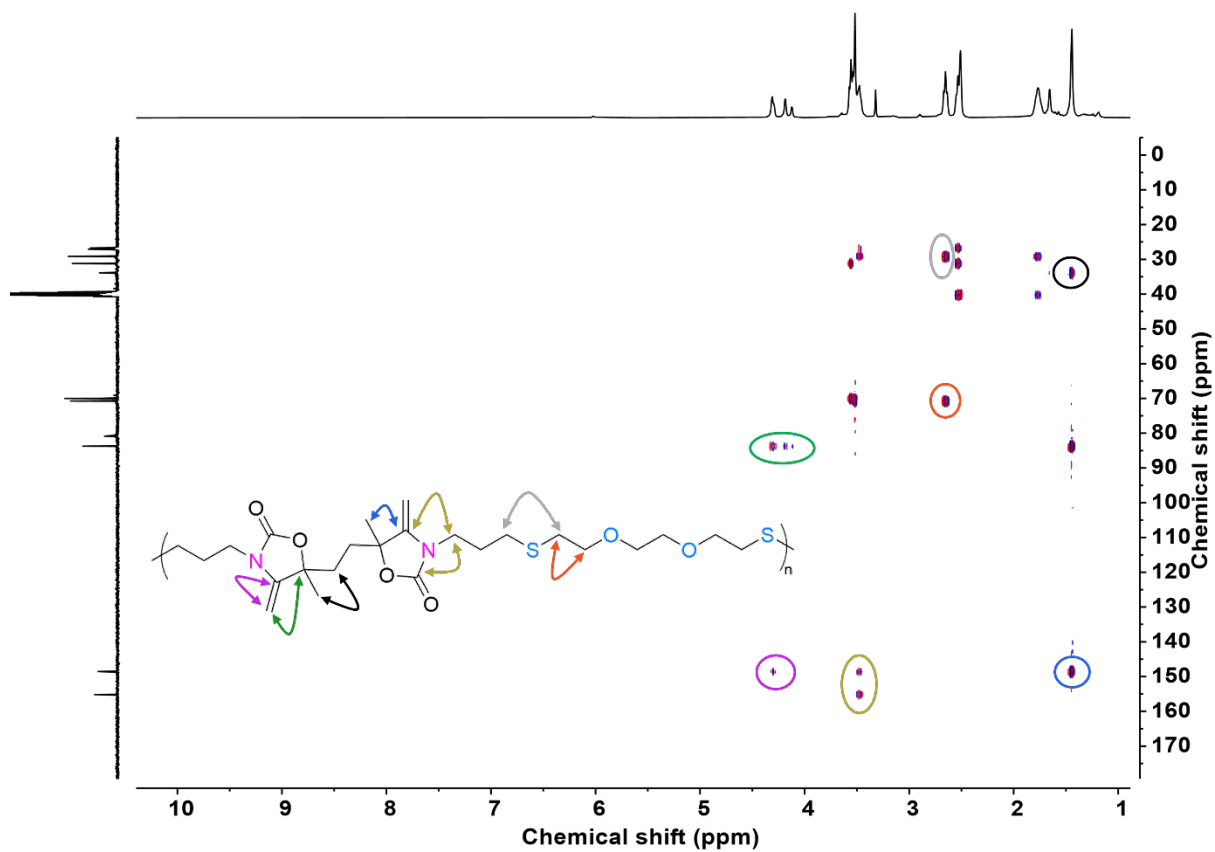


Figure S66. HMBC NMR spectrum of P2a-dehydrated (400 MHz, DMSO- d_6).

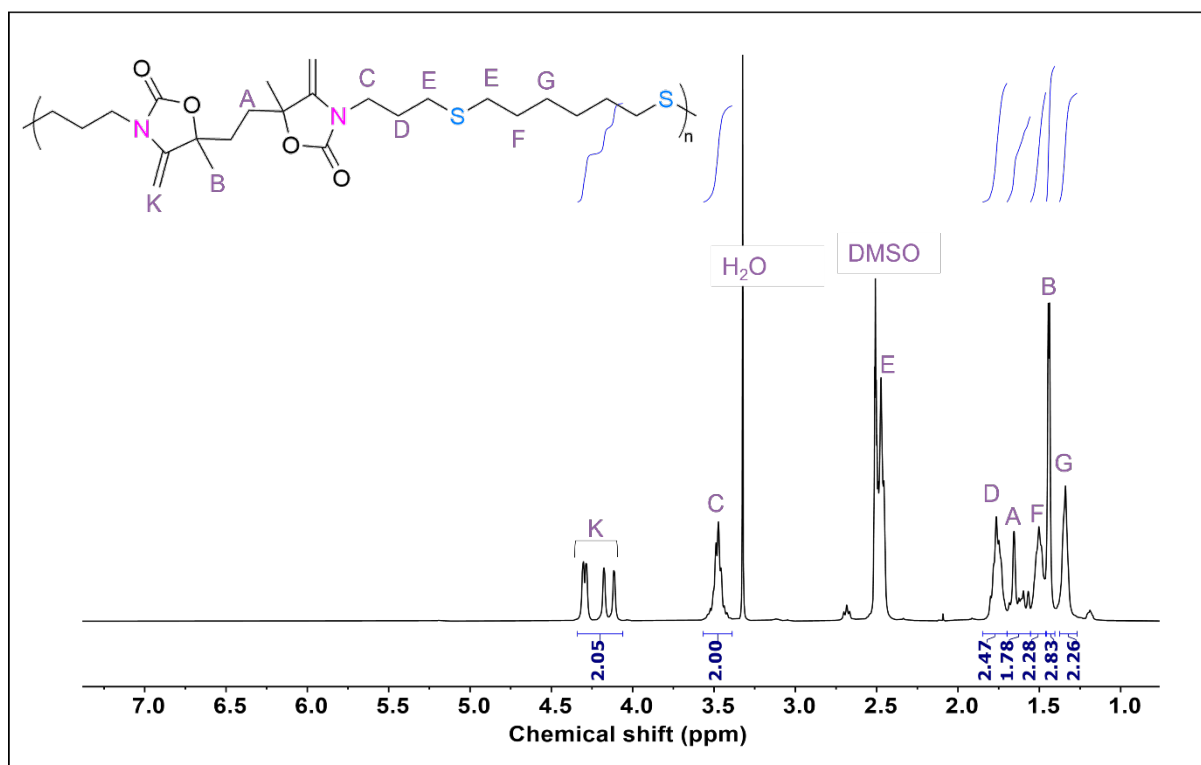


Figure S67. $^1\text{H-NMR}$ spectrum of **P2b-dehydrated** (400 MHz, $\text{DMSO-}d_6$).

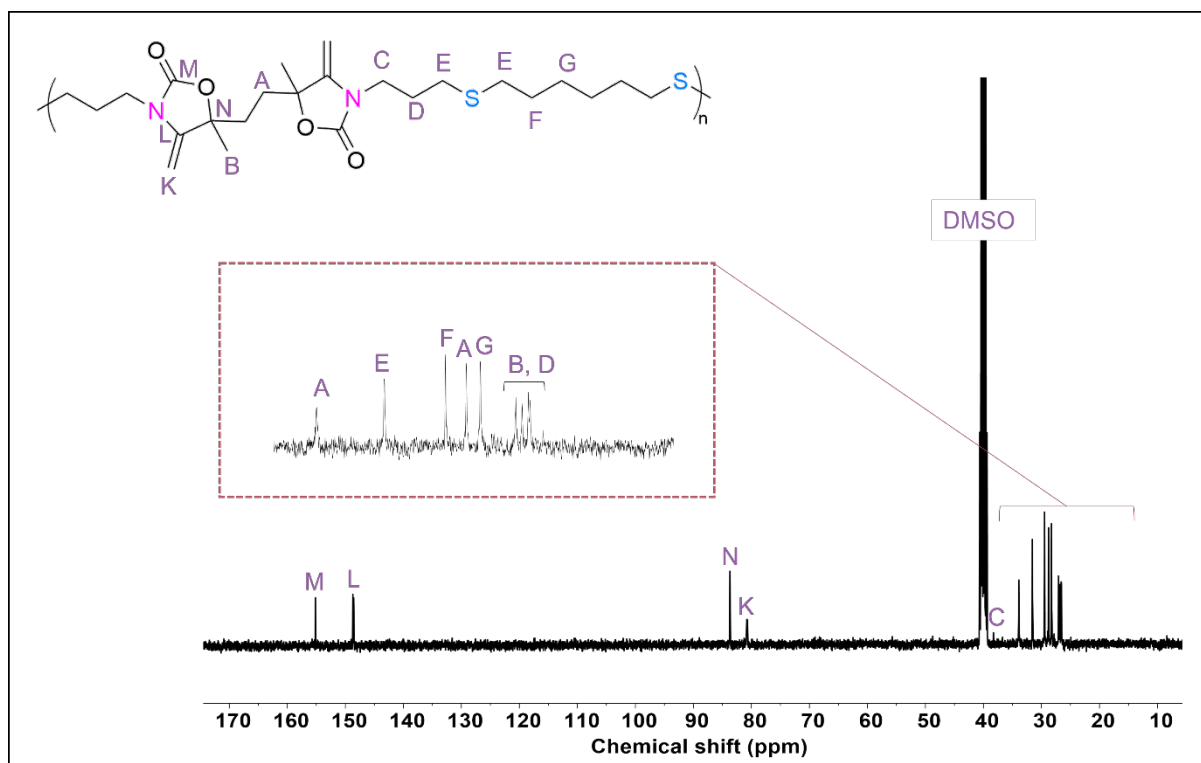


Figure S68. $^{13}\text{C-NMR}$ spectrum of **P2b-dehydrated** (100 MHz, $\text{DMSO-}d_6$).

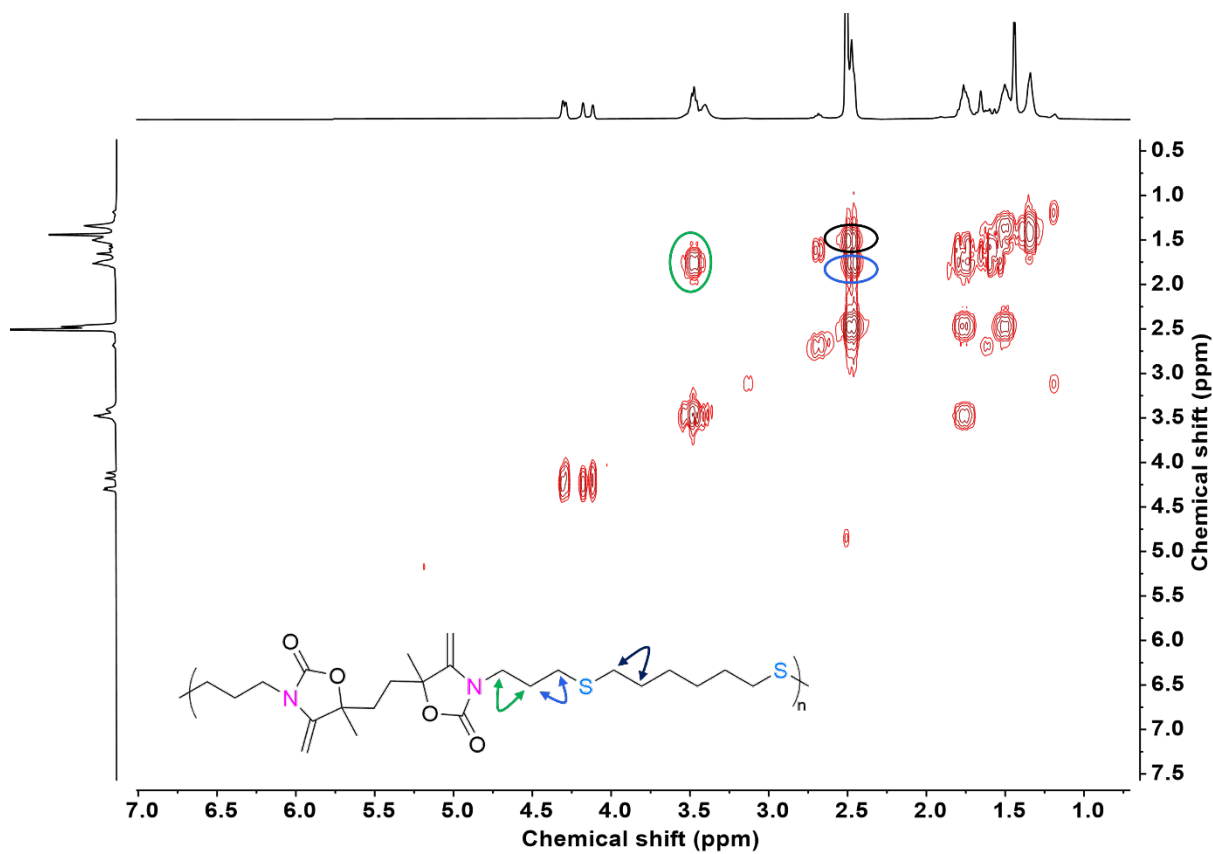


Figure S69. COSY NMR spectrum of **P2b-dehydrated** (400 MHz, DMSO- d_6).

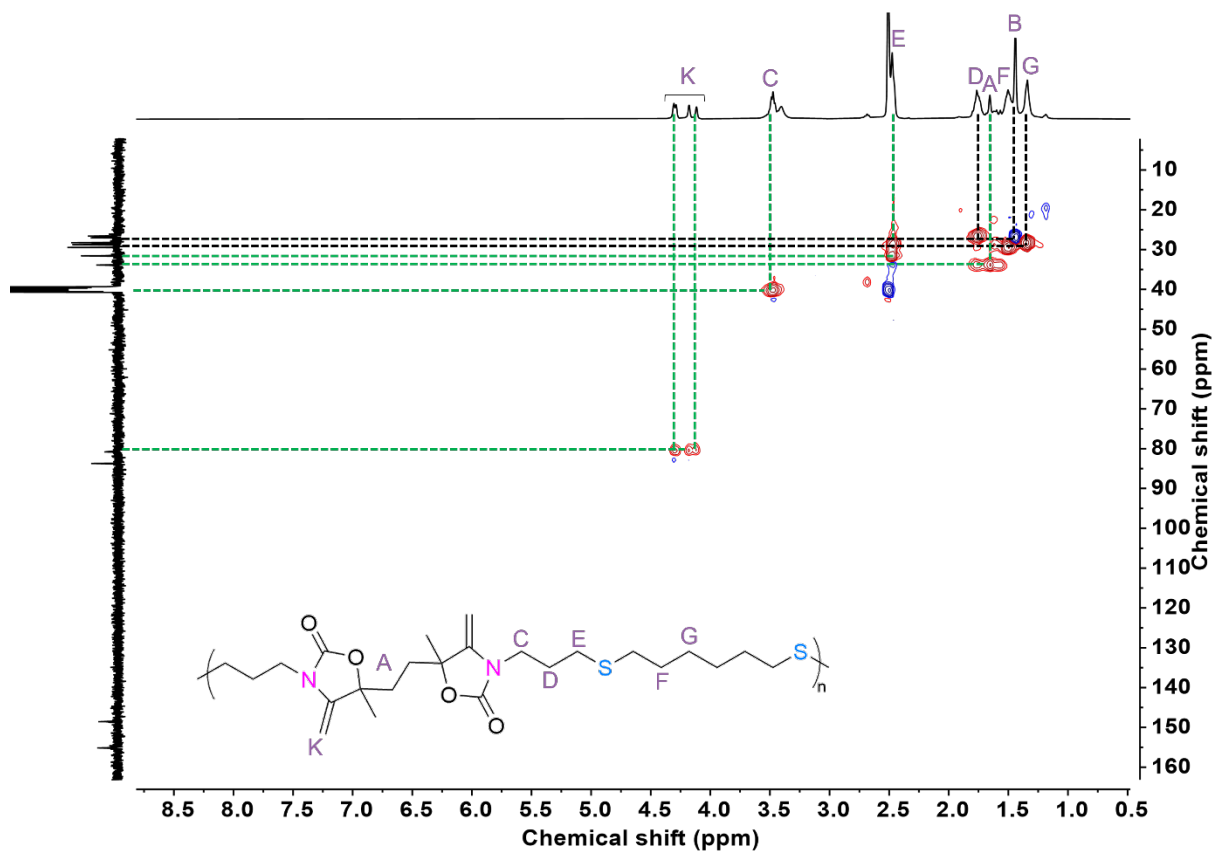


Figure S70. ^1H - ^{13}C HSQC NMR spectrum of **P2b-dehydrated** (400 MHz, DMSO- d_6).

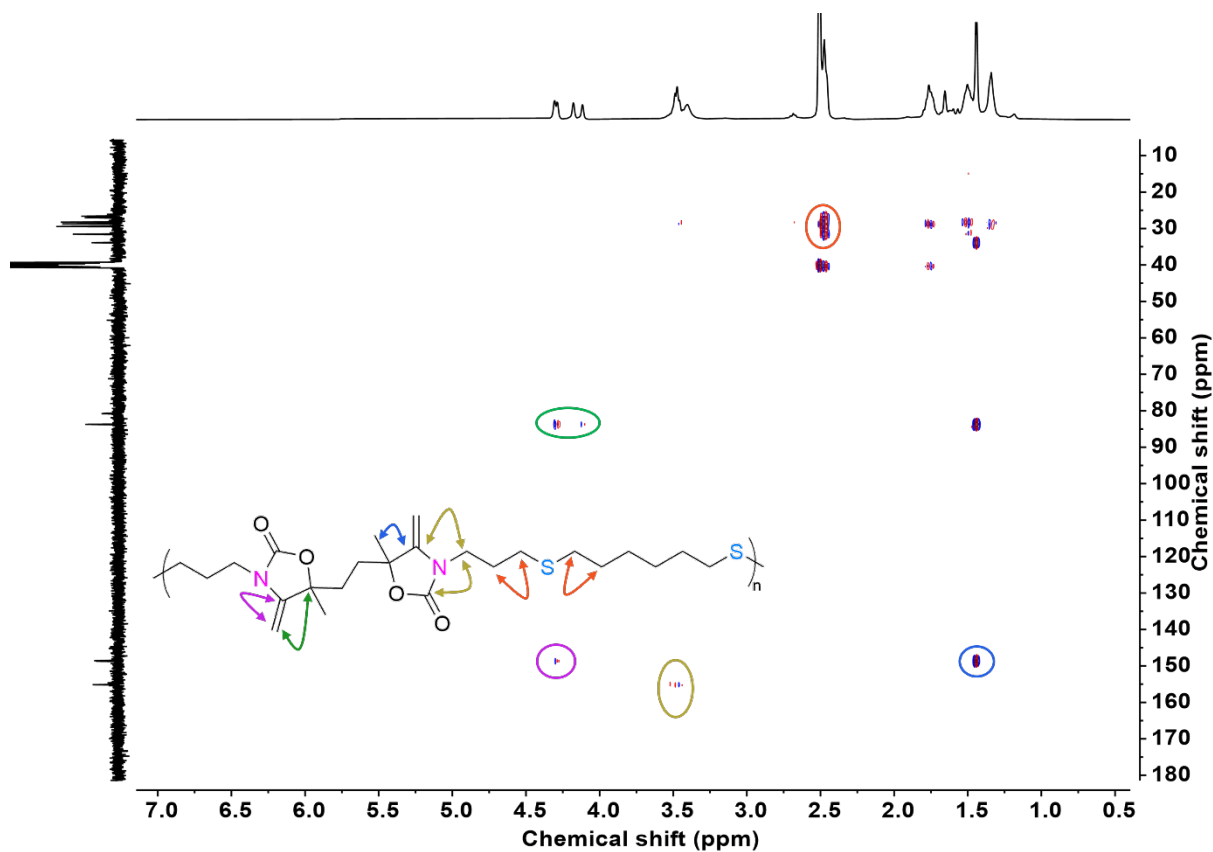


Figure S71. HMBC NMR spectrum of P2b-dehydrated (400 MHz, DMSO-*d*₆).

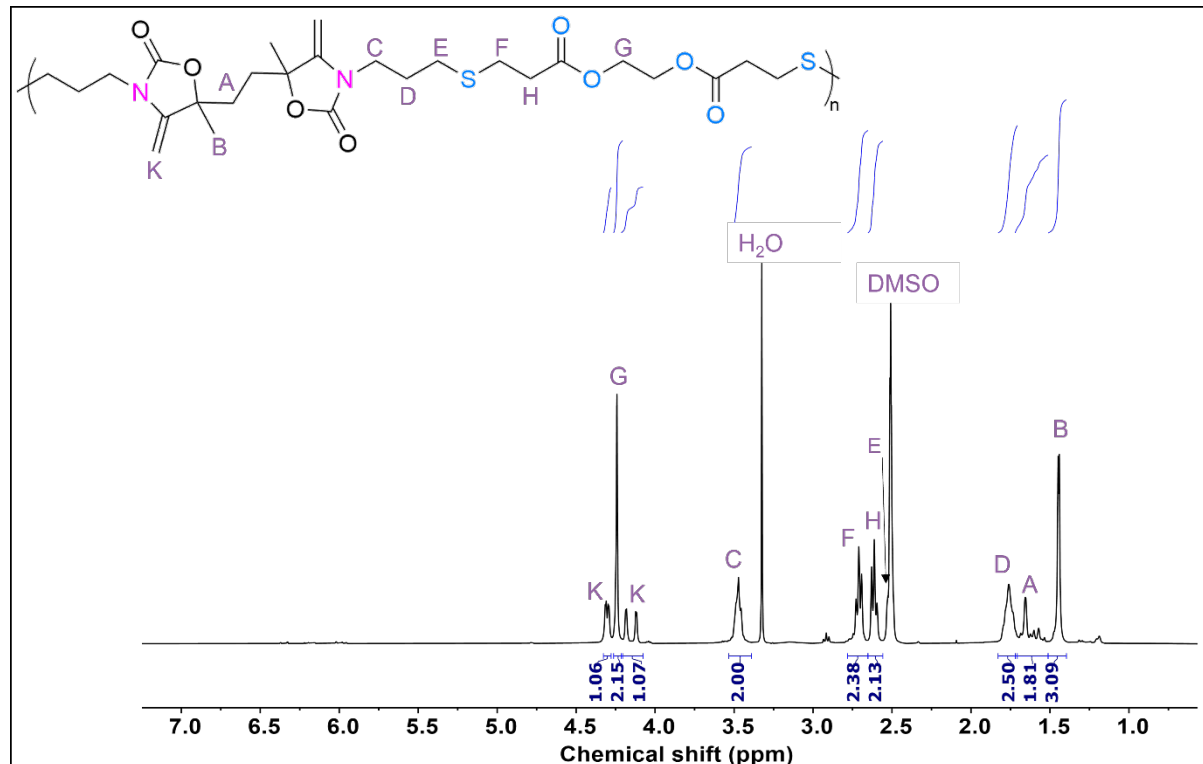


Figure S72. ¹H-NMR spectrum of P2c-dehydrated (400 MHz, DMSO-*d*₆).

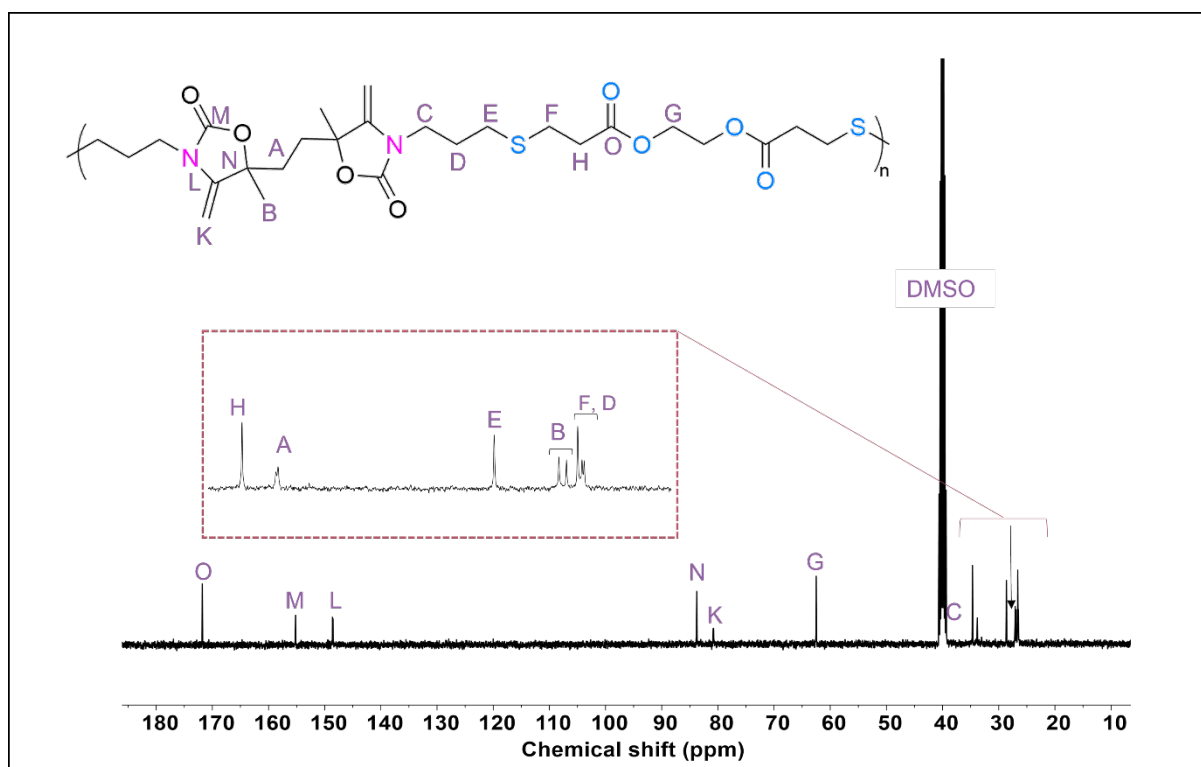


Figure S73. ^{13}C -NMR spectrum of P2c-dehydrated (100 MHz, $\text{DMSO-}d_6$).

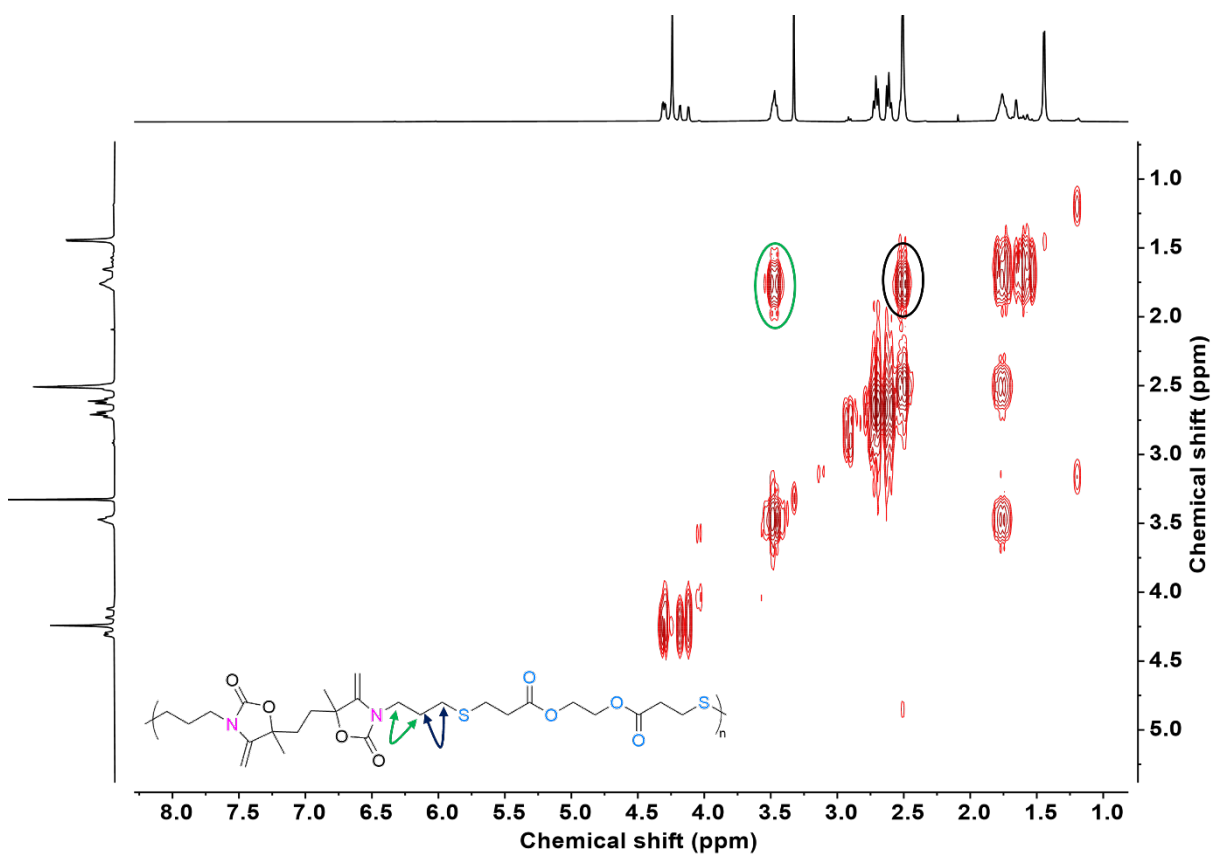


Figure S74. COSY NMR spectrum of P2c-dehydrated (400 MHz, $\text{DMSO-}d_6$).

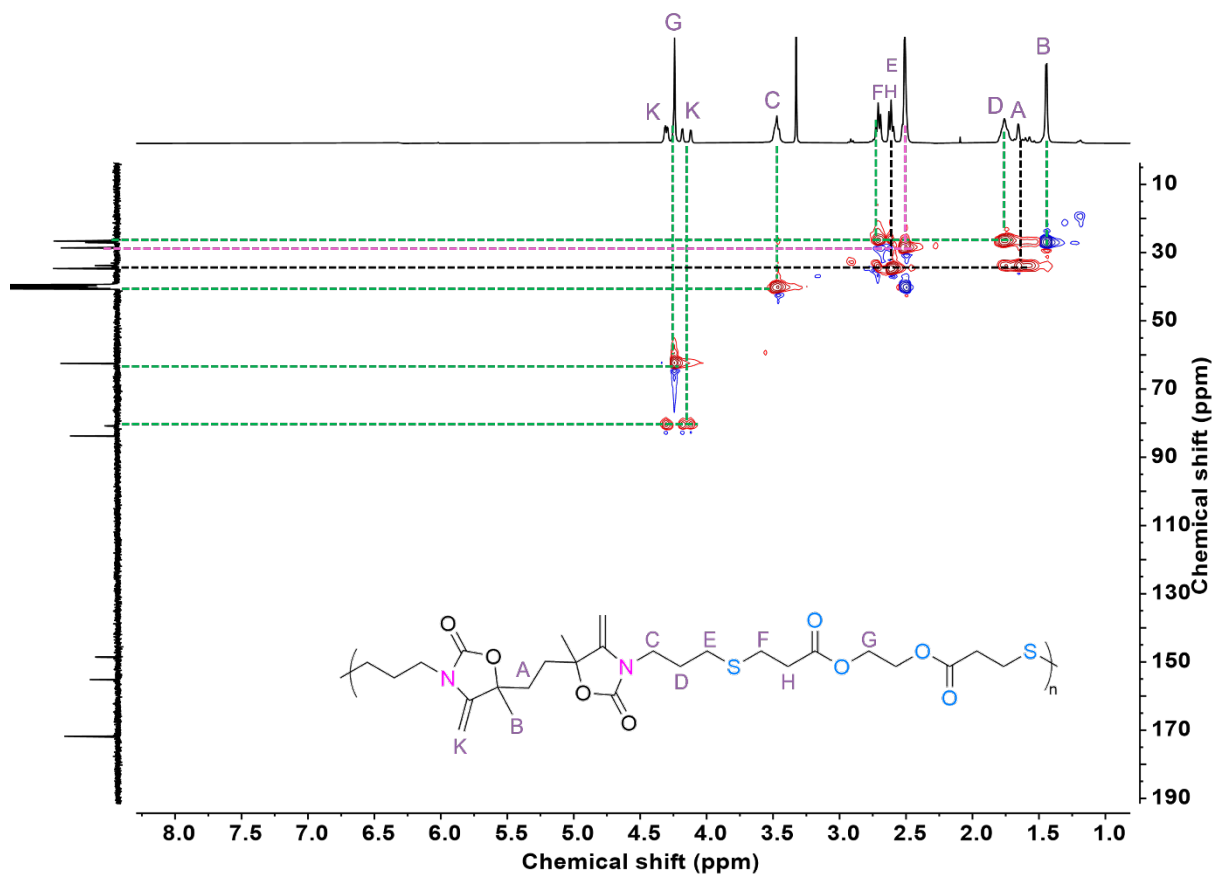


Figure S75. ^1H - ^{13}C HSQC NMR spectrum of P2c-dehydrated (400 MHz, $\text{DMSO-}d_6$).

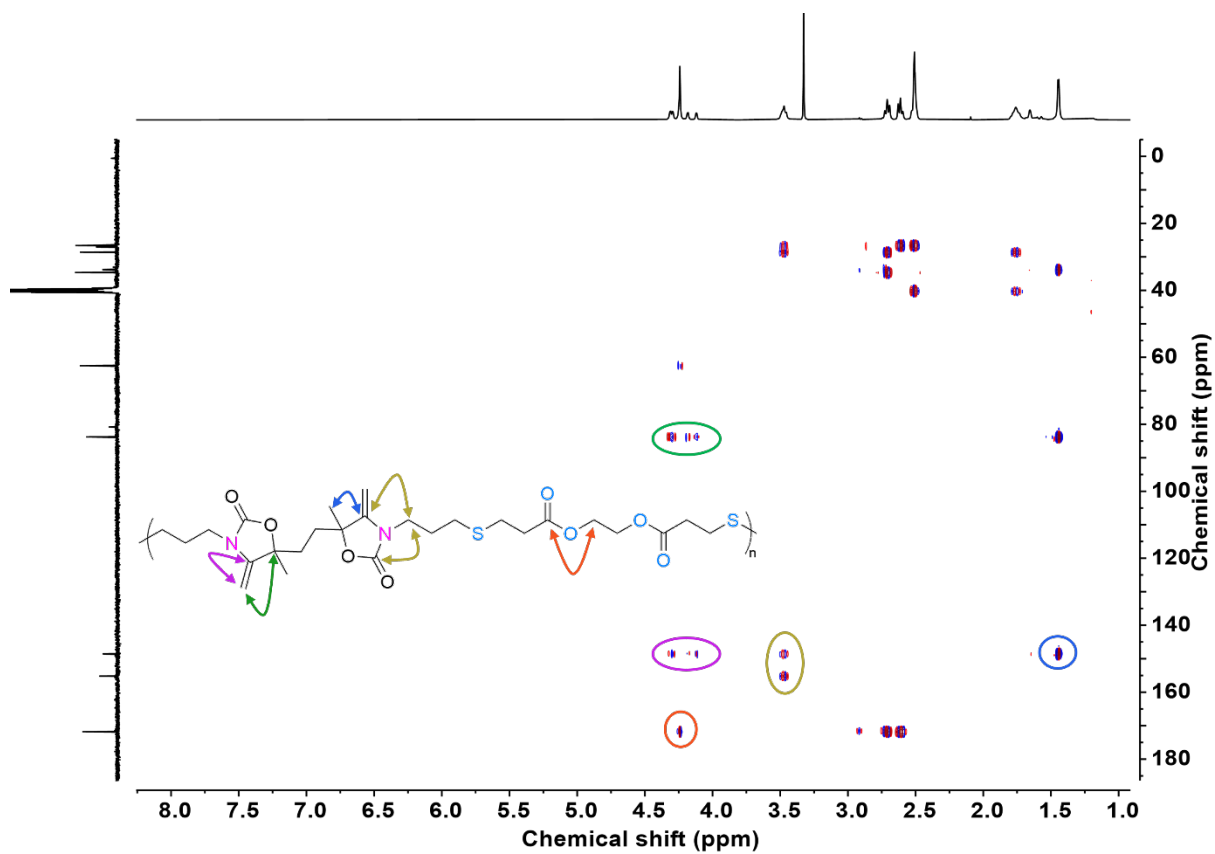


Figure S76. HMBC NMR spectrum of P2c-dehydrated (400 MHz, DMSO- d_6).

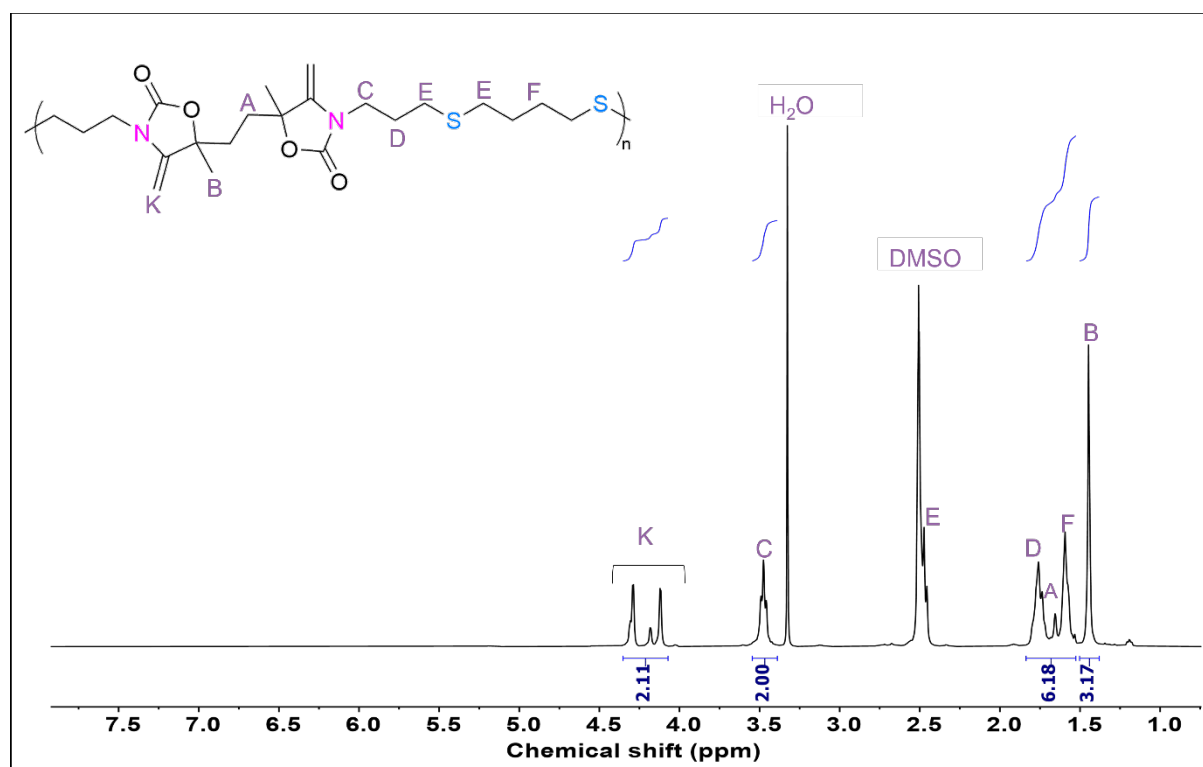


Figure S77. ^1H -NMR spectrum of P2d-dehydrated (400 MHz, DMSO- d_6).

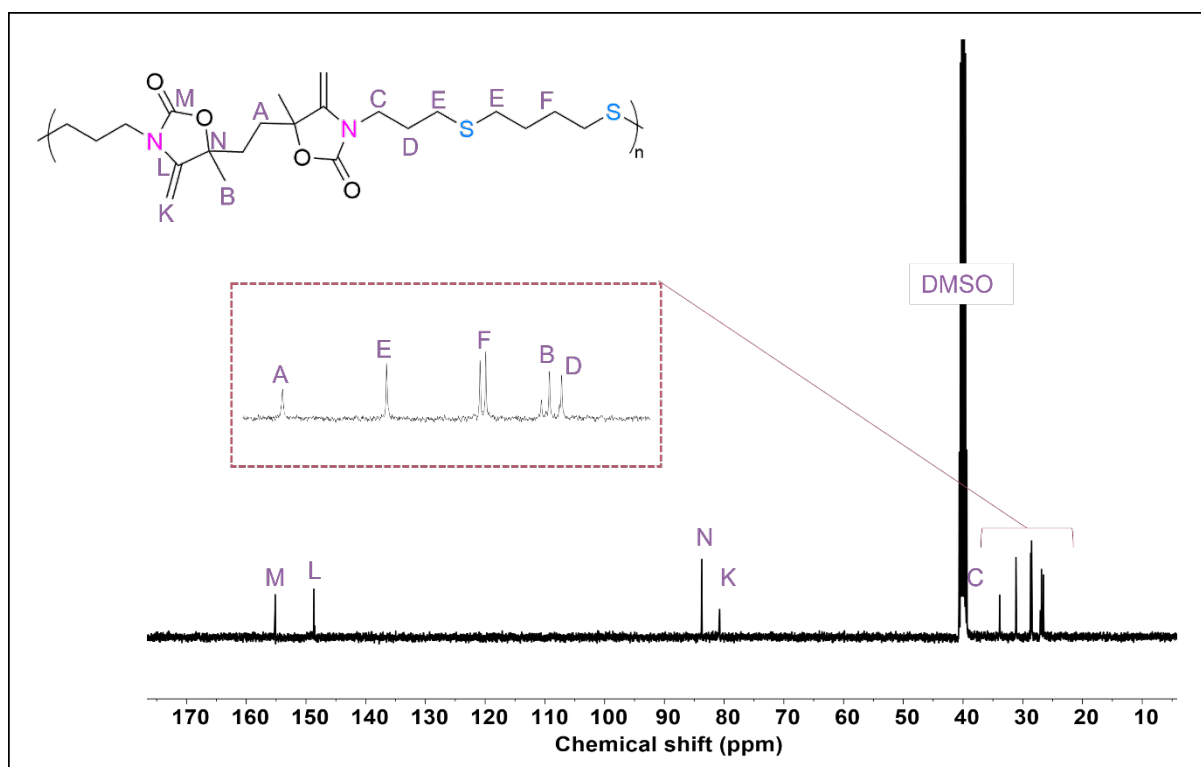


Figure S78. ^{13}C -NMR spectrum of P2d-dehydrated (100 MHz, $\text{DMSO-}d_6$).

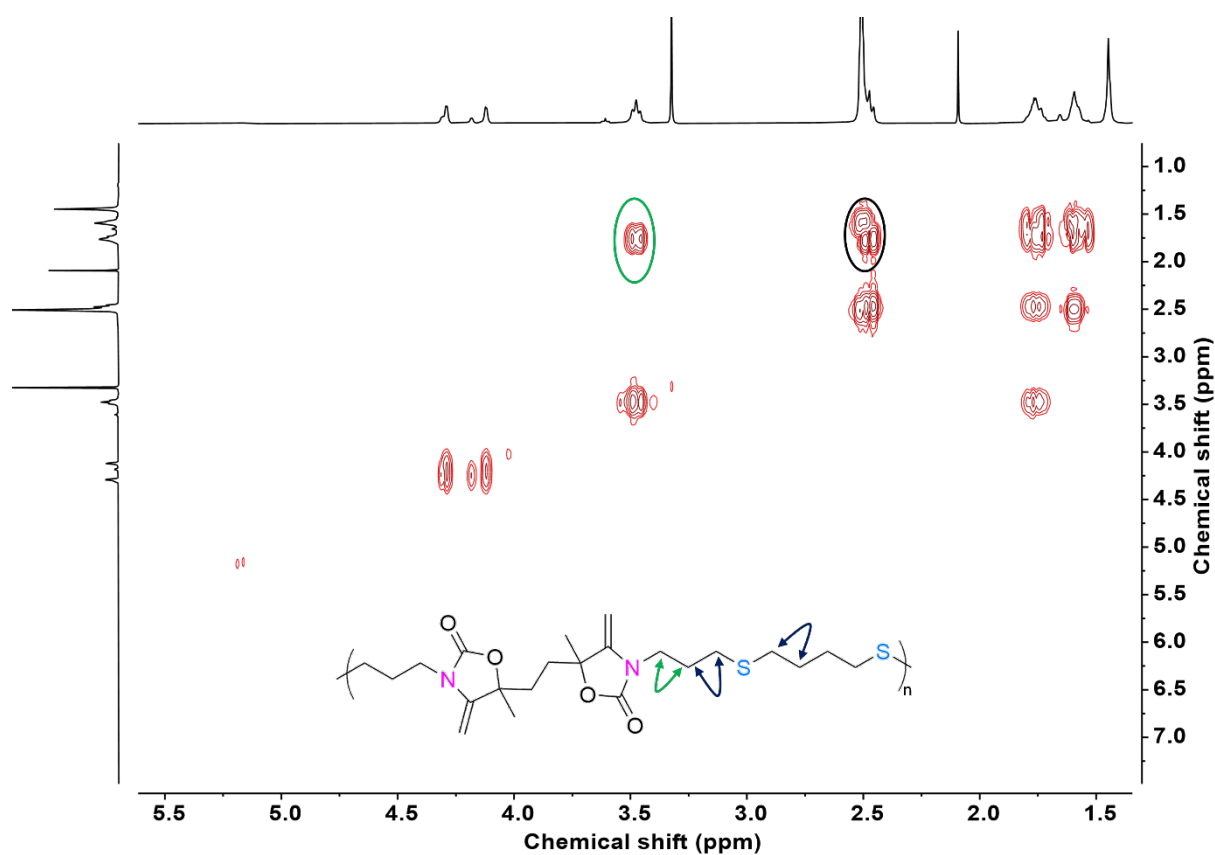


Figure S79. COSY NMR spectrum of P2d-dehydrated (400 MHz, $\text{DMSO-}d_6$).

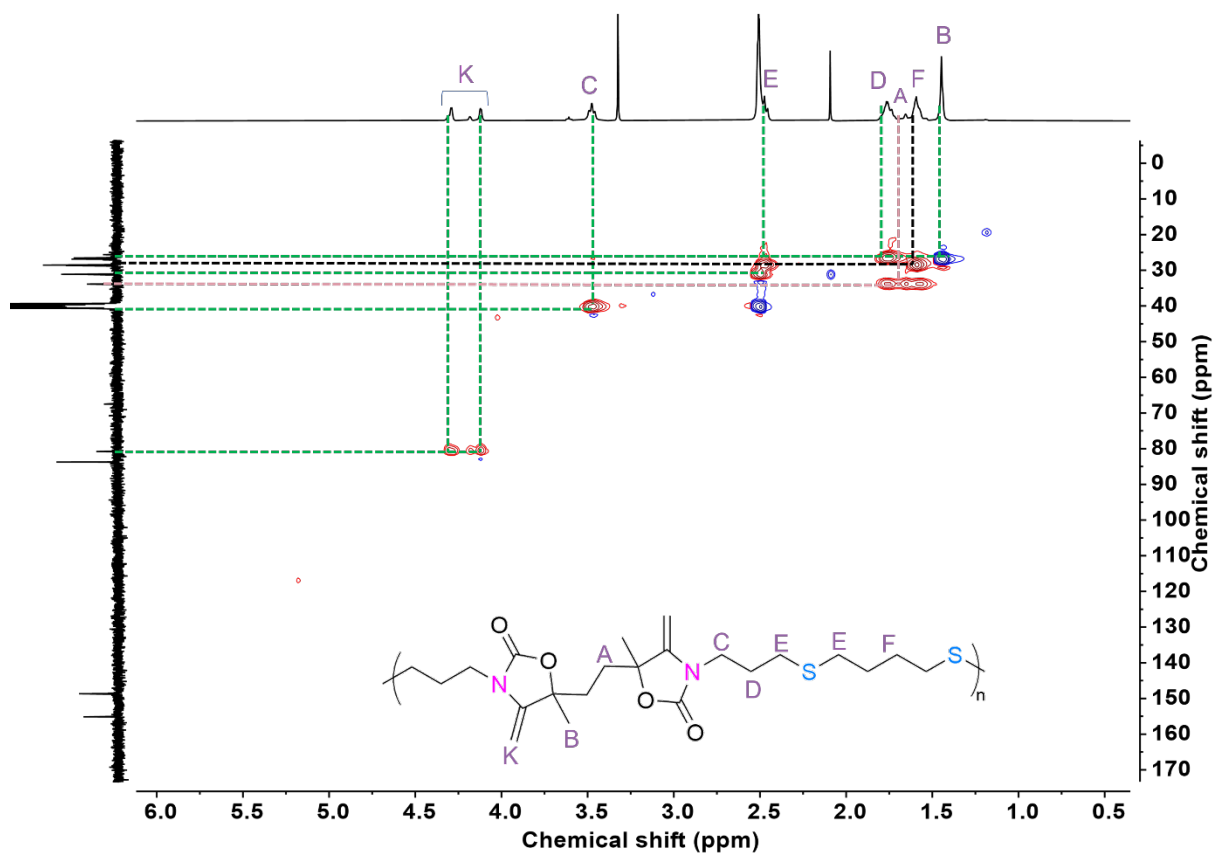


Figure S80. ^1H - ^{13}C HSQC NMR spectrum of P2d-dehydrated (400 MHz, $\text{DMSO-}d_6$).

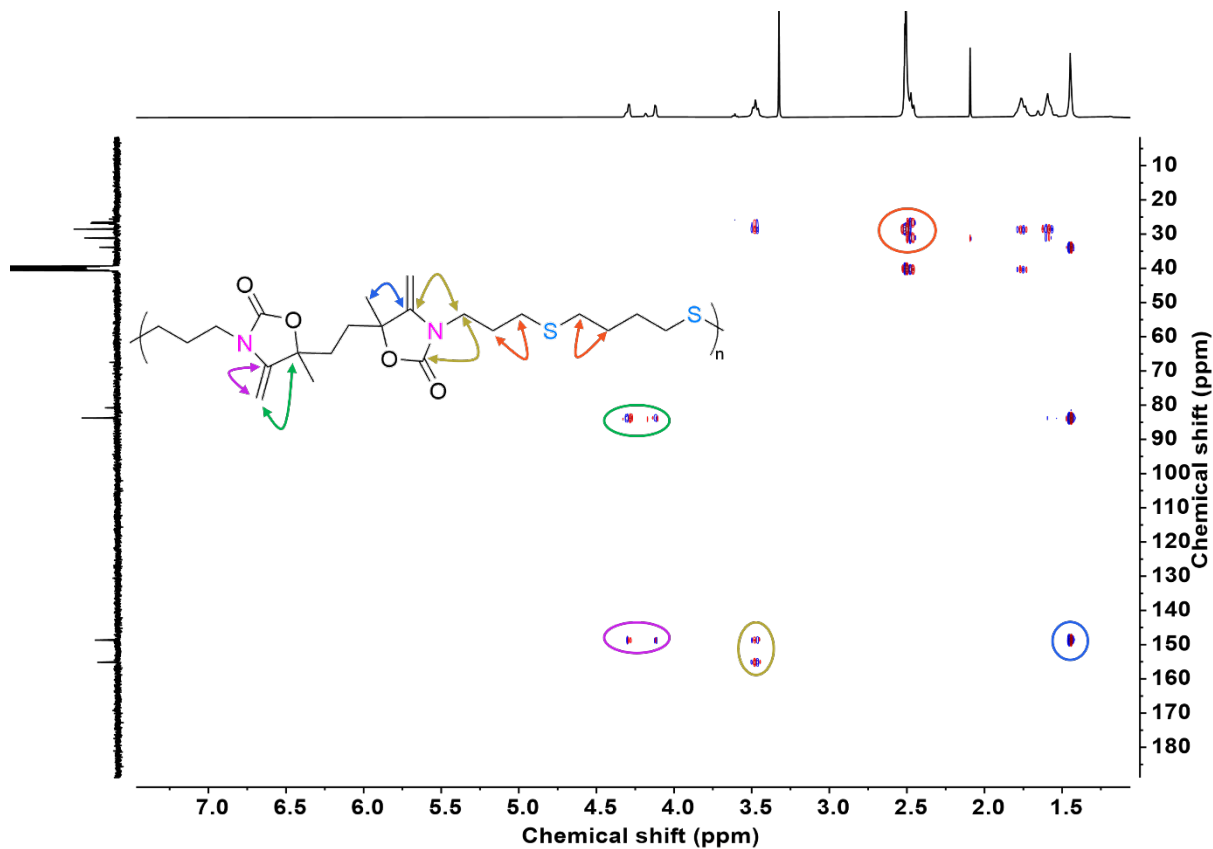


Figure S81. HMBC NMR spectrum of P2d-dehydrated (400 MHz, $\text{DMSO-}d_6$).

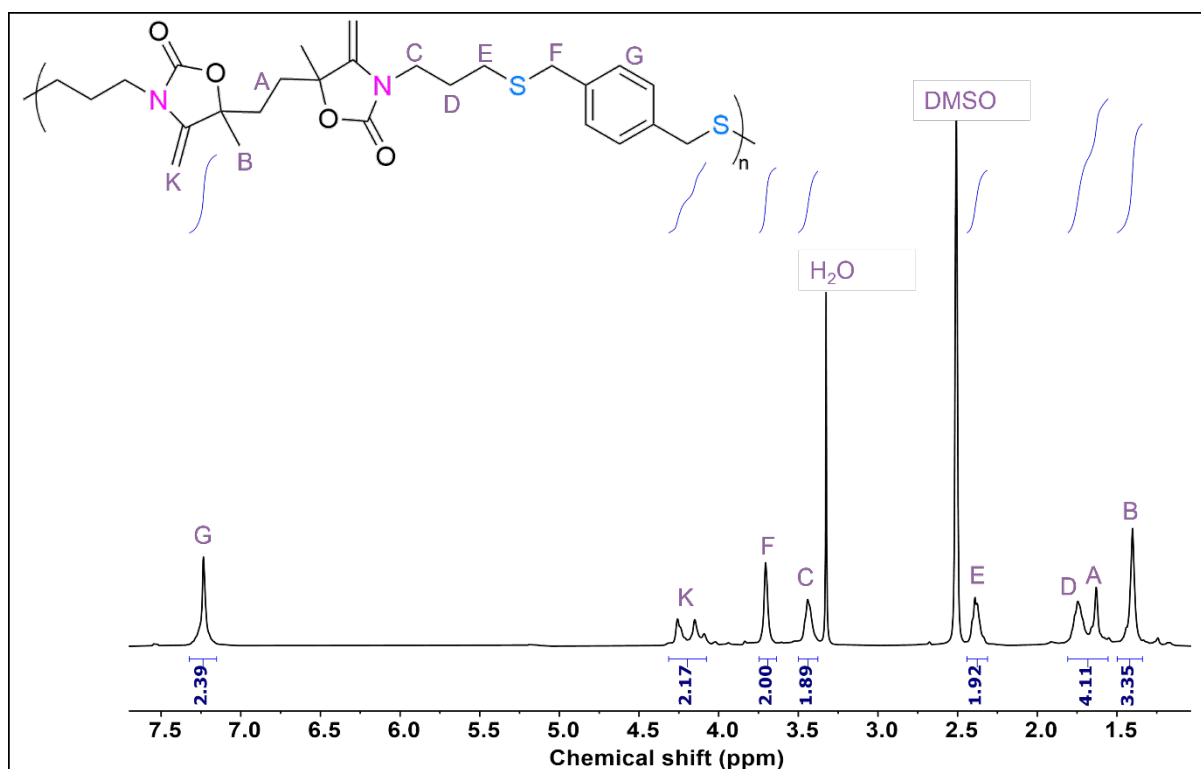


Figure S82. $^1\text{H-NMR}$ spectrum of P2e-dehydrated (400 MHz, DMSO- d_6).

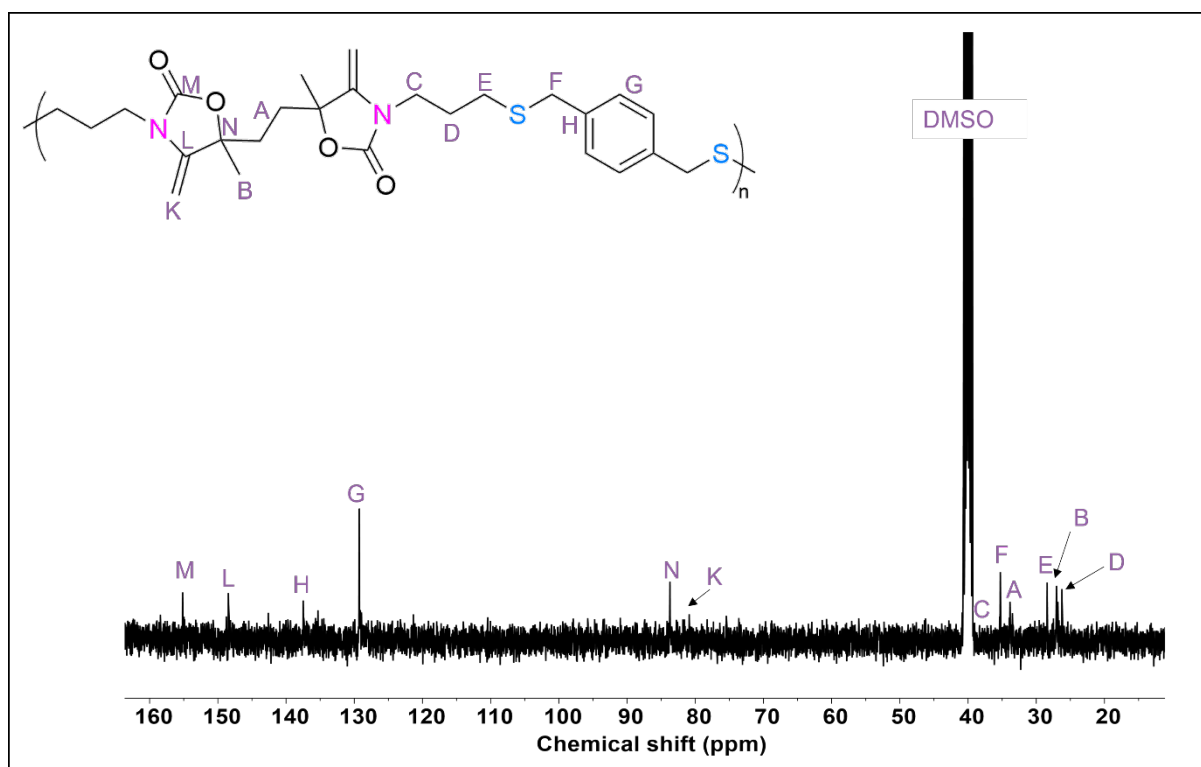


Figure S83. $^{13}\text{C-NMR}$ spectrum of P2e-dehydrated (100 MHz, DMSO- d_6).

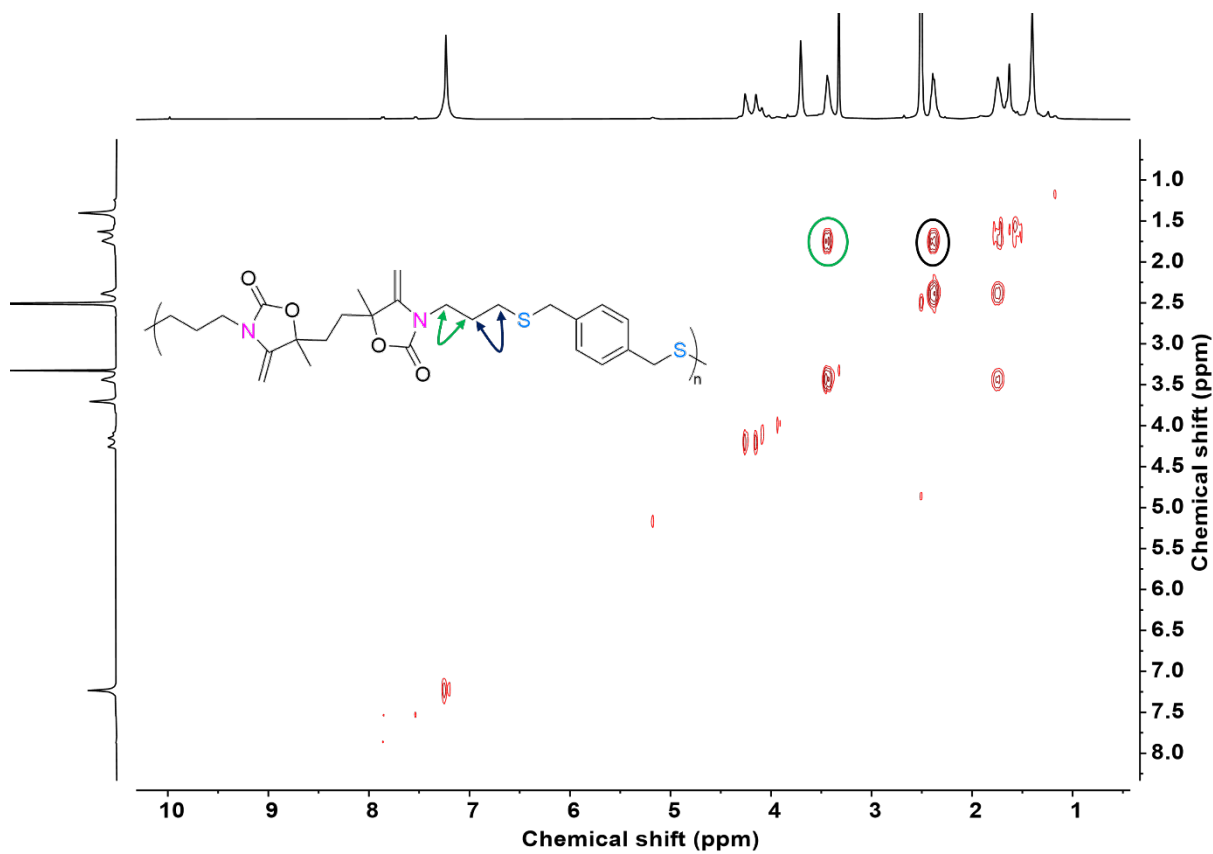


Figure S84. COSY NMR spectrum of P2e-dehydrated (400 MHz, DMSO- d_6).

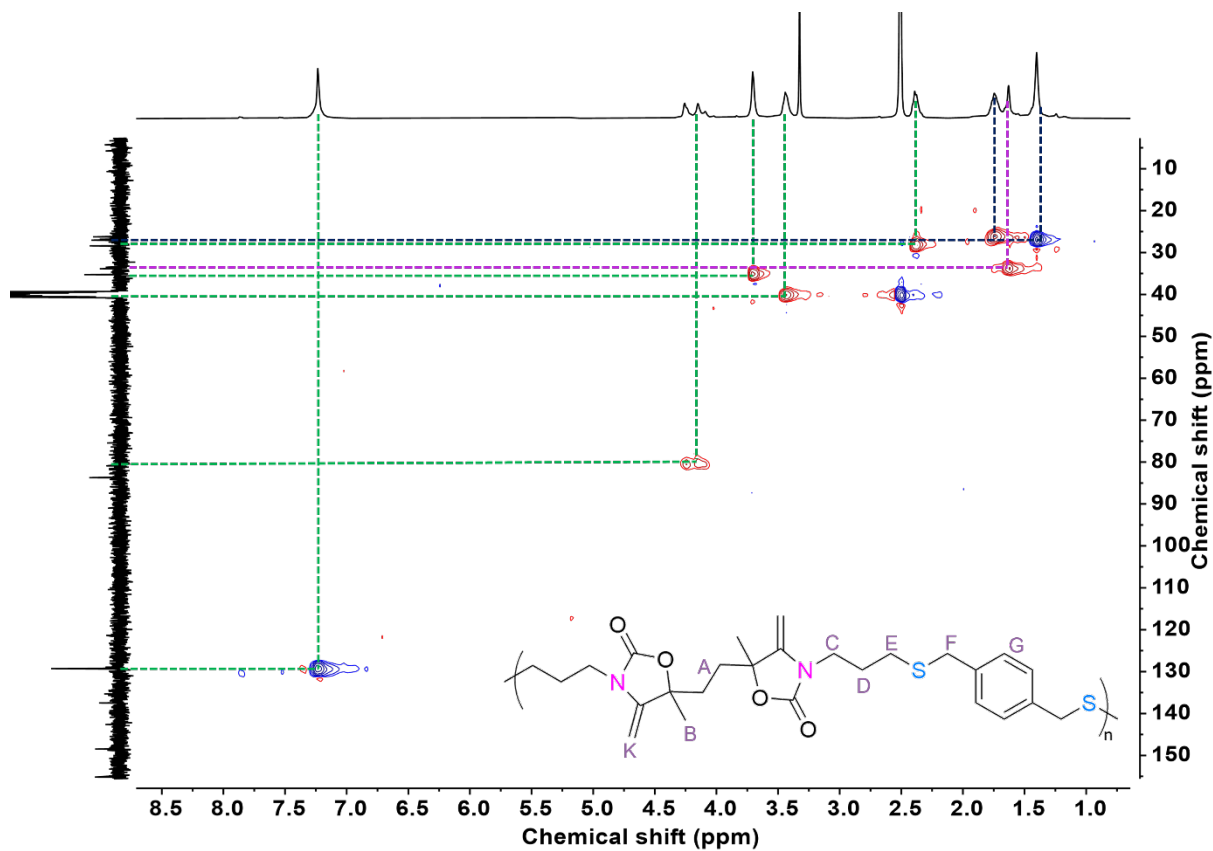


Figure S85. ^1H - ^{13}C HSQC NMR spectrum of P2e-dehydrated (400 MHz, DMSO- d_6).

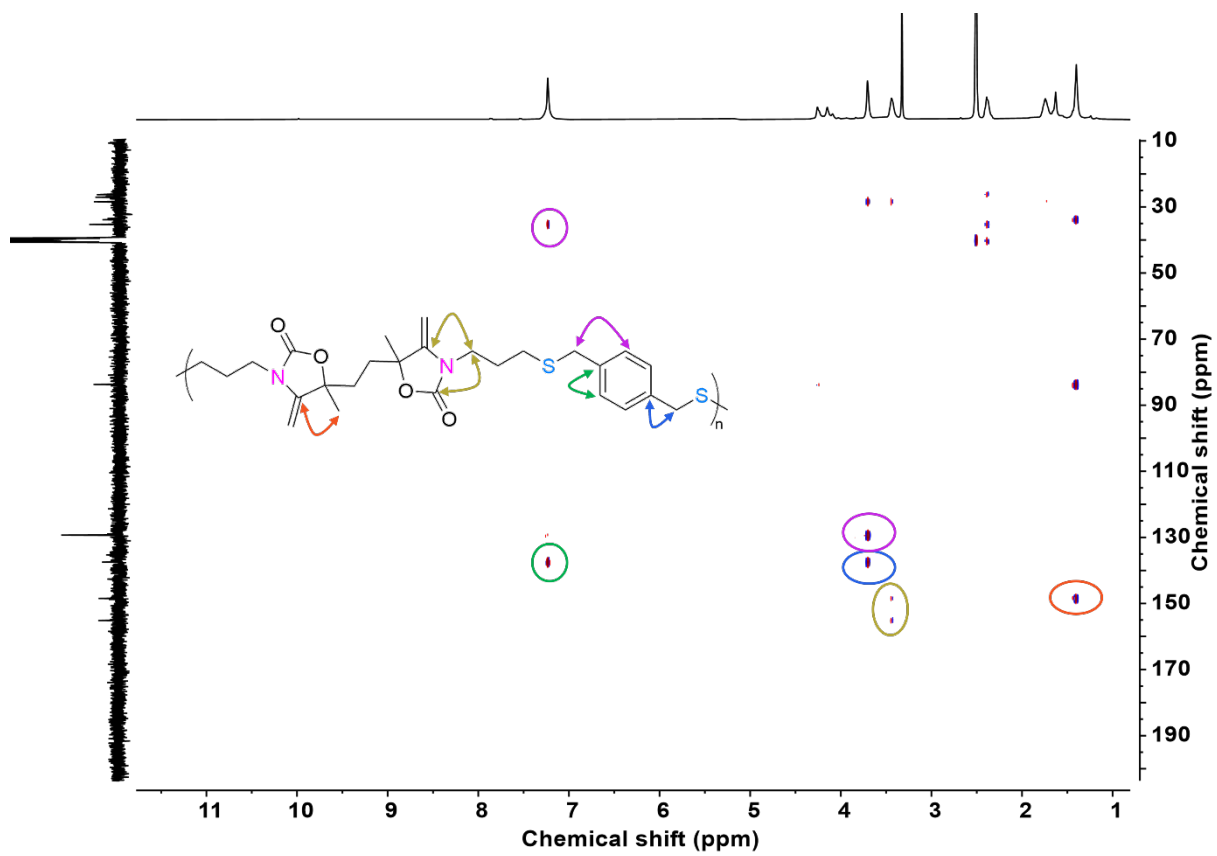


Figure S86. HMBC NMR spectrum of P2e-dehydrated (400 MHz, DMSO- d_6).

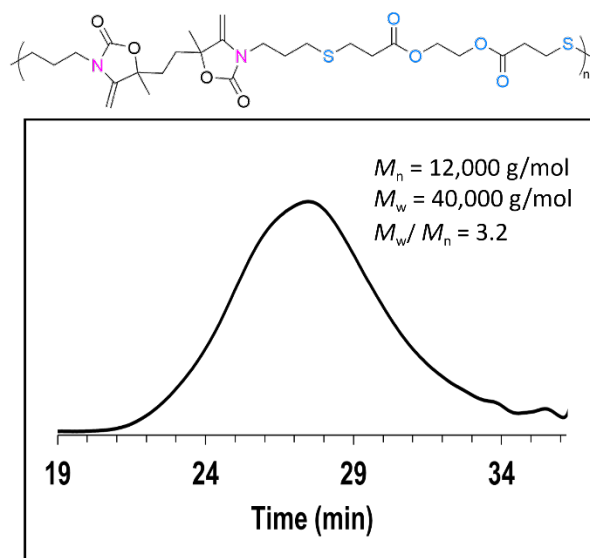


Figure S89. SEC chromatogram of **P2c-dehydrated** (in DMF/LiBr).

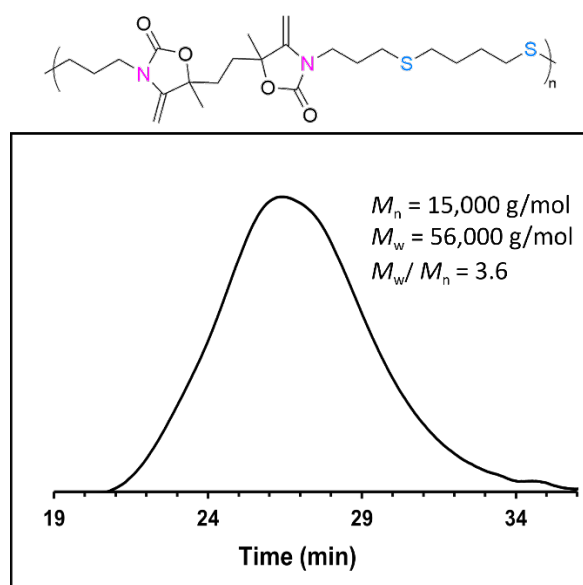


Figure S90. SEC chromatogram of **P2d-dehydrated** (in DMF/LiBr).

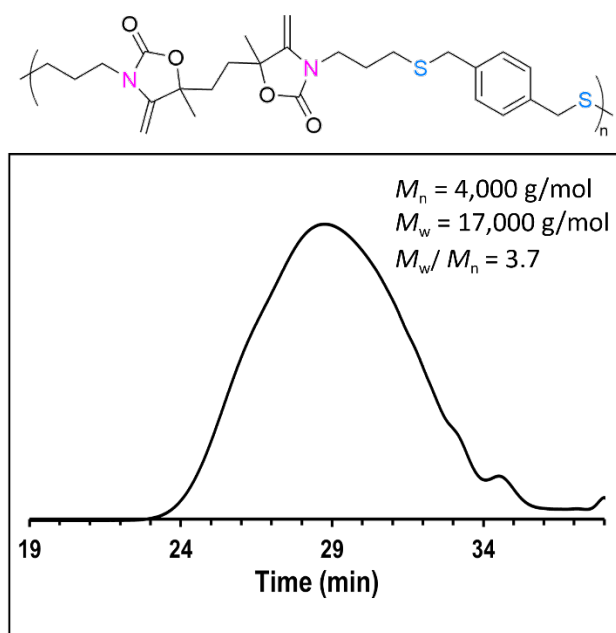


Figure S91. SEC chromatogram of **P2e-dehydrated** (in DMF/LiBr).

Table S3. Molecular characteristics of hydrated and dehydrated copolymers

Entry	Polymer	POxa-hydrated			POxa-dehydrated		
		M_n^a (g/mol)	M_w^a (g/mol)	Dispersity ^a	M_n^a (g/mol)	M_w^a (g/mol)	Dispersity ^a
1	P2a	31,000	101,000	3.2	11,000	41,000	3.5
2	P2b	20,000	57,000	2.7	15,000	56,000	3.7
3	P2c	21,000	64,000	3.0	12,000	40,000	3.2
4	P2d	23,000	69,000	3.0	15,000	56,000	3.6
5	P2e	8,000	20,000	2.5	4,000	17,000	3.7

^a Determined on pure products by SEC in DMF/LiBr calibrated with PS standards

15- TGA of dehydrated samples

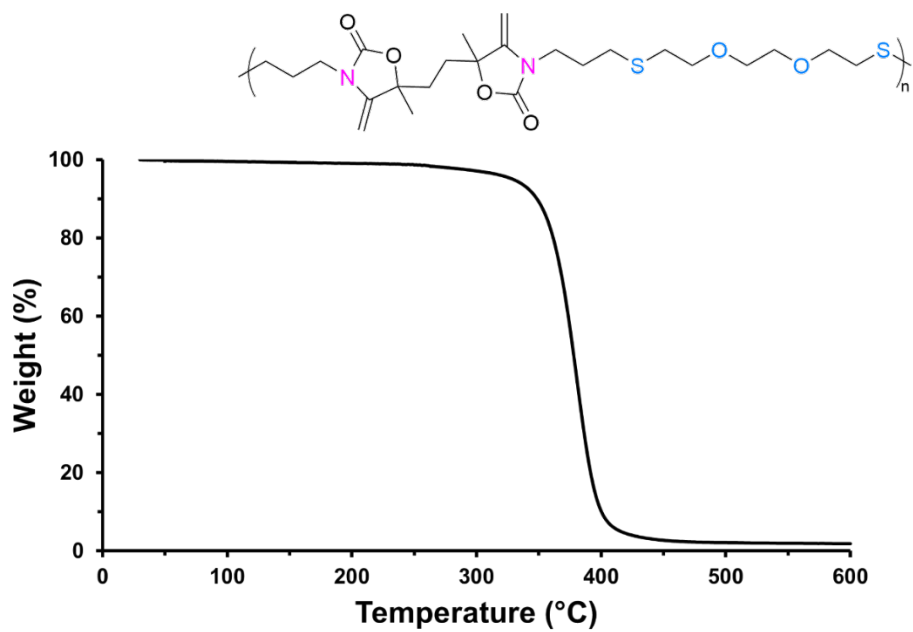


Figure S92. TGA thermogram of P2a-dehydrated

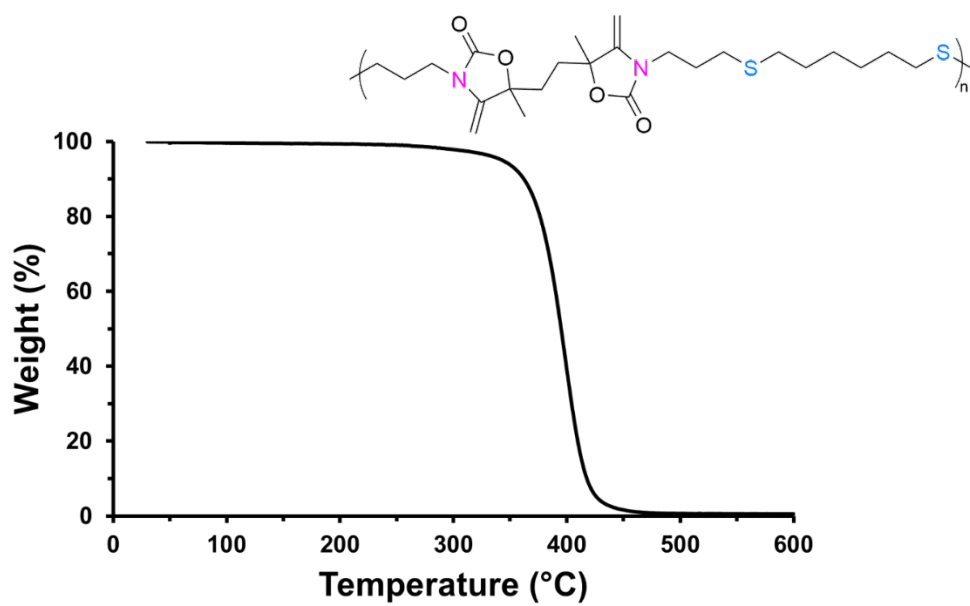


Figure S93. TGA thermogram of P2b-dehydrated

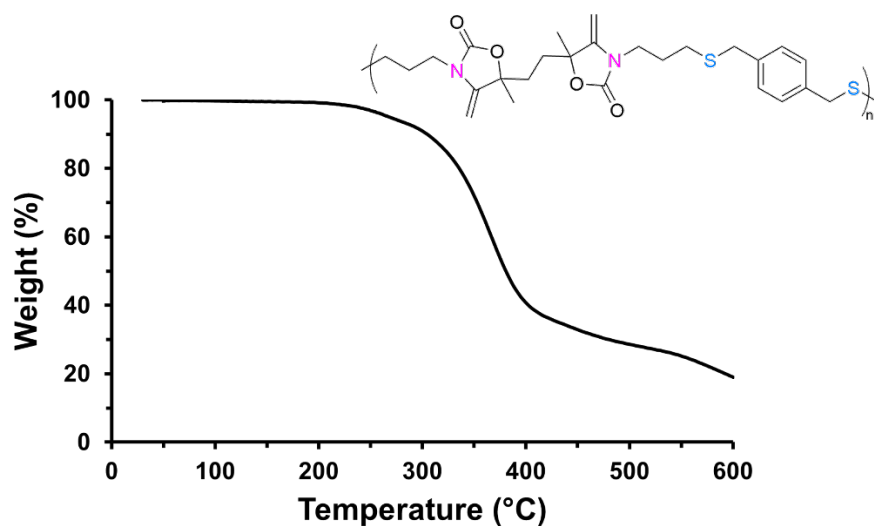


Figure S96. TGA thermogram of P2e-dehydrated

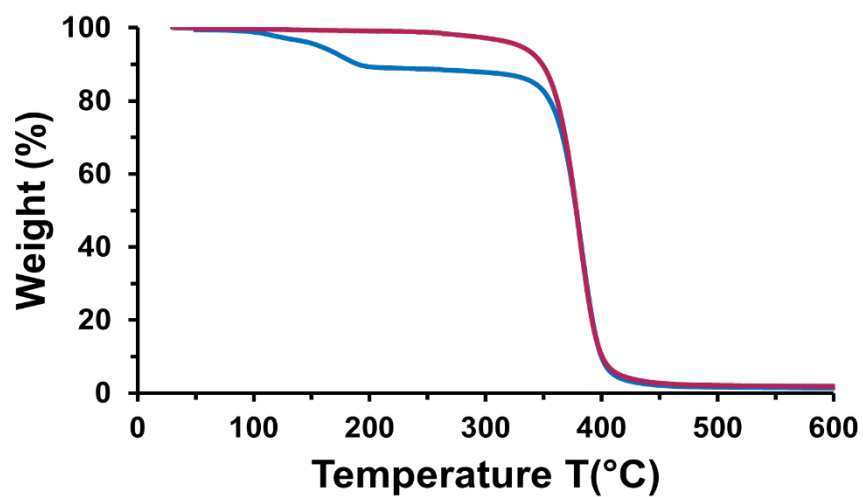


Figure S97. overlay of TGA curves for POxa (blue) and POxa-dehydrated (magenta); (samples P2b and P2b-dehydrated as a representative example)

16- DSC characterization of hydrated polymers

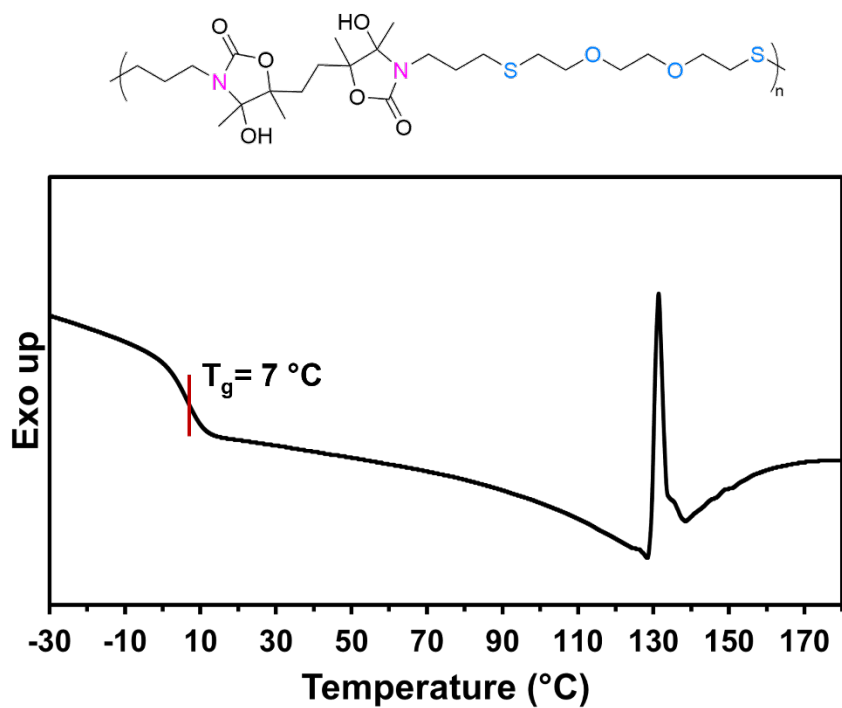


Figure S98. Reversing heat flow using modulated DSC of P2a

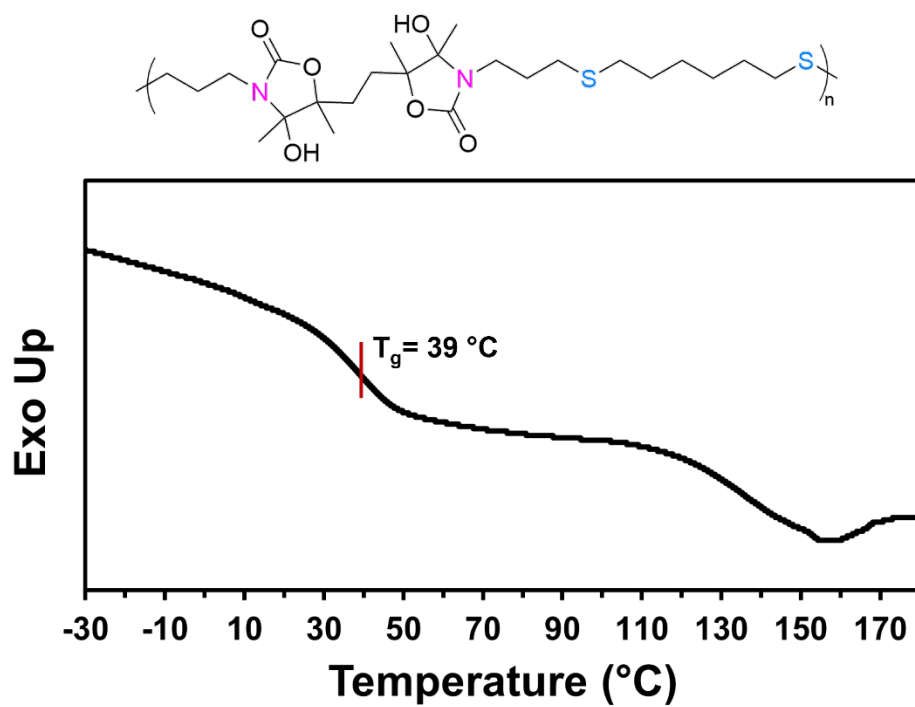


Figure S99. Reversing heat flow using modulated DSC of P2b

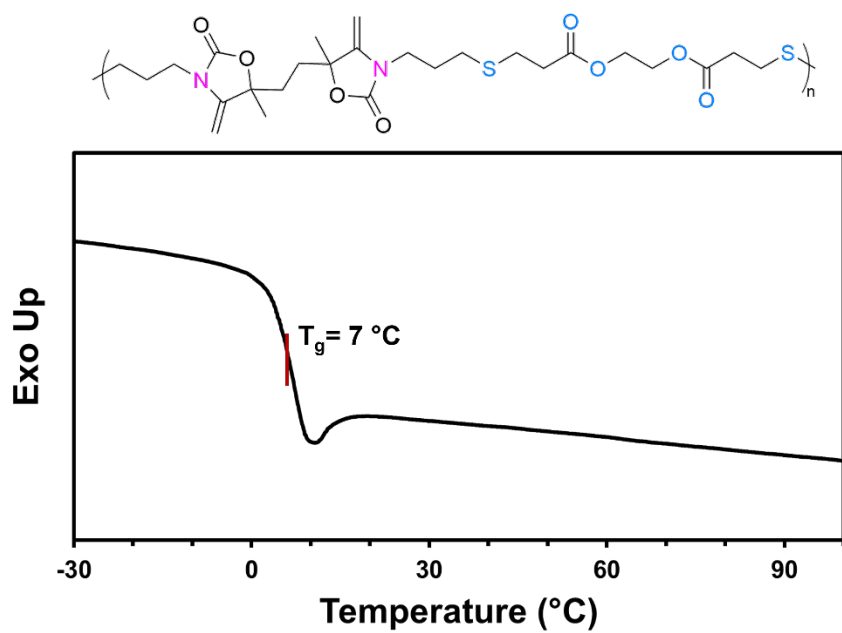


Figure S105. DSC characterization of P2c-dehydrated

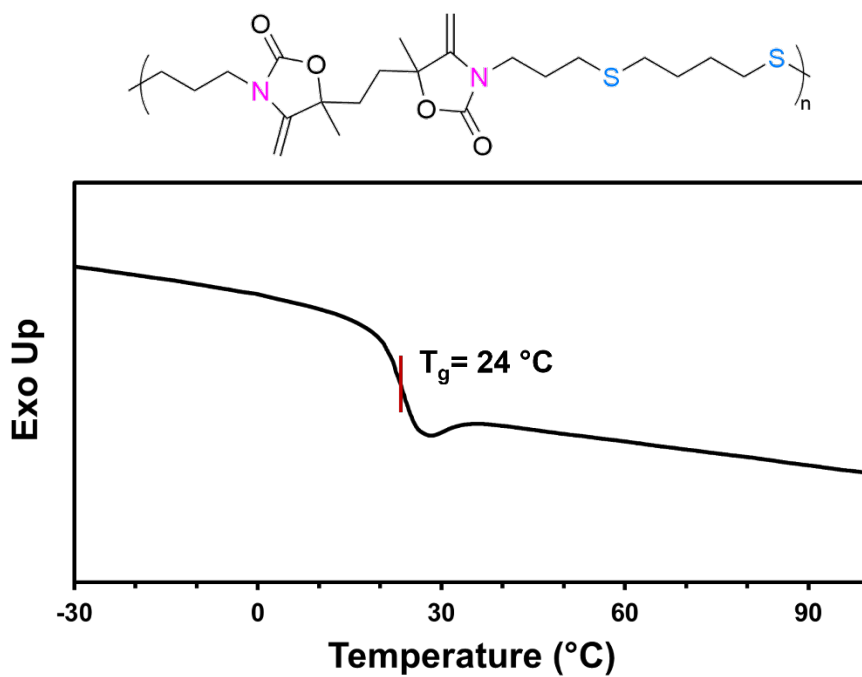


Figure S106. DSC characterization of P2d-dehydrated

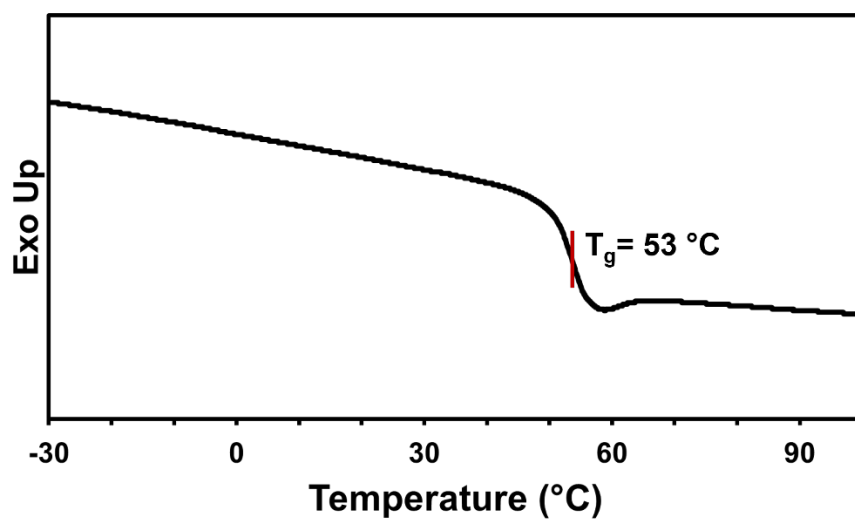
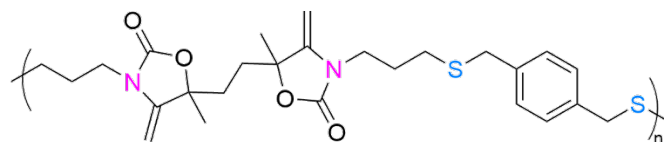


Figure S107. DSC characterization of P2e-dehydrated

18- Mechanical properties – Tensile test

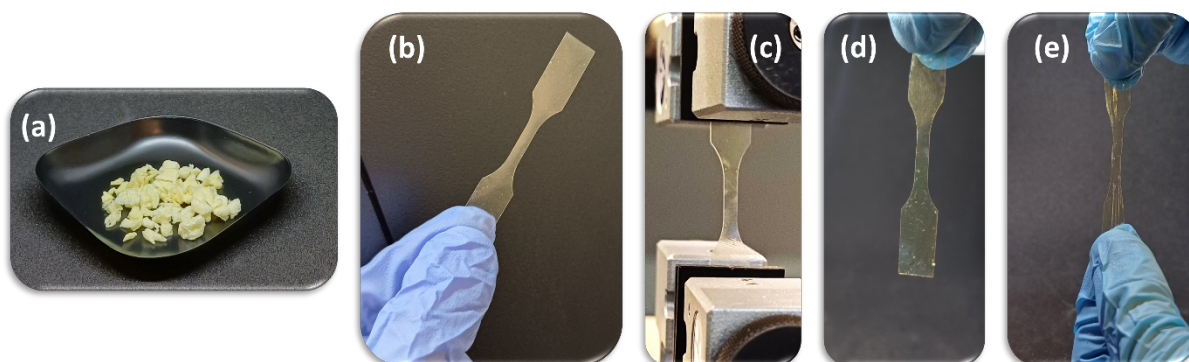


Figure S108. (a) Polymer **P2a** sectioned into small fragments, (b) dog-bone shaped sample of **P2a**, (c) tensile strength experimental setup for **P2a**, (d) dog-bone shaped sample of **P2a-dehydrated**, (e) representative figure of **P2a-dehydrated**'s behavior when exposed to stress

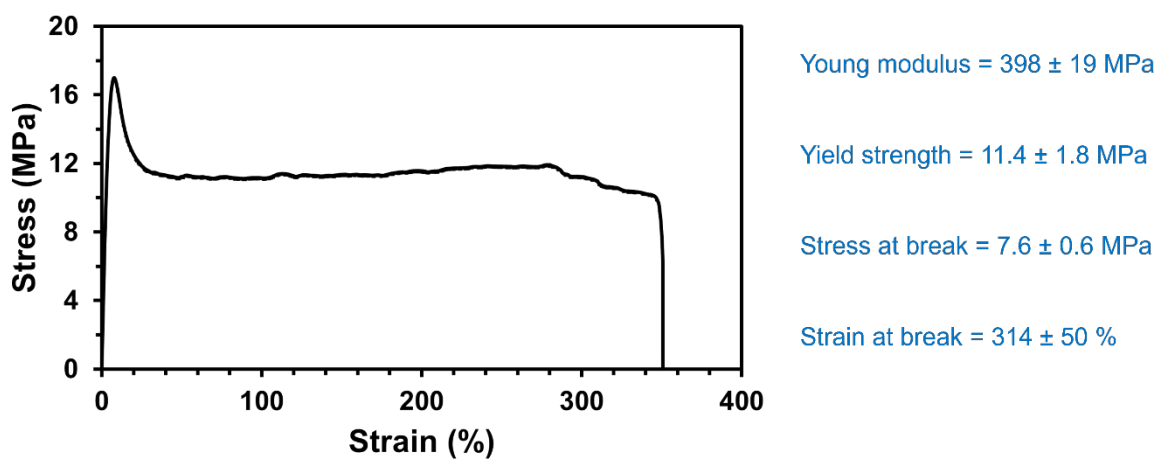


Figure S109. Representative stress-strain curve of **P2a** and mechanical properties determined over five tests.

19- Chemical stability

Pressed polymer films of **P2a** were cut into small pieces (50 mg) and immersed in 6 mL of sulfuric acid and sodium hydroxide aqueous solutions of different concentrations of (0.1 M, 1 M and 5 M) for 48 h. Except in the case of the 1 M NaOH solution, all polymers remained insoluble. The recovered solids were characterized by $^1\text{H-NMR}$ spectroscopy (Figure S112 and Figure S114) and by SEC (Figure S111 and Figure S113).

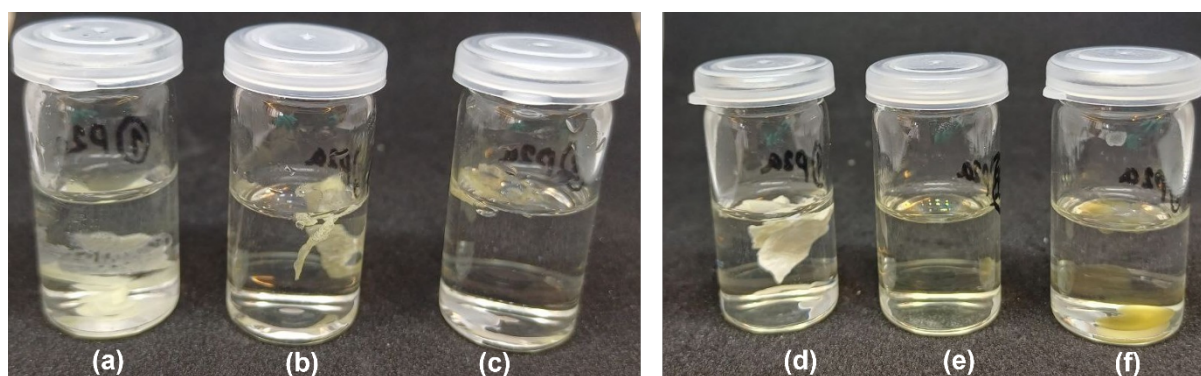


Figure S110. Comparative visual documentation of **P2a** polymer samples after 48 hours exposure to acidic and basic environments (a) in H_2SO_4 (0.1 M), (b) in H_2SO_4 (1 M), (c) in H_2SO_4 (5 M); (d) in NaOH (0.1 M), (e) in NaOH (1 M), (f) in NaOH (5 M)

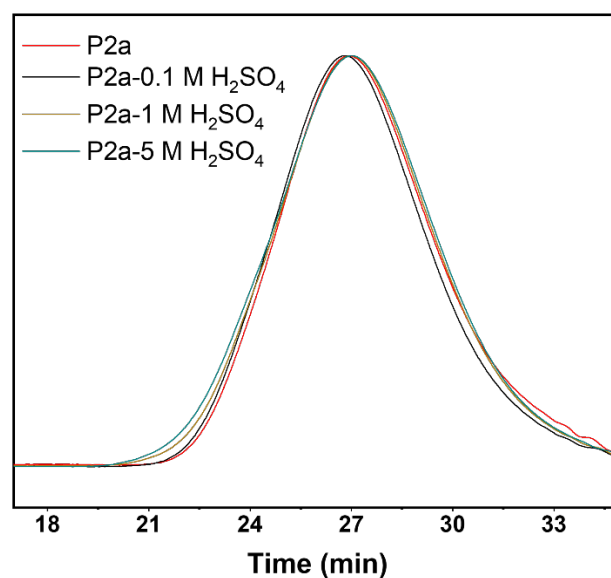


Figure S111. SEC chromatograms comparing **P2a** before and after a 48-hour immersion in an acidic environment, highlighting the polymer's stability (in DMF/LiBr).

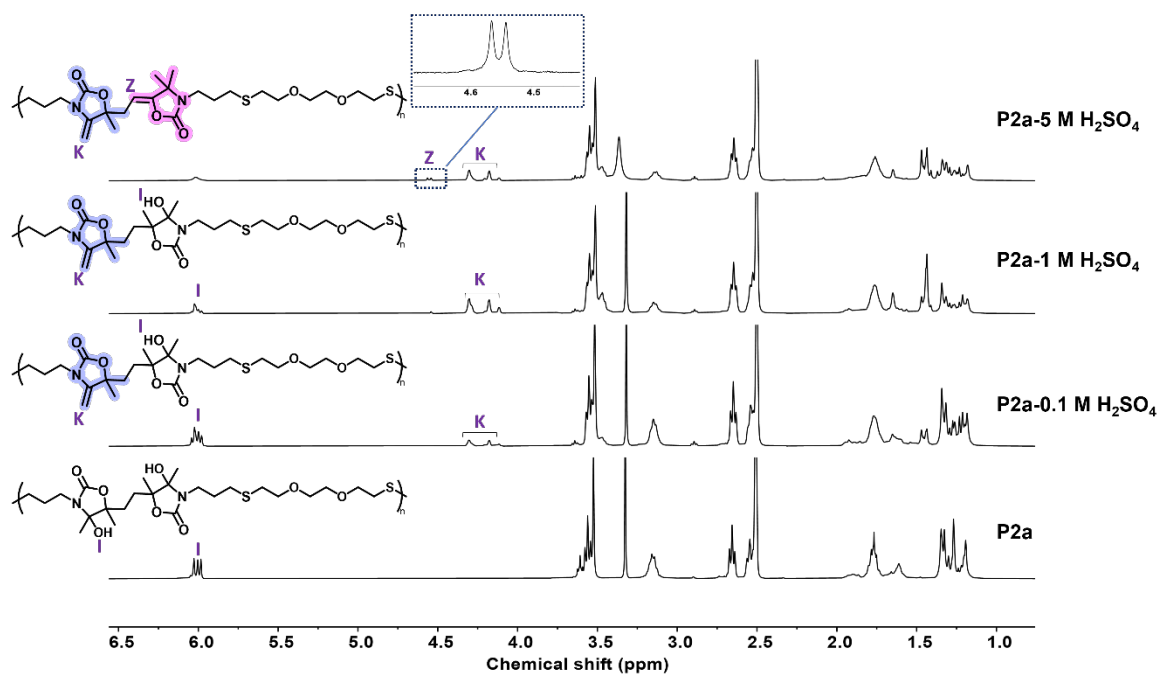


Figure S112. $^1\text{H-NMR}$ spectrum comparing **P2a** before and after a 48-hour immersion in an acidic environment (400 MHz, $\text{DMSO-}d_6$).

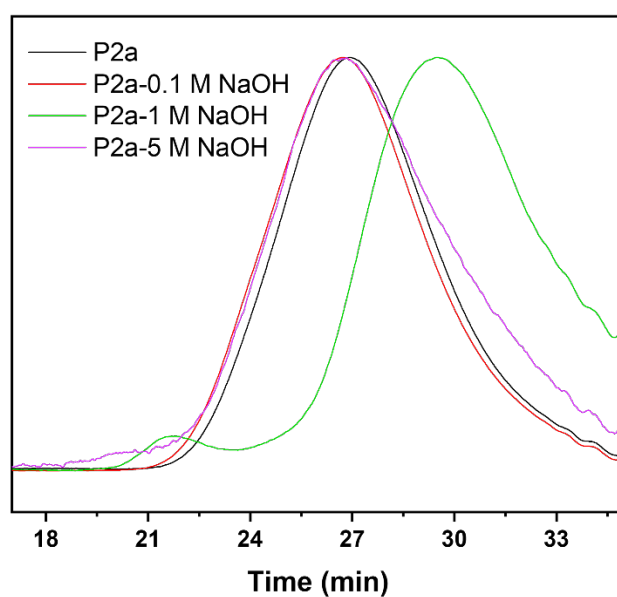


Figure S113. SEC chromatograms comparing **P2a** before and after a 48-hour immersion in basic environment, highlighting the polymer's stability (in DMF/LiBr).

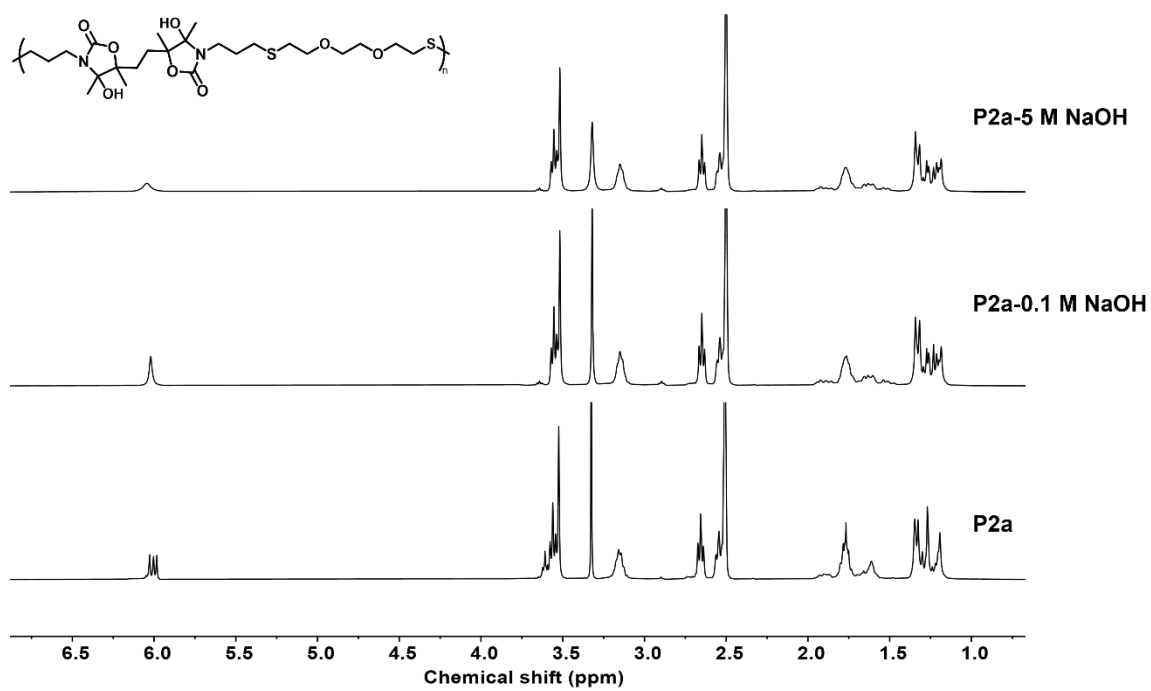


Figure S114. ¹H-NMR spectrum comparing **P2a** before and after a 48-hour immersion in basic environment (400 MHz, DMSO-*d*₆).

20- Structure characterizations of P2b-Sulfoxide (oxidation to sulfoxide)

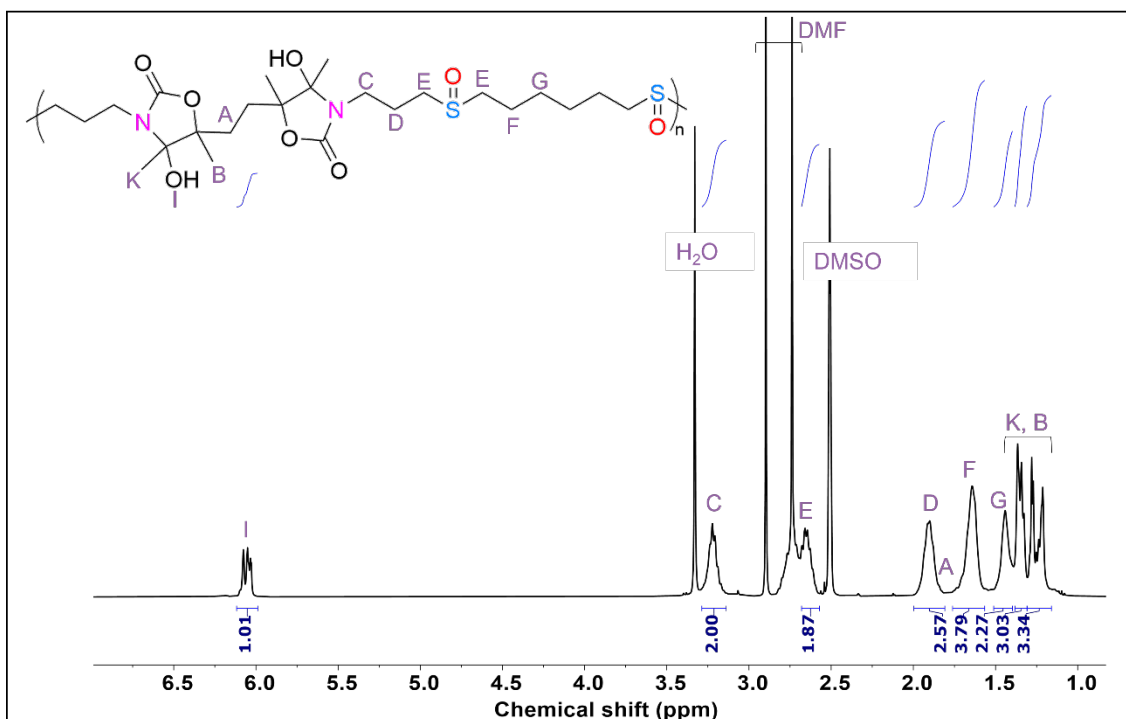


Figure S115. $^1\text{H-NMR}$ spectrum (400 MHz, DMSO-d_6) of P2b-Sulfoxide.

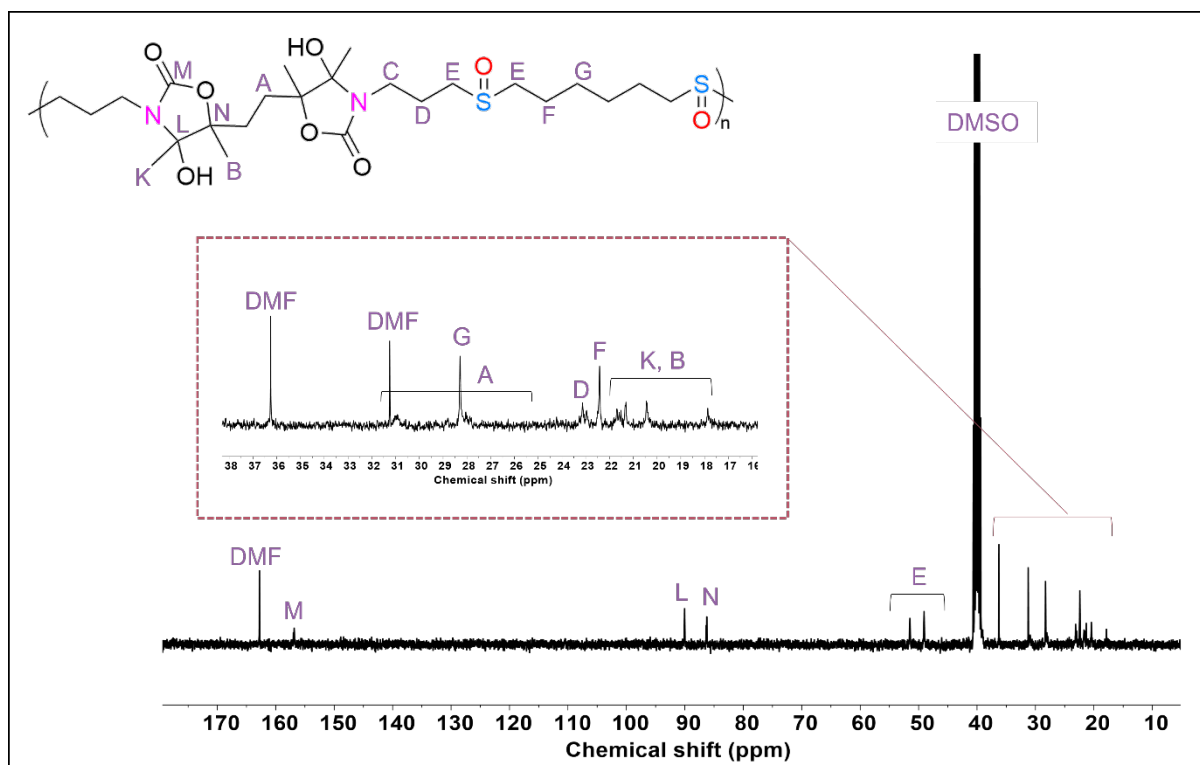


Figure S116. $^{13}\text{C-NMR}$ spectrum (100 MHz, DMSO-d_6) of P2b-Sulfoxide.

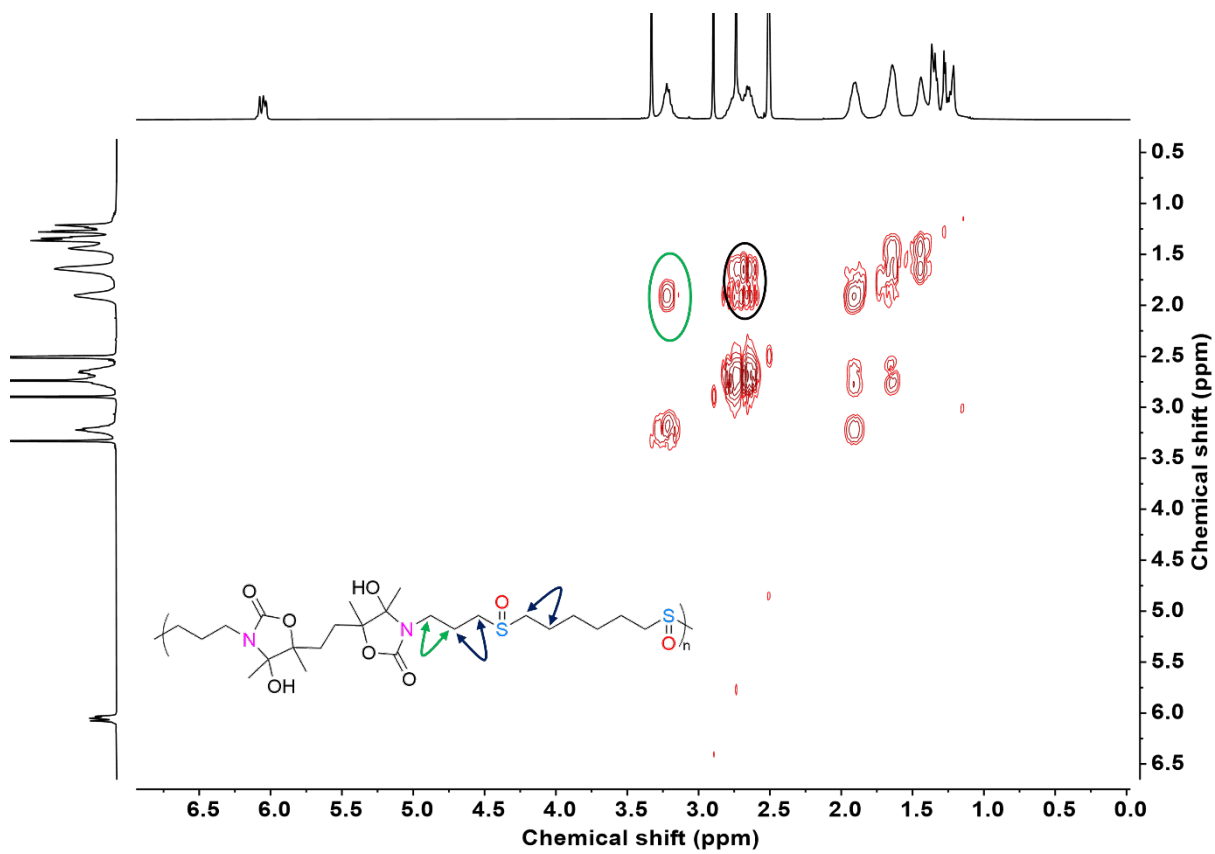


Figure S117. COSY NMR spectrum of P2b-Sulfoxide (400 MHz, DMSO-*d*₆).

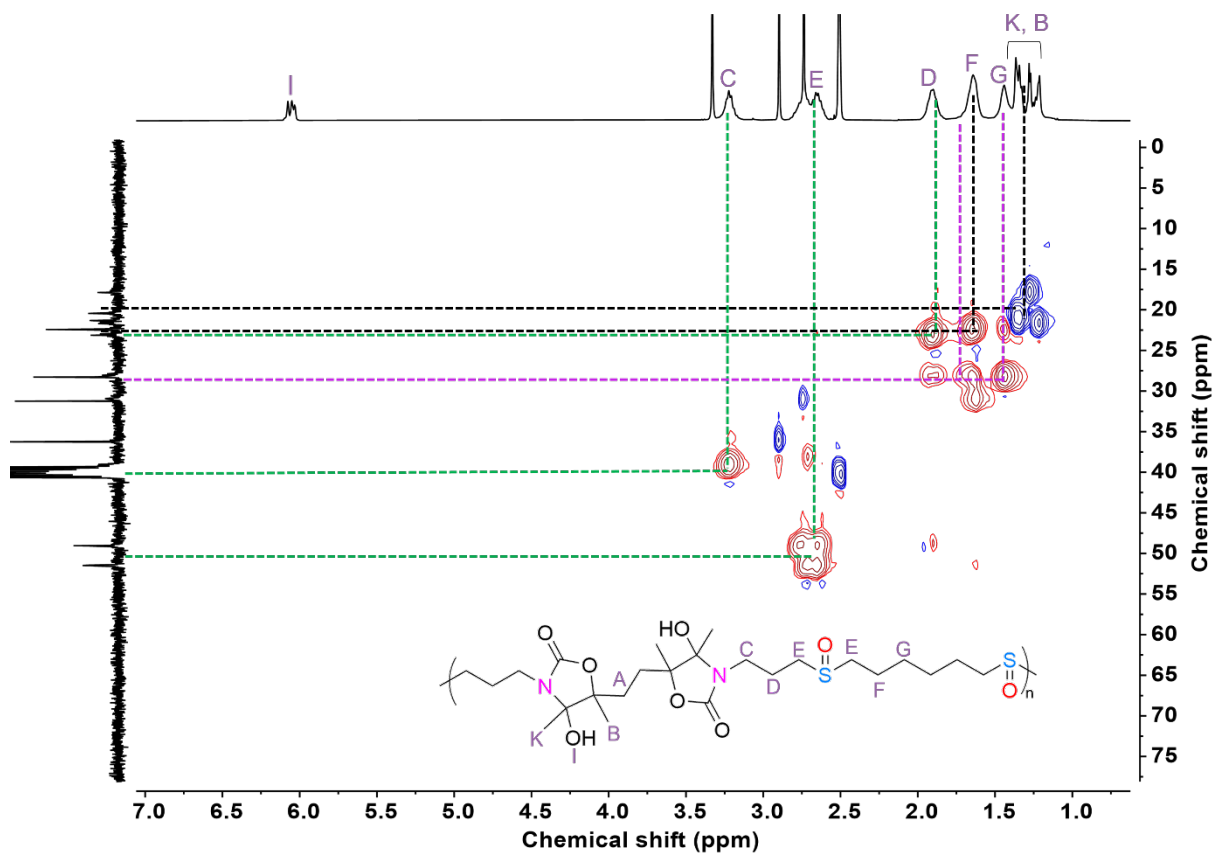


Figure S118. ^1H - ^{13}C HSQC NMR spectrum of **P2b-Sulfoxide** (400 MHz, $\text{DMSO-}d_6$).

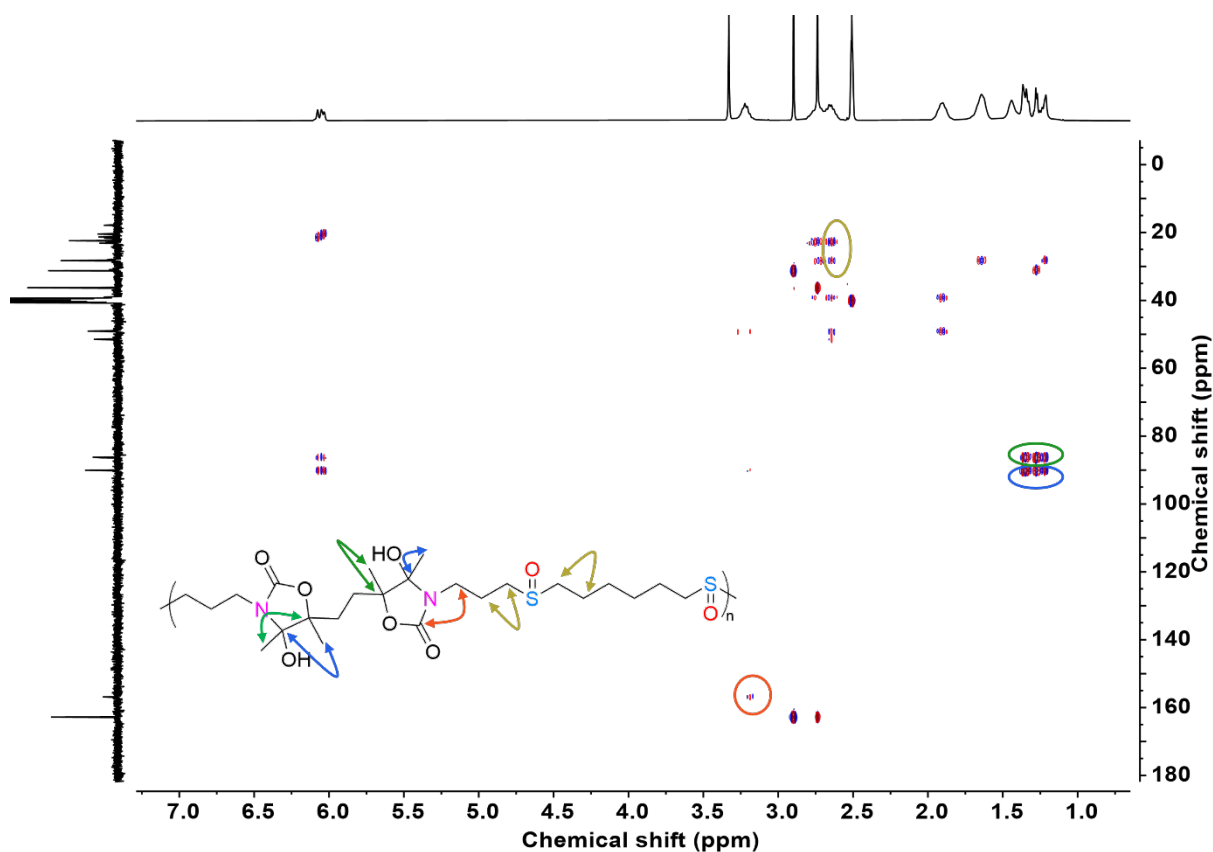


Figure S119. HMBC NMR spectrum of **P2b-Sulfoxide** (400 MHz, $\text{DMSO-}d_6$).

To further confirm the quantitative sulfoxide formation, ^1H -NMR was also conducted in $\text{DMF-}d_7$ as a solvent (Figure S73). It is verified that signals associated to protons adjacent to thioethers ($\delta=2.51$ - 2.64 ppm) were vanished, substituted with a new downfield peak ($\delta=2.70$ - 2.90 ppm) corresponding to the methylene protons adjacent to the sulfoxide groups ($-\text{SOCH}_2$).

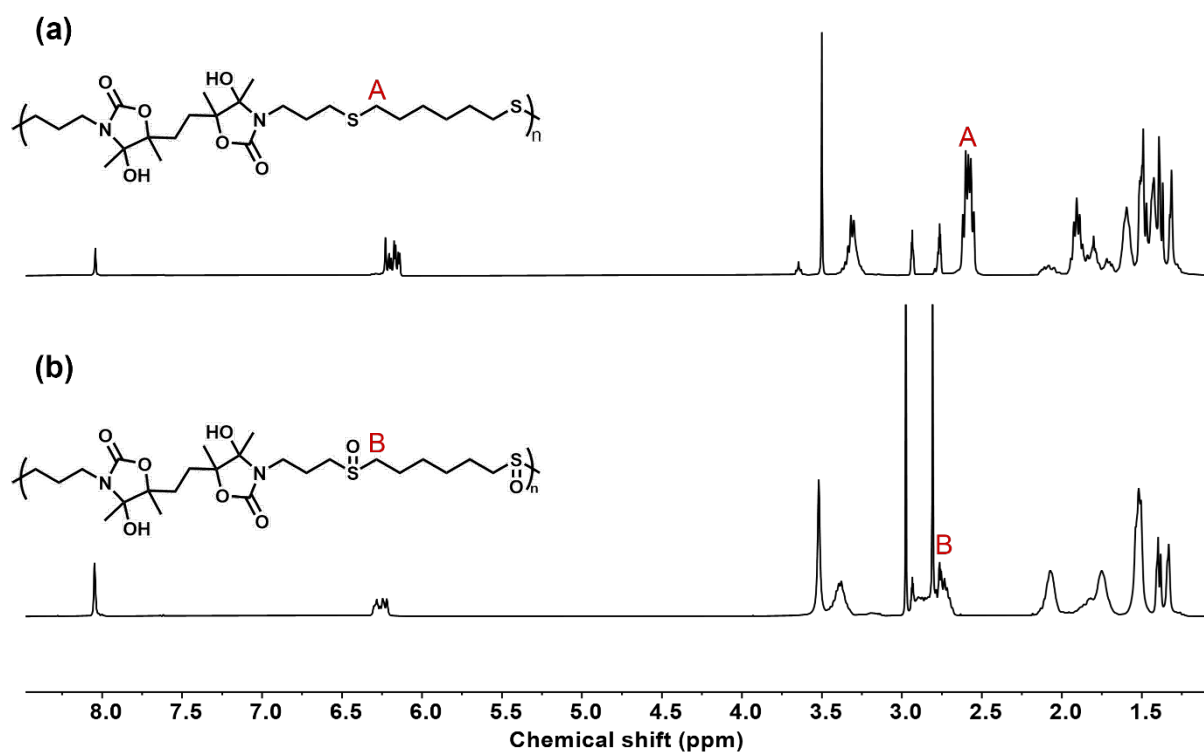


Figure S120. ^1H -NMR spectrum (400 MHz, DMF-d_7) of (a) P2b; (b) P2b-Sulfoxide

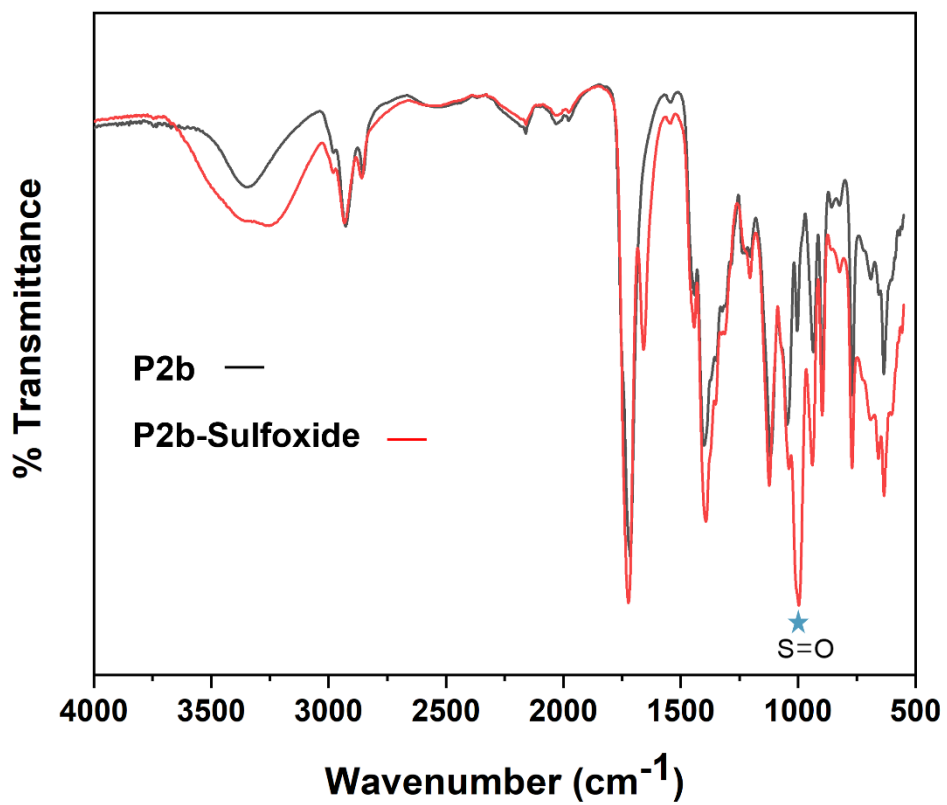


Figure S121. FT-IR spectra of P2b and P2b-Sulfoxide.

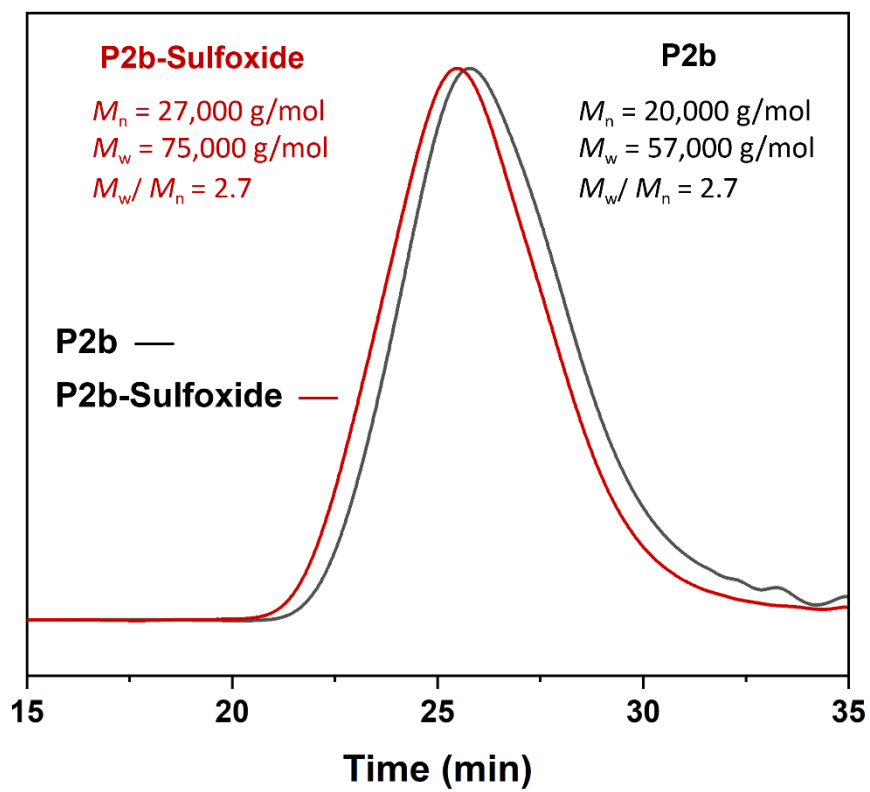


Figure S122. SEC chromatogram of P2b and P2b-Sulfoxide

21- Structure characterizations of P2b-Sulfone (oxidation to sulfone)

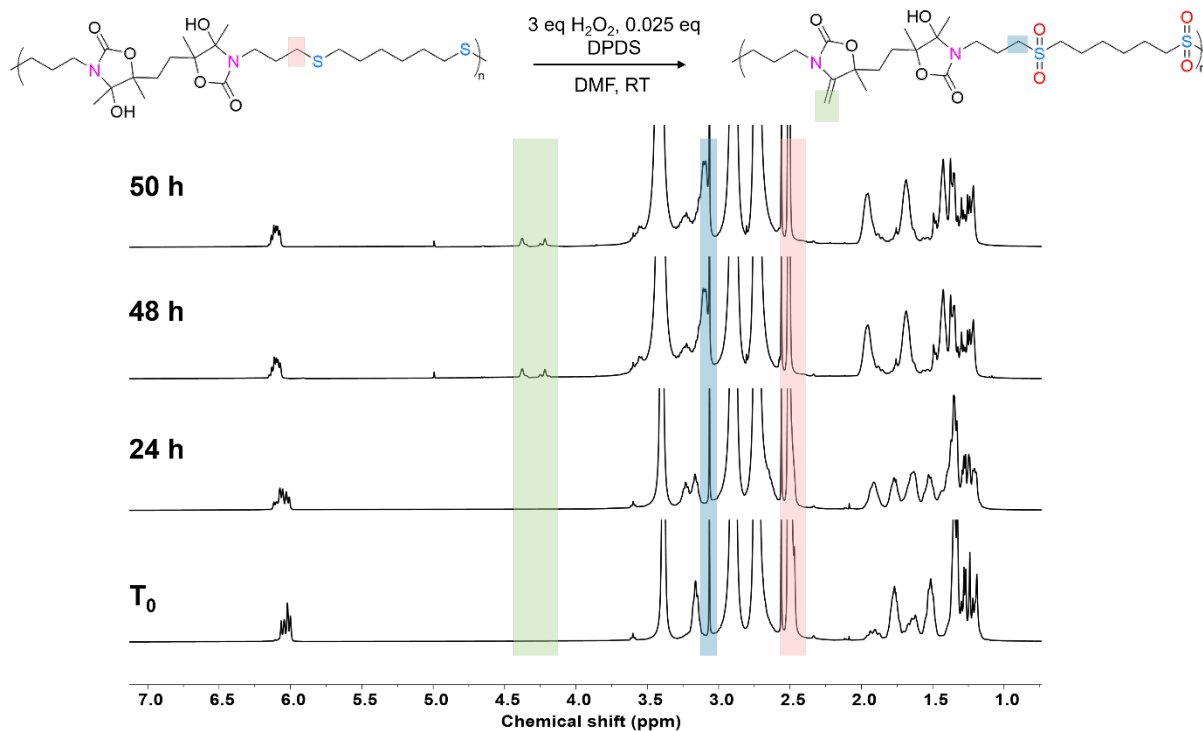


Figure S123. Kinetic study of oxidation of **P2b** to **P2b-Sulfone** containing sulfone groups using $^1\text{H-NMR}$ (400 MHz, DMSO-d_6).

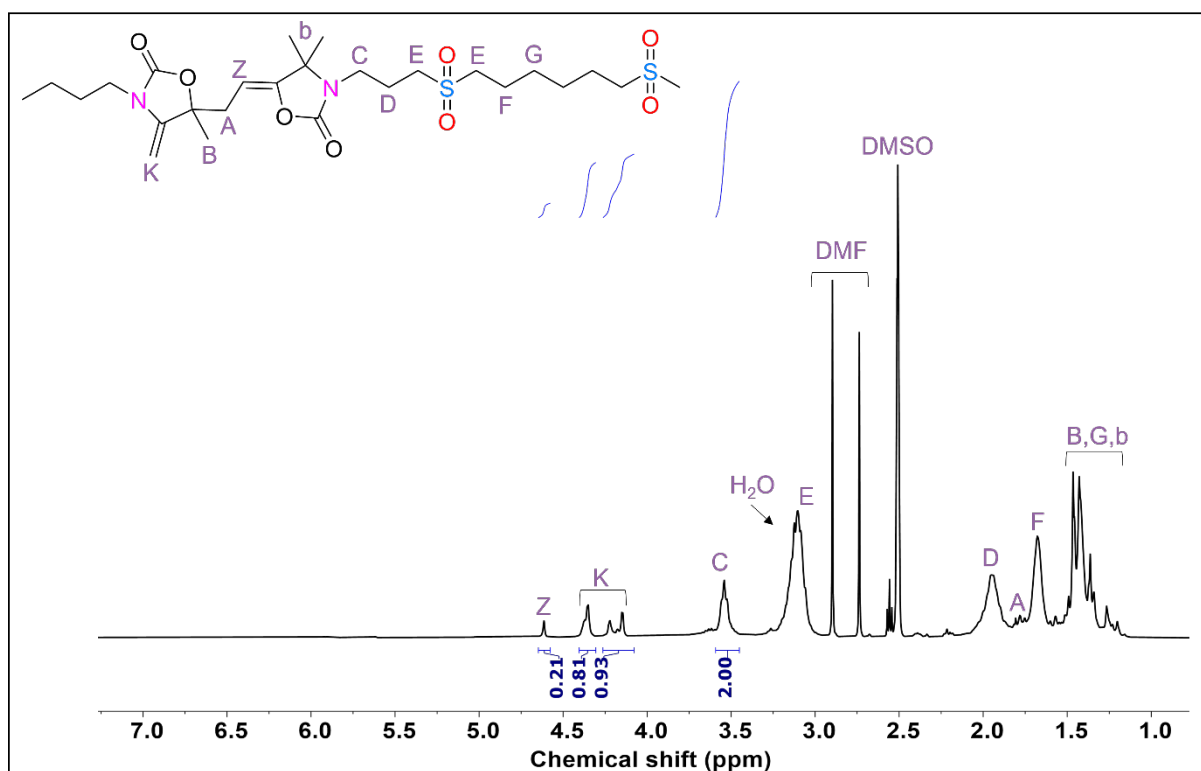


Figure S124. $^1\text{H-NMR}$ spectrum (400 MHz, DMSO-d_6) of **P2b-Sulfone**.

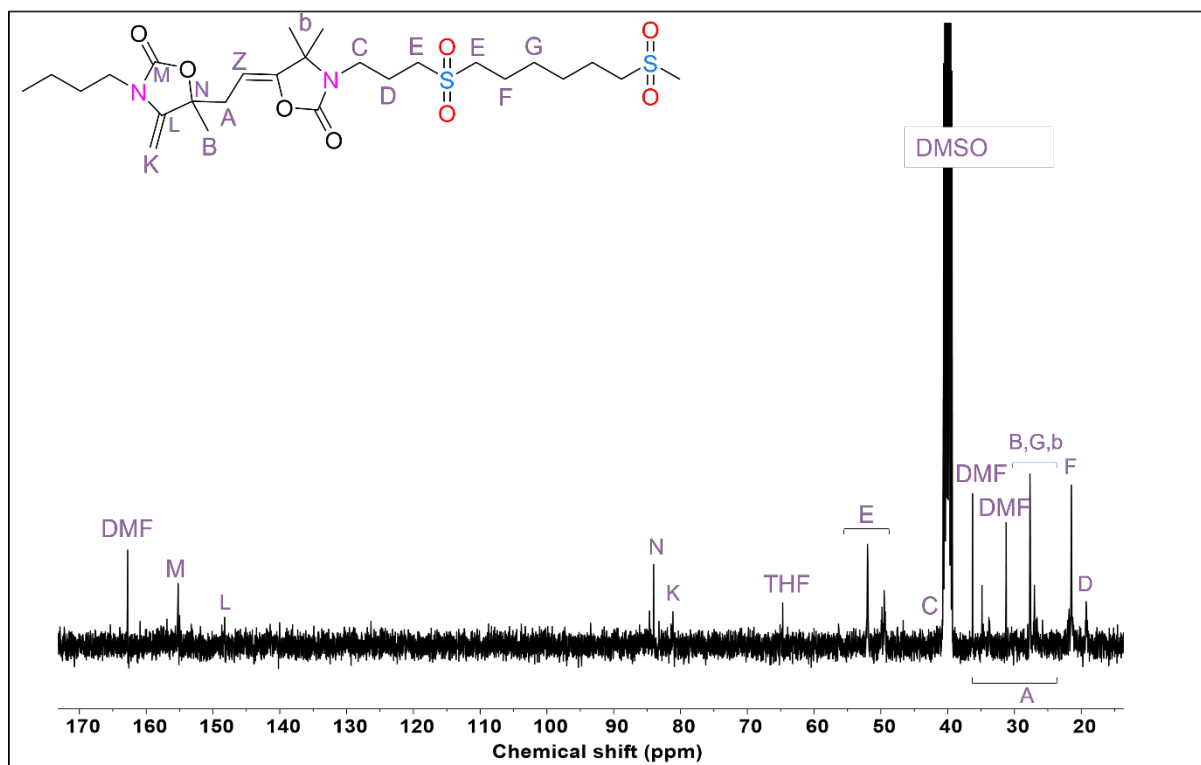


Figure S125. ^{13}C -NMR spectrum (100 MHz, $\text{DMSO-}d_6$) of P2b-Sulfone.

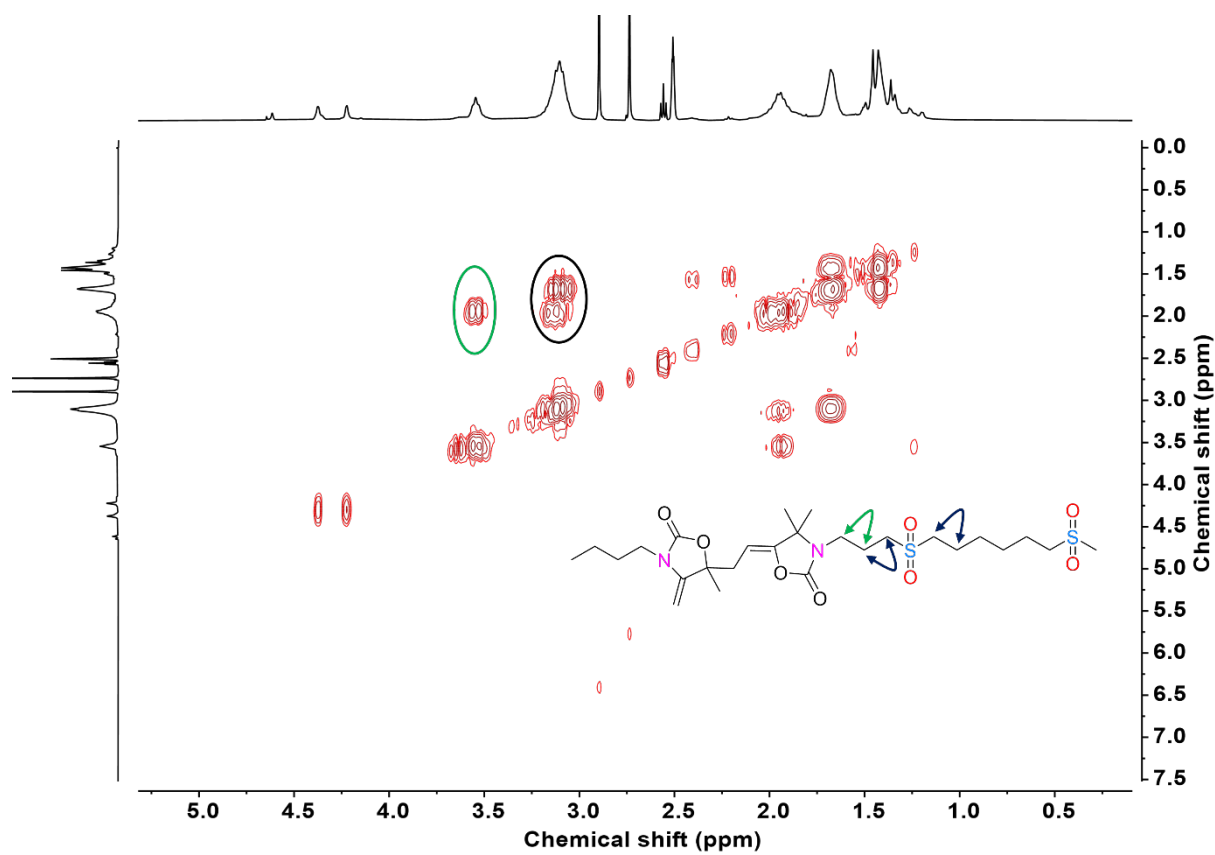


Figure S126. COSY NMR spectrum of P2b-Sulfone (400 MHz, $\text{DMSO-}d_6$).

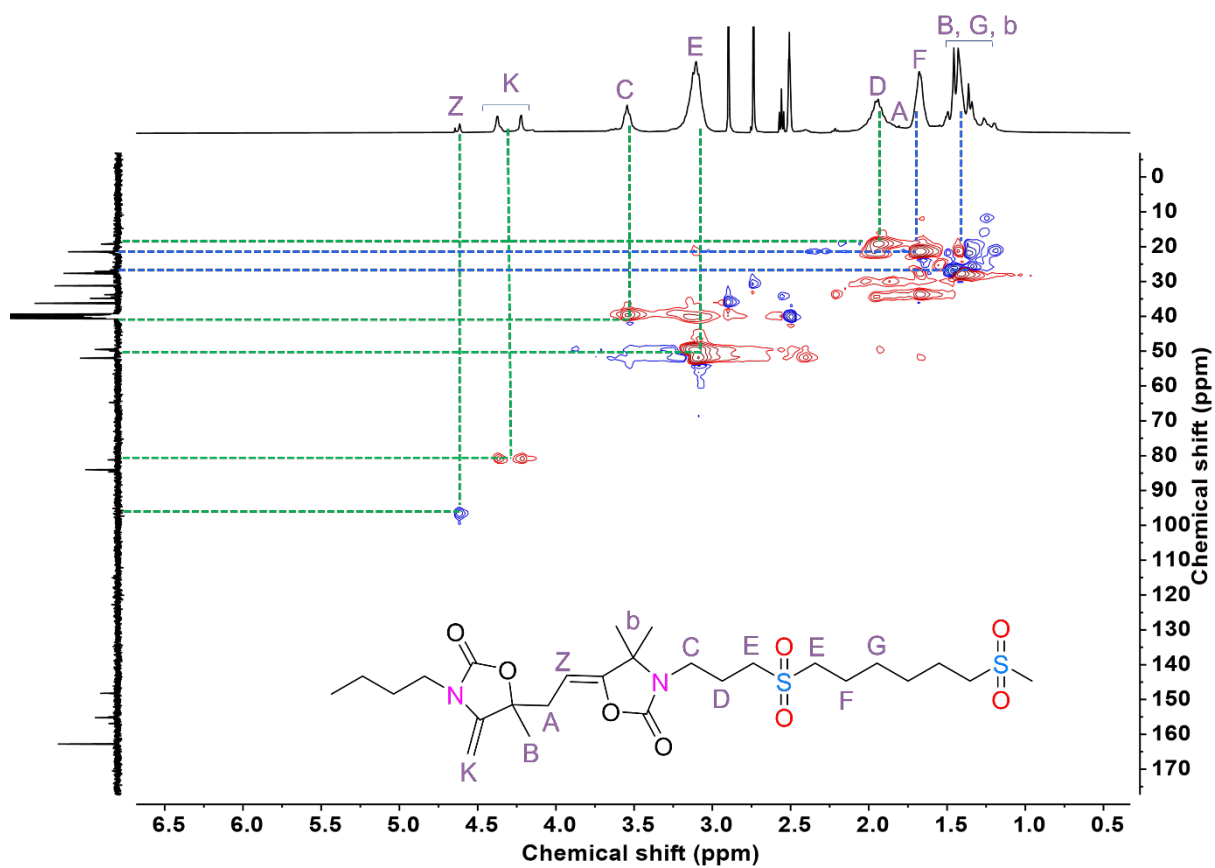


Figure S127. ^1H - ^{13}C HSQC NMR spectrum of P2b-Sulfone (400 MHz, $\text{DMSO-}d_6$).

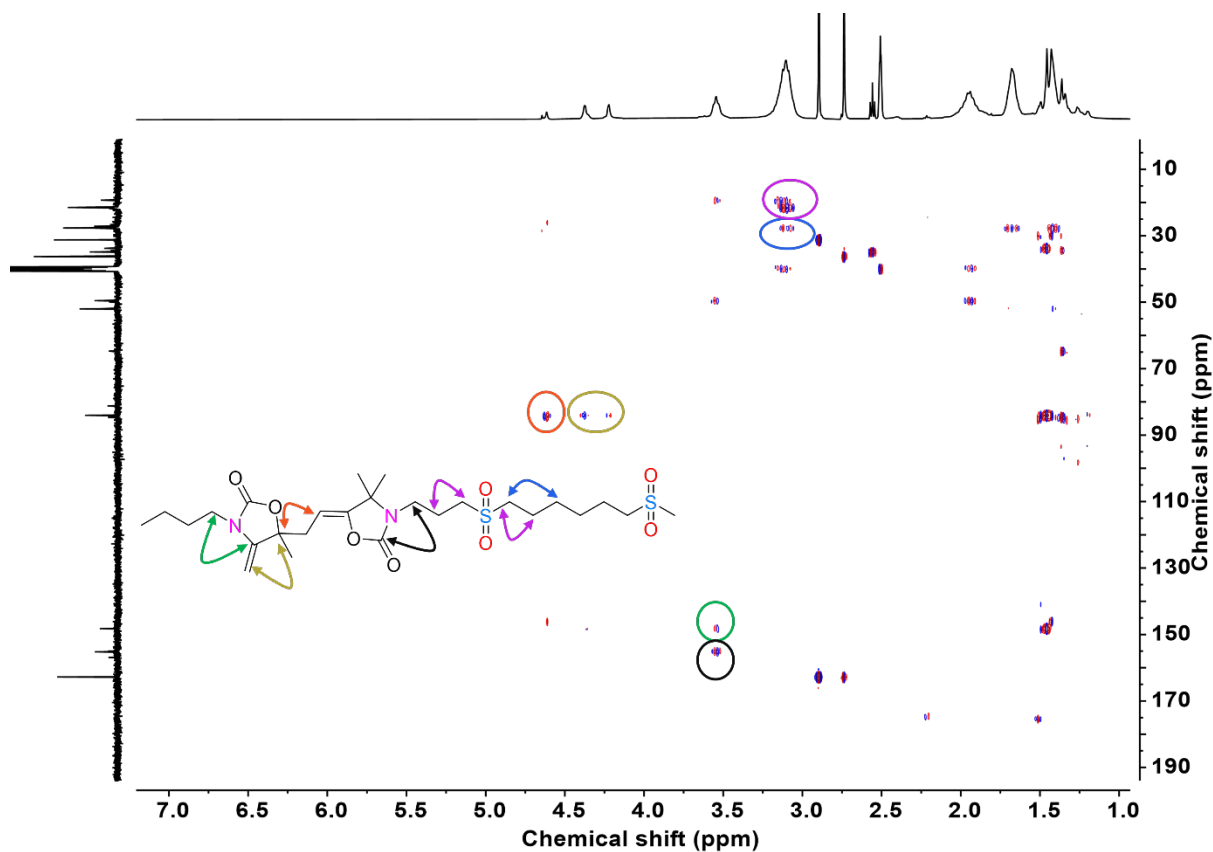


Figure S128. HMBC NMR spectrum of **P2b-Sulfone** (400 MHz, DMSO-*d*₆).

To corroborate the quantitative formation of sulfone groups, an additional verification was conducted using ¹H-NMR in DMF-*d*₇ as the solvent (Figure S79), which the peak associated to protons adjacent to thioethers ($\delta=2.51\text{-}2.64$ ppm) were vanished, substituted with a new downfield peak ($\delta=3.27\text{-}3.52$ ppm) corresponding to the methylene protons neighboring the sulfone groups ($-\text{SO}_2\text{CH}_2$).

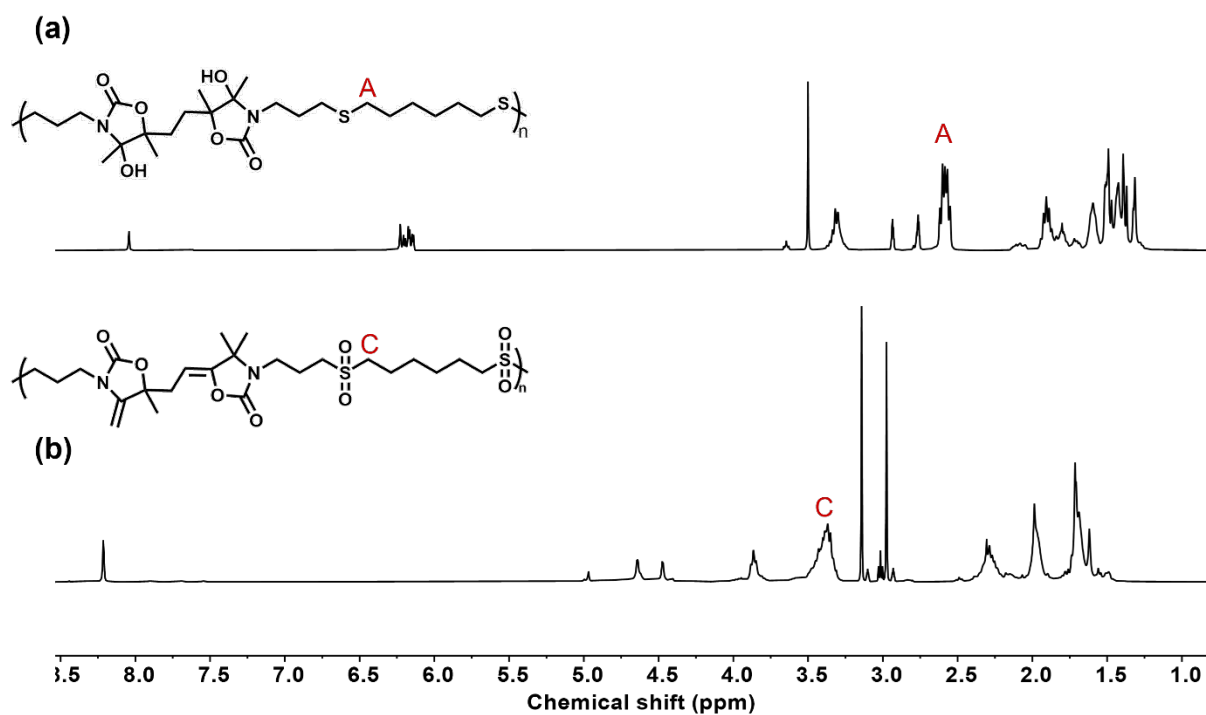


Figure S129. $^1\text{H-NMR}$ spectrum (400 MHz, DMF-d_7) of (a) **P2b**; (b) **P2b-Sulfone**.

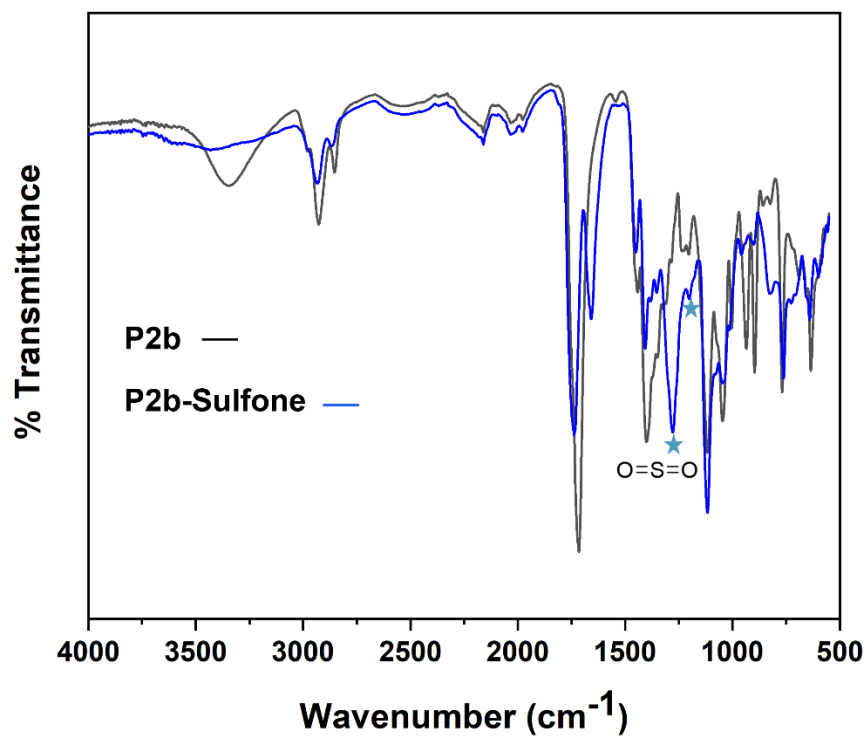


Figure S130. FT-IR spectra of P2b and P2b-Sulfone.

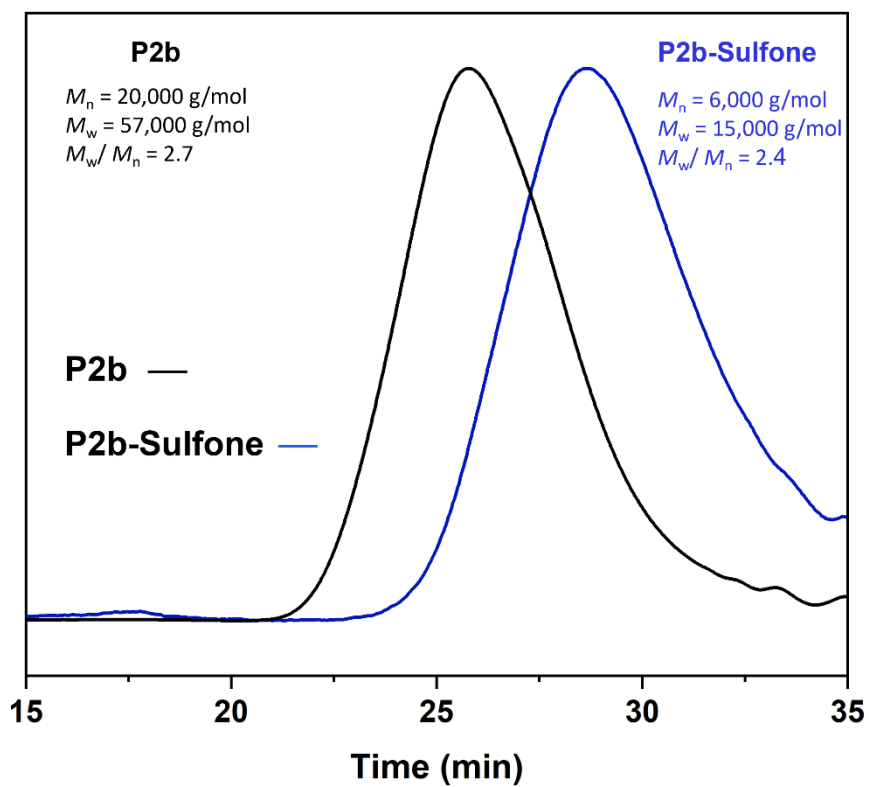


Figure S131. SEC chromatogram of P2b and P2b-Sulfone

22- TGA characterization of post-modified polymers

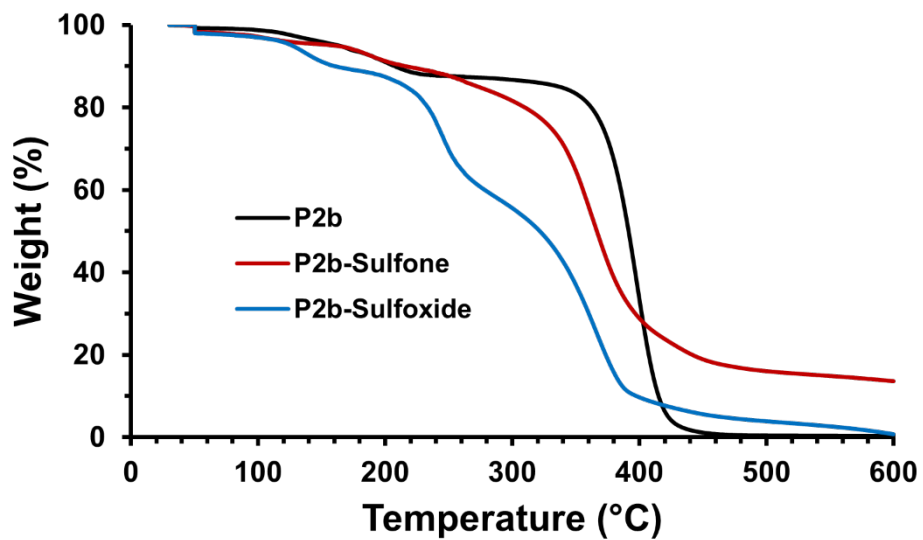


Figure S132. Overlay of TGA curves for polymers **P2b**, **P2b-Sulfoxide**, and **P2b-Sulfone**

23- Structure characterizations of P2b-Sulfonium (S-alkylated)

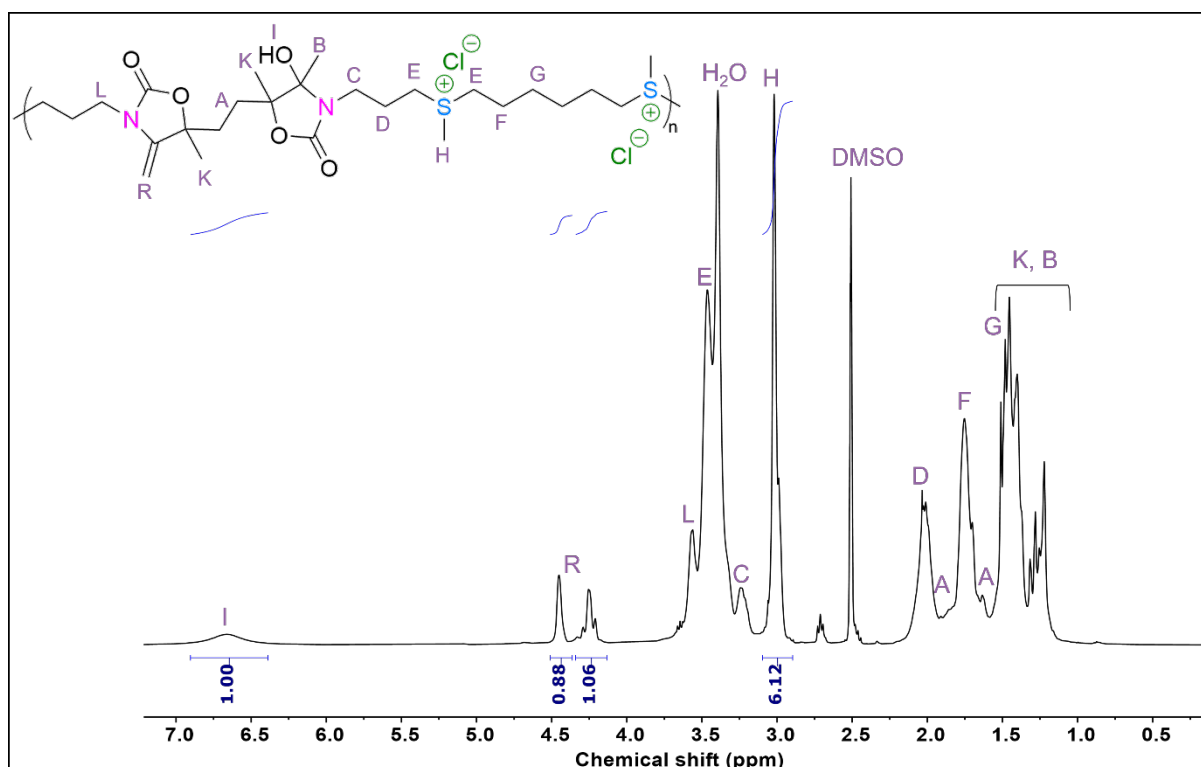


Figure S133. ¹H-NMR spectrum (400 MHz, DMSO-d₆) of P2b-Sulfonium.

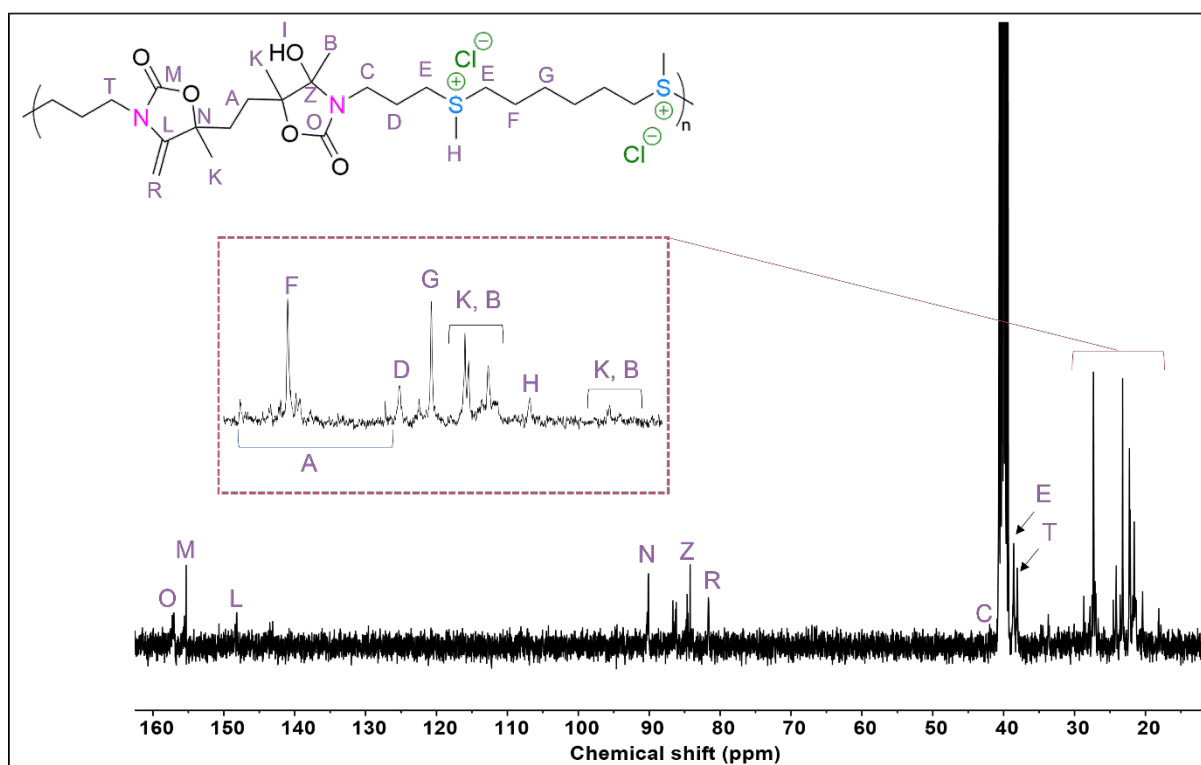


Figure S134. ¹³C-NMR spectrum (100 MHz, DMSO-d₆) of P2b-Sulfonium.

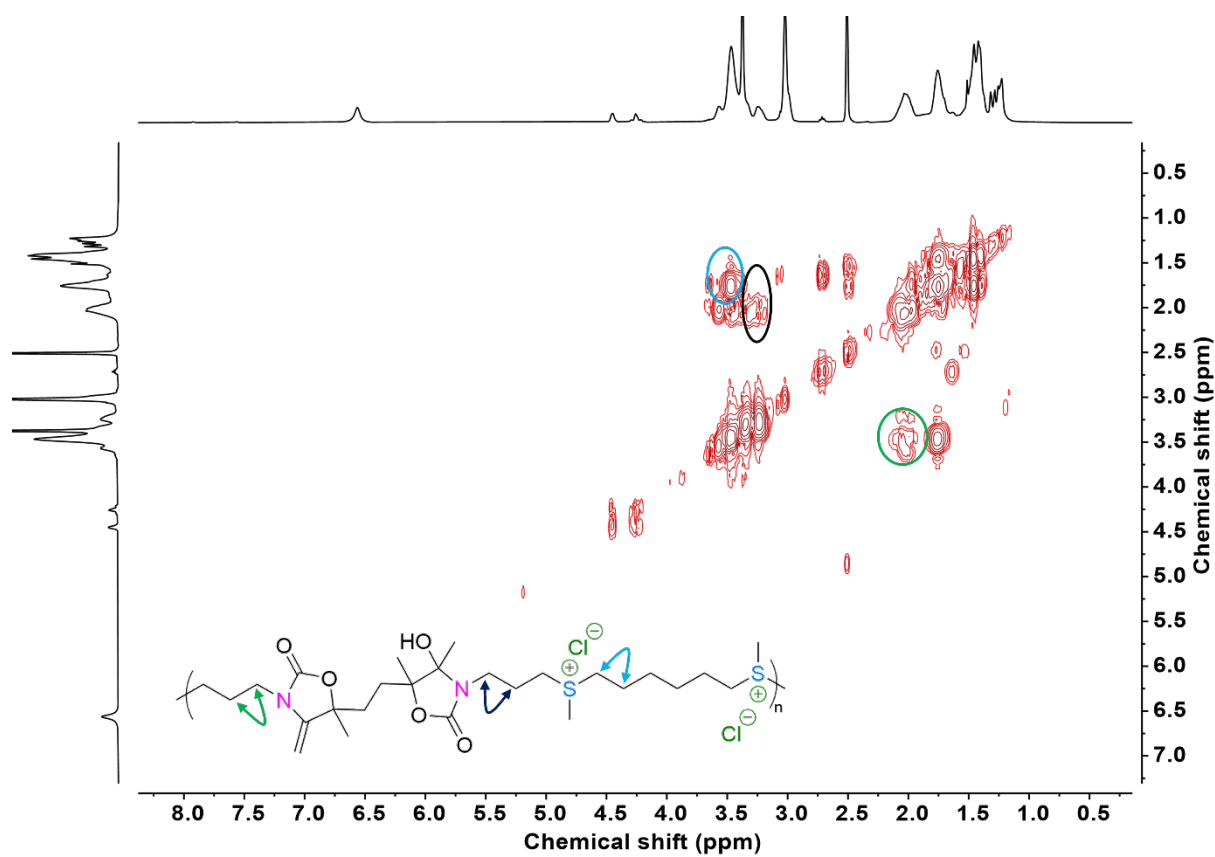


Figure S135. COSY NMR spectrum of **P2b-Sulfonium** (400 MHz, DMSO- d_6).

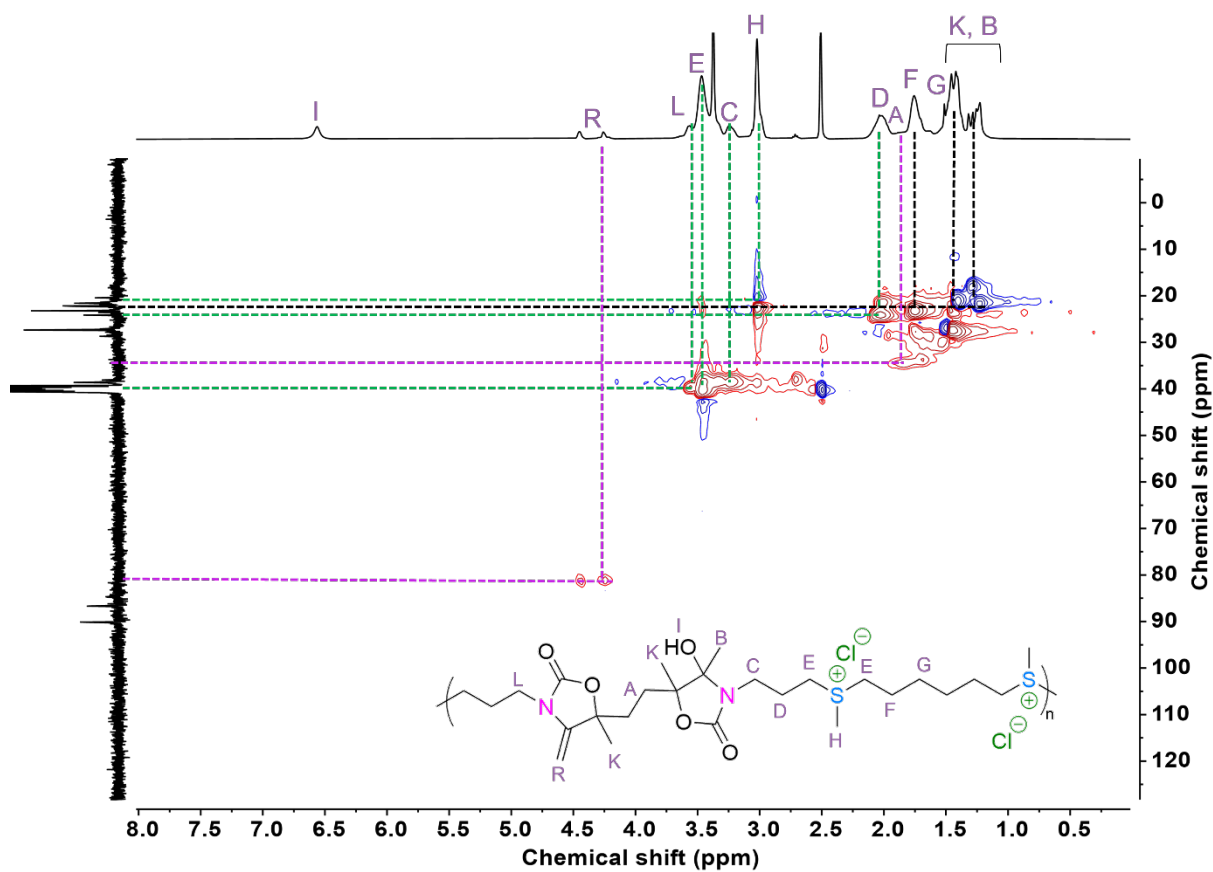


Figure S136. ^1H - ^{13}C HSQC NMR spectrum of P2b-Sulfonium (400 MHz, $\text{DMSO-}d_6$).

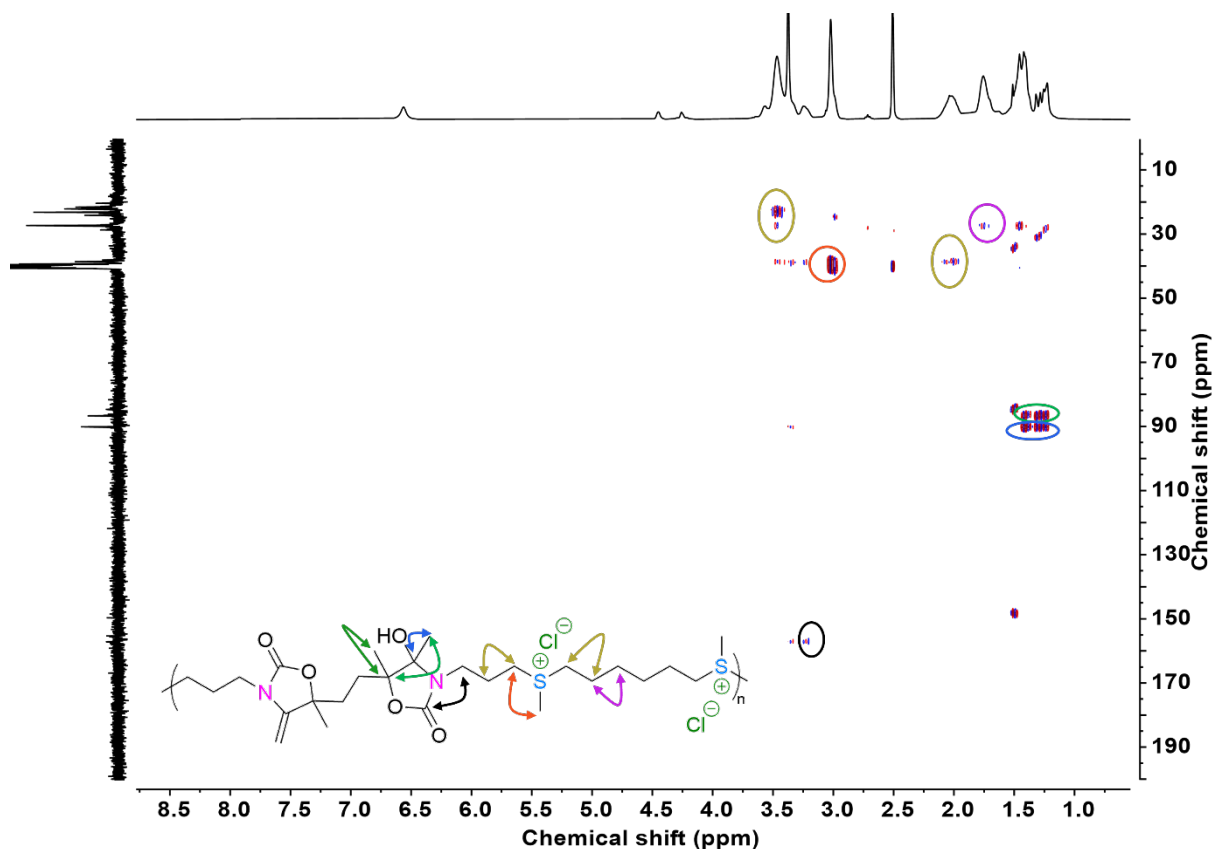


Figure S137. HMBC NMR spectrum of **P2b-Sulfonium** (400 MHz, DMSO- d_6).

To corroborate the quantitative formation of sulfonium groups, an additional verification was conducted using $^1\text{H-NMR}$ in D_2O as the solvent. As shown in S85, no resonance corresponding to protons adjacent to thioethers ($\delta=2.51\text{-}2.64$ ppm) were detected, while two new distinctive downfield peaks emerged at $\delta=3.19\text{-}3.44$ ppm and $\delta=2.81\text{-}2.89$ ppm, signifying the presence of the methylene ($\text{CH}_2\text{-S}^+$) and the methyl ($\text{CH}_3\text{-S}^+$) groups of the sulfonium moiety.

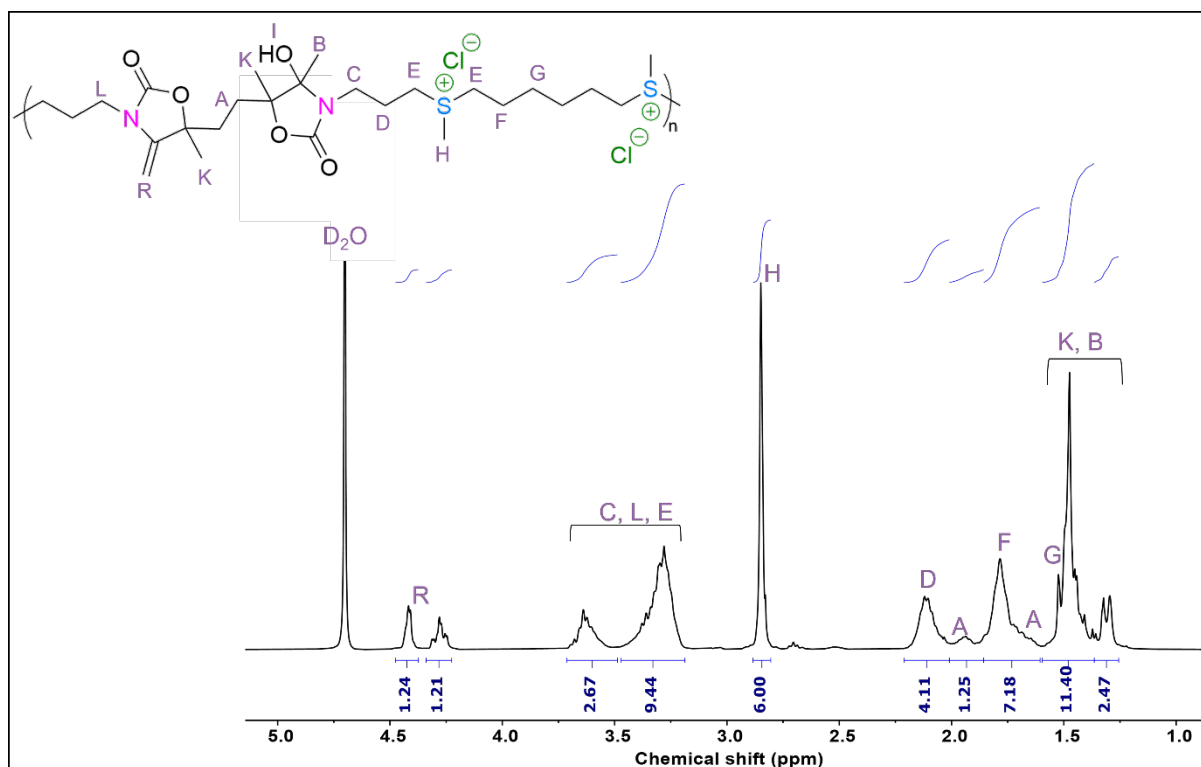


Figure S138. ¹H-NMR spectrum (400 MHz, D₂O) of P2b-Sulfonium.

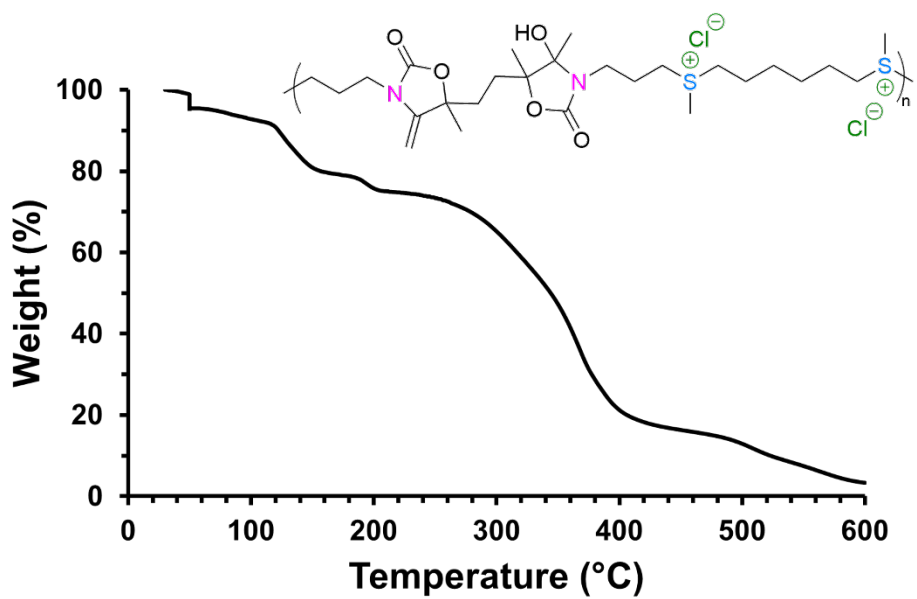


Figure S139. TGA thermogram for polymer P2b-Sulfonium

24- DSC characterization of alkylated polymer

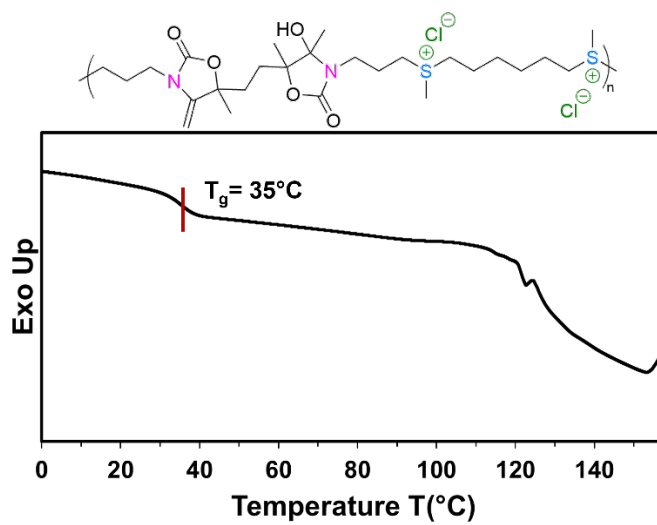


Figure S140. DSC trace of P2b-Sulfonium

25- References

1. Gennen, S., et al., *CO₂-Sourced α -Alkylidene Cyclic Carbonates: A Step Forward in the Quest for Functional Regioregular Poly(urethane)s and Poly(carbonate)s*. *Angew. Chem. Int. Ed.* 2017. **129**, 10394-10398.